

Effect of mix scale and rejuvenators on the performance of asphalt binders and asphalt mixtures containing 50% RAP materials- a statistical investigation

by

Zahra Sotoodeh-Nia

A dissertation submitted to the graduate faculty
in partial fulfillment of the requirements for the degree of
DOCTOR OF PHILOSOPHY

Major: Civil Engineering (Civil Engineering Materials)

Program of Study Committee:
R. Christopher Williams, Major Professor
Eric Cochran
Derrick Rollins
Vernon Schaefer
Martin Thuo
Ashley Buss

The student author, whose presentation of the scholarship herein was approved by the program of study committee, is solely responsible for the content of this dissertation. The Graduate College will ensure this dissertation is globally accessible and will not permit alterations after a degree is conferred.

Iowa State University

Ames, Iowa

2019

Copyright © Zahra Sotoodeh-Nia, 2019. All rights reserved.

DEDICATION

*To my parents,
because they always cared, understood, and inspired to dream big.*

*To my husband, Amin,
for all the unconditional love, support, happiness, and inspiration he has always offered.*

*To my brother, Saeid,
for his constant support and encouragements.*

TABLE OF CONTENTS`

	Page
LIST OF FIGURES	v
LIST OF TABLES	vii
ACKNOWLEDGEMENTS	ix
ABSTRACT	xi
CHAPTER 1 GENERAL INTRODUCTION	1
1.1 Background and Problem Statement	1
1.2 Objective and Tasks	3
1.3 Outline	4
1.4 Acknowledgements	5
1.5 Funding	6
1.6 References	6
CHAPTER 2 EFFECT OF TWO NOVEL BIO-BASED REJUVENATORS ON THE PERFORMANCE OF 50% RAP MIXES- A STATISTICAL STUDY ON COMPLEX MODULUS OF ASPHALT BINDERS AND ASPHALT MIXTURES	8
Abstract	8
2.1 Introduction	9
2.2 Experimental Plan	12
2.2.1 Materials	12
2.2.2 Mix design	13
2.2.3 Testing plan	14
2.3 Results and discussions	18
2.3.1 Binder evaluation	18
2.3.2 Mixture evaluation	30
2.4 Conclusions	33
2.5 References	34
CHAPTER 3 EFFECT OF HIGH RAP AND TWO NOVEL BIO-BASED REJUVENATORS ON THE LOW AND INTERMEDIATE TEMPERATURE PROPERTIES OF ASPHALT BINDERS AND ASPHALT MIXTURES	38
Abstract	38
3.1 Introduction	39
3.2 Experimental Plan	42
3.3.1 Materials	42
3.3.2 Extraction and recovery	43
3.3.3 Mix design	44
3.3.4 Testing plan	45
3.3 Results and discussion	48
3.4.1 Rejuvenator compatibility	48
3.4.2 Glover-Rowe damage parameter	50
3.4.3 Binder fatigue properties	51
3.4.4 Low temperature mixture fracture resistance	54
3.4.5 Mixture fatigue resistance	60

3.5	Conclusions and Recommendations.....	64
3.6	References	66
CHAPTER 4 HIGH TEMPERATURE PERFORMANCE OF ASPHALT MIXTURES AND ASPHALT BINDERS CONTAINING HIGH AMOUNTS OF RAP AND TWO NOVEL BIO-BASED REJUVENATORS.....		70
	Abstract	70
4.1	Introduction	71
4.2	Experimental Materials and Mix Designs.....	75
4.2.1	Materials	75
4.2.2	Mix design	76
4.2.3	Laboratory testing	77
4.3	Results and Discussion.....	78
4.3.1	Rotational Viscosity.....	78
4.3.2	Superpave specification parameter, $G * \sin\delta$	80
4.3.3	Complex Viscosity and shear rate influence.....	81
4.3.4	Zero Shear Viscosity and Cross model.....	83
4.3.5	Flow number	87
4.3.6	Stripping and moisture Susceptibility.....	89
4.3.7	Study on the recovered binders.....	91
4.4	Conclusions	94
4.5	References	95
CHAPTER 5 CONCLUSIONS AND RECOMMENDATIONS.....		98
5.1	Effect of bio-rejuvenators and mix scale on the complex modulus of binders and mixtures.....	98
5.2	Effect of bio-rejuvenators and mix scale on the low and intermediate temperature properties of asphalt binders and asphalt mixtures	99
5.3	Effect of bio-rejuvenators and mix scale on the high temperature properties of asphalt binders and asphalt mixtures.....	100
5.4	Recovered binders after short-term aging	101
5.5	Future research	102

LIST OF FIGURES

	Page
Figure 2.1 $ G^* $ master curves for unaged binders at 70°C	22
Figure 2.2 $ G^* $ master curves for RTFO-aged binders at 70°C.....	22
Figure 2.3 $ G^* $ master curves for RTFO+PAV-aged binders at 22°C.....	23
Figure 2.4 Normal quantile plot for the measured $ G^* $	23
Figure 2.5 Normal quantile plot for the model error	25
Figure 2.6 Comparison between measured and predicted $ G^* $ for RTFO+PAV aged binders	27
Figure 2.7 Black Space diagrams for unaged, RTFO-aged, and PAV-aged binders.....	30
Figure 2.8 $ E^* $ master curves for asphalt mixtures at 21°C reference temperature.....	31
Figure 2.9 Black Space diagram for the mixtures.....	33
Figure 3.1 Mix design gradations	45
Figure 3.2 Testing plan	46
Figure 3.3 Heating curves obtained from DSC testing.....	49
Figure 3.4 Glover-Rowe diagram	51
Figure 3.5 Cycles to failure at 28°C	53
Figure 3.6 Mean peak load results obtained from DCT testing.....	55
Figure 3.7 Mean peak load results obtained from DCT testing.....	55
Figure 3.8 Variation of peak load in the rejuvenated mixtures.....	58
Figure 3.9 Variation of fracture energy in the rejuvenated mixtures.....	58
Figure 3.10 Correlation between mix fracture energy and binder m-value.....	59
Figure 3.11 Correlation between mix fracture energy and binder stiffness.....	60
Figure 3.12 Schematic of RDEC curve(Ghuzlan 2001)	61
Figure 3.13 Comparison of PVs obtained from flexural beam fatigue testing	62

Figure 3.14 Comparison of Fatigue life obtained from flexural beam fatigue testing	63
Figure 4.1 Conventional viscosity measurements	79
Figure 4.2 Variation of rutting parameter $G * \sin(\delta)$ with temperature	80
Figure 4.3 Variation of complex viscosity with shear rate and temperature for the control and the rejuvenated binders	82
Figure 4.4 Normal quantile plot for the differences between pairs	82
Figure 4.5 Variation of ZSV with temperature and aging conditions for the binders	85
Figure 4.6 Variation of critical shear rate with the temperature and aging conditions for the binder	85
Figure 4.7 Example of Dunnett test output showing significant differences between the ZSV values of the control binder and the rejuvenated binders	86
Figure 4.8 Variation of ZSV with temperature	87
Figure 4.9 Example of MATLAB output for determining the flow number	88
Figure 4.10 Comparison of rutting resistance.....	89
Figure 4.11 Example of HWTD output	90
Figure 4.12 average rut depth for lab-produced and plant-produced groups.....	91

LIST OF TABLES	Page
Table 2.1 Aggregate gradation.....	15
Table 2.2 Volumetric properties	17
Table 2.3 Summary of performance grading	20
Table 2.4 Goodness-of-fit p-values from the normality test for measured and predicted log(G*) values	24
Table 2.5 Goodness-of-fit p-values from the normality test for model errors.....	25
Table 2.6 Wilcoxon signed rank test p-values for the differences between each model and the measured values	25
Table 2.7 Wilcoxon signed rank test p-values for the differences between the two models	27
Table 2.8 Wilcoxon signed rank test p-values for the differences between the two rejuvenated binders and the control binder.....	28
Table 3.1 Binder contents of the fractionated RAP	44
Table 3.2 Mix design proportions.....	45
Table 3.3 Proportions of fresh binder, RAP binder, and the rejuvenators.....	45
Table 3.4 Statistical comparison between the control and the rejuvenated mixtures-peak load ..	56
Table 3.5 Statistical comparison between the control and the rejuvenated mixtures-fracture energy.....	57
Table 3.6 Statistical comparison between the lab and plant-produced rejuvenated mixtures- peak load	57
Table 3.7 Statistical comparison between the lab and plant-produced rejuvenated mixtures- fracture energy	57
Table 4.1 Common Types of Rejuvenators	72

Table 4.2 Binder mix design.....	76
Table 4.3 VTS values.....	80
Table 4.4 ANOVA test results for the ZSV measurements	86
Table 4.5 ANOVA results for PG of the control binder	93
Table 4.6 ANOVA results for PG of the BM-1 binder.....	93
Table 4.7 ANOVA results for PG of the BM-2 binder.....	93

ACKNOWLEDGEMENTS

Thank God for his countless blessings during this entire journey especially the strength to finish this work and the abundant patience and perseverance over the past year.

I would like to express my deepest gratitude to my major professor, Dr. R. Christopher Williams for his selfless support during my graduate studies, for the many valuable advice and research opportunities he provided for me, and for the lifetime lesson he taught me, being patient during tough situations and believe they will eventually get resolved in favor.

I would like to thank my committee members, Dr. Eric Cochran, Dr. Derick Rollins, Dr. Vern Schaefer, Dr. Martin Thuo, and Dr. Ashley Buss for their guidance and encouragement in completing this dissertation.

I would like to extend my gratitude to all my colleagues in the BioRePavation project for all their contributions to the success of this project. I gratefully acknowledge the funding received from the European commission on the Infravation program for this project.

I would also like to thank all my colleagues in the asphalt materials lab especially Dr. Nicholas Manke, Paul Ledtje, Dr. Joseph Podolsky, and Dr. Ka Lai Ng Puga for their support and assistance.

Many thanks to all my friends in Ames for their part in this journey, and special thanks to my dear friends, Dr. Parnian Ghasemi, Dr. Raha Hamzeie, and Soheila Shabaniverki who went through hard times together with me and always cheered me on.

My very special thanks to my parents and my brother for always supporting me with their best wishes and prayers.

Finally, I acknowledge my dear husband for being the best company in this journey and for all the joy and unique adventures he has brought to my life. Without his support this dissertation would have never been completed.

ABSTRACT

Over the past decades, reclaimed asphalt pavement (RAP) materials have been increasingly used in asphalt pavements due to their significant contribution in reducing asphalt production costs and energy consumption. The main drawback associated with using RAP materials is the excessive amount of stiffness which the aged RAP binder introduces to the mixtures, thus reducing the resistance of mixtures to rutting, stripping, fatigue, and thermal cracking. In response to these limitations, researchers have suggested different techniques to avoid such distresses. The most common technique which is widely being practiced recently, is to use rejuvenators in the mix designs.

Currently, there are many rejuvenators available in the market with many variations in their origins and description. A successful rejuvenator is one that can be applied to the mix design in low dosages while restoring the chemical and rheological properties of the aged RAP binder as well as improving the performance of mixtures to adequate levels. Several petroleum-based rejuvenators have been used in the asphalt mix designs successfully, and recently, bio-based rejuvenators have attracted the attention of researchers due to the value they add to the sustainability of infrastructures.

In this research, two bio-based rejuvenators, one a by-product of the paper industry, and one derived from soybean oil, are introduced to enhance the properties of asphalt mixtures containing 50% RAP materials, and their respective binders. The first bio-rejuvenator is recommended by the manufacturer to be applied directly to the RAP, and then to the mixture, while the second bio-rejuvenator is recommended to be blended with the virgin binder, and then the blend added to the mixture.

In the first phase of the study, the alternative binders were produced based on the proportions in the mix design. First, the RAP binders were recovered from the coarse-graded and the fine-graded RAP mixtures in accordance with ASTM standards. A control binder containing 62.4% virgin binder and 37.6% RAP binder was compared with the two rejuvenated binders containing same amount of RAP binder, smaller amount of virgin binder, and a low dosage of the rejuvenators. The initial screening of the binders in terms of their density, viscosity, and performance grade was done according to the AASHTO standards. For the rheological properties evaluation, binders were tested in three aging conditions: unaged, RTFO aged, and RTFO+PAV aged, using a dynamic shear rheometer (DSR) and a bending beam rheometer (BBR). The complex modulus master curves of the binders were constructed based on the two common models: Sigmoidal and Christensen-Anderson- Marasteanu (CAM). The compatibility of the rejuvenators with the RAP and virgin binder was also assessed using a differential scanning calorimetry (DSC) equipment. The results of this phase proved that the rejuvenators can effectively improve the low and intermediate-temperature properties of the control binder, as well as reducing the complex modulus and viscosity, and decreasing the critical high-temperature performance grade. Statistical analysis on the two master curve models indicated no significant differences between the measured and predicted complex modulus data, and no significant differences between the two models at unaged and RTFO-aged conditions. At PAV-aged conditions, a greater R^2 value was observed for the Sigmoidal model. Viscosity measurements with the conventional method using a viscometer revealed a decrease in the viscosity of the control binder with the use of rejuvenator. Further study on the complex viscosity of the binders using the DSR equipment indicated statistically significant decrease in the zero shear viscosity (ZSV) values when using the two rejuvenators. From the DSC

results the compatibility of the rejuvenators with the binder was validated and possible disaggregation of some of the asphaltenes was observed.

In the second phase of the research, because the effectiveness of the rejuvenators was of interest at different mixing locations, asphalt mixtures were mixed in two locations: in the lab, and at the asphalt plant where the large-scale phase of the project was being handled. The plant-produced mixtures were then transported to the laboratory and both the plant-produced mixtures and lab-produced mixtures were compacted in the lab using a gyratory shear compactor (GSC). The specimens were then tested for their dynamic modulus, rutting and stripping resistance, and thermal cracking resistance. For the fatigue resistance, asphalt mixtures were compacted in the shape of slabs using a linear kneading compactor. Testing on the specimens was conducted in accordance with the ASTM/AASHTO standards. The dynamic modulus results indicated lower stiffness of the mixtures at low, intermediate, and high temperatures with the use of rejuvenators. The flow number of the mixtures as a measure of rutting resistance was also decreased with the use of rejuvenators due to the lower stiffness at high temperatures. Using the Hamburg wheel tracking test (HWT), no stripping inflection point (SIP) was identified before 20,000 wheel passes for the control mixture and both the rejuvenated mixtures and it was an indication of excellent stripping resistance in the mixtures and proved that the positive effect of high RAP content was not diminished by using the rejuvenators. The results from DCT testing on the mixtures revealed significant improvement in the fracture energy of the control mixtures after being rejuvenated. Although a significant improvement was observed in the fatigue resistance of the control binder after rejuvenation, however, no significant improvement was detected for the fatigue life of the rejuvenated mixtures, indicating that the existing beam fatigue procedure needs revision to integrate the effect of high RAP contents on the mix performance.

CHAPTER 1 GENERAL INTRODUCTION

1.1 Background and Problem Statement

Over the past decades, recycling of asphalt pavements to re-use, repair, reconstruct, and maintain highways has been found as a valuable approach as a result of increased demand and limited aggregate and binder supply (FHWA)[1]. The use of RAP not only helps in conserving energy and lowering construction costs, but it also decreases the amount of waste produced, and helps preserve the environment by decreasing the use of natural resources.

Despite increasing interest in the use of RAP, many agencies are still reluctant to use high amounts of RAP. In 2011, the average use of RAP in the United States was estimated at 12 percent in hot mix asphalt (HMA) [1]. Currently, many departments of transportations (DOTs) in the United States are allowed to increase the amount of RAP up to 50% in flexible pavements. However, such a high amount of RAP has the potential to adversely influence durability and structural performance of the pavements [2]. The reason is that, during the aging process over its service life, the asphalt binder hardens through various mechanisms such as oxidation, volatilization, and separation [3]. The structure of an asphalt binder could be seen as a colloid structure in which high molecular weight asphaltene micelles are dispersed in a low molecular weight medium known as maltenes. Upon aging, asphalt binder loses a large amount of its maltene phase, thus gaining a high proportion of asphaltenes, which are the stiffest component of asphalt binder. As the asphaltene content increases, the asphaltene micelles start to flocculate and create a continuous network with higher viscosity and lower ductility [4]. On the other hand, when asphalt binder loses its low-viscosity components, it requires higher conditioning temperatures and longer conditioning times to blend with other asphalt binders [5]. The durability problems related to the high stiffness and low ductility of recycled materials, coupled with concerns related to the

interactions between virgin and recycled materials, make the HMA more susceptible to low-temperature and fatigue cracking [6].

Several techniques have been developed to more effectively produce HMA containing high amounts of RAP while maintaining the high quality of pavement infrastructures to address the issues regarding the use of high RAP in HMA. One approach is to use a softer virgin binder to compensate for the increased stiffness and achieve the desired performance grade of the binder blend [7]. Recently, binders made from renewable resources have shown good potential to be used with high amounts of RAP [8]. Another approach is to utilize warm mix asphalt (WMA) technologies which significantly reduce the production and paving temperature of HMA, thus reducing oxidation during the production and transportation of asphalt mixtures, known as short-term aging [9]. Another approach is to use a recycling agent to lower the viscosity and restore the rheological properties of the recycled binder [10]. The recycling agents are classified as softening agents or rejuvenators. The distinction between these two groups is that softening agents are solely used to lower the viscosity of aged binders [9], while rejuvenators recover the aged binder's rheological properties and reconstitute their chemical compositions [11]. The focus of this study is on the effect of rejuvenators on the performance of HMA containing high amounts of RAP.

Researchers who used aromatic oils or petroleum-based rejuvenators, have concluded that when a rejuvenator was blended with the recycled asphalt binder, first, a low viscosity layer formed around the RAP aggregates coated with aged binder. The rejuvenator then diffused into the aged binder layer and softened it. After a period of time, no raw rejuvenator remained, but the diffusion process still continued until equilibrium was reached [12]. A number of studies have investigated the viability of rejuvenators in asphalt binders and their respective mixtures [3, 10, 12-15]. It has been concluded that rejuvenators containing high proportions of maltene constituents and a low

content of saturates help the aged binder to re-balance its composition through gaining the maltenes which were lost during short-term and long-term aging [16]. The new generation of engineered rejuvenators, however, are being added to the asphalt binder matrix at a low dosage which does not change as such the chemical composition. To ensure durability of the aged binder, the rejuvenator should provide a homogenous system where the asphaltenes are prevented from precipitation or flocculation [3].

The behavior of asphalt binder primarily depends on the temperature and the loading conditions. Therefore, rheology, which studies the behavior of materials under loading, can significantly contribute to understanding the properties of asphalt binders at various temperatures and loading conditions. It is essential that the asphalt binder demonstrate high resistance against stress related loading to mitigate permanent deformation and possess a thermal stability over a wide range of temperatures experiencing during its service life. On the other hand, it is also essential to characterize the structural behavior of asphalt mixtures for the critical distress modes including rutting, fatigue, and thermal cracking.

1.2 Objective and Tasks

This dissertation presents the preliminary findings of a research project called BioRePavation as part of the Infravation program on the use of novel bio-materials. The main objective of this proposed project is to investigate the performance of novel bio-materials from bio-mass as potential binders and rejuvenators in the asphalt mixtures containing high amounts of RAP and demonstrate that alternative bio-based binders can be used in asphalt mixtures with the same level of performance as of the conventional solutions with petroleum-based binders. To achieve this objective, the following tasks were undertaken:

1. Evaluate the effectiveness of two bio-based materials as potential rejuvenators on the rheological and thermal properties of binders including recycled binders by using Dynamic Shear Rheometer (DSR), Bending Beam Rheometer (BBR), and Differential Scanning Calorimetry (DSC).
2. Characterize the effect of the bio-rejuvenators on the critical distress modes of asphalt mixtures at low-temperatures, intermediate-temperatures, and high-temperatures known as thermal cracking, fatigue cracking, and rutting, respectively.
3. Conduct statistical analyses on the results obtained from experiments and identify the significant differences between the existing prediction models.
4. Investigate the effect of aging and thermal history of the binders on the presence of bio-rejuvenators in the recovered binders from mixes.

1.3 Outline

The dissertation is organized into five chapters as follows:

Chapter 1 provides a brief background about the use of RAP and rejuvenators in HMA followed by the required tasks to address the current issues in this subject and the dissertation organization.

In Chapter 2, a thorough analysis of the rheological properties of the rejuvenated binders as well as the dynamic modulus of their respective mixtures is conducted. A statistical analysis is performed to compare two existing models used to construct binder master curves and identify the significant differences between them. The mix study is performed on two sets of specimens: lab-produced, lab-compacted, and plant-produced, lab-compacted specimens. The statistical analysis in this part included identification of any significant differences between the complex modulus of

the rejuvenated mixtures and the control mixture (with no rejuvenator), based on different testing temperatures and the location they were mixed (lab/plant).

Chapter 3 focuses on evaluation of the low and intermediate temperature properties of the rejuvenated binders and their respective mixtures, followed by some statistical analyses performed to identify the differences between lab-produced and plant-produced mixtures. The compatibility of the rejuvenators with the binders is also assessed in this chapter.

In Chapter 4, the high-temperature properties of the asphalt binders in terms of their viscosity is discussed and the rutting and stripping properties of the mixtures is evaluated. Finally, the recovered asphalt binders from lab-produced and plant-produced mixtures are characterized based on their performance grade and compared with those of the blended binders and the differences are highlighted.

Chapter 5 summarizes the conclusions and presents recommendations for future work.

1.4 Acknowledgements

The authors appreciate the involvement of Jean-Pascal Planche, Ryan Boysen, Ana Jiménez del Barco Carrión, Davide Lo Presti, Simon Pouget, François Olard, Erik Bessmann, Juliette Blanc, Pierre Hornyh, Vincent Gaudefroy, and Ka Lai N. Ng Puga as other partners in this project. The authors gratefully acknowledge Eiffage Company for supplying the aggregates and Shell for providing the binder. In addition, authors are thankful to Kraton Company for providing SYLVAROAD™ RP1000 as a bio-rejuvenator and Adventus & ADM for providing Epoxidized Methyl Soyate (EMS) as a potential bio-rejuvenator for use in this research work.

1.5 Funding

The research presented here was financially supported through the European Union's seventh framework programme for research, technological development and demonstration. The BioRePavation project is co-funded by funding partners of the ERA-NET plus Infravation and the European Commission.

1.6 References

1. Copeland, A., *Reclaimed asphalt pavement in asphalt mixtures: State of the practice*. 2011.
2. Al-Qadi, I.L., et al., *Impact of high RAP contents on structural and performance properties of asphalt mixtures*. 2012.
3. Karlsson, R. and U. Isacson, *Material-related aspects of asphalt recycling—state-of-the-art*. *Journal of Materials in Civil Engineering*, 2006. **18**(1): p. 81-92.
4. Corbett, L.W., *Reaction variables in the air blowing of asphalt*. *Industrial & Engineering Chemistry Process Design and Development*, 1975. **14**(2): p. 181-187.
5. Rad, F.Y., *Estimating blending level of fresh and RAP binders in recycled hot mix asphalt*. Master of Science, University of Wisconsin Madison, 2013.
6. Al-Qadi, I.L., M. Elseifi, and S.H. Carpenter, *Reclaimed asphalt pavement—a literature review*. 2007.
7. McDaniel, R.S., et al., *Recommended use of reclaimed asphalt pavement in the Superpave mix design method*. NCHRP Web document, 2000. **30**.
8. Barco Carrión, A.J.d., et al., *Linear viscoelastic properties of high reclaimed asphalt content mixes with biobinders*. *Road Materials and Pavement Design*, 2017. **18**(sup2): p. 241-251.
9. Zaumanis, M. and R.B. Mallick, *Review of very high-content reclaimed asphalt use in plant-produced pavements: state of the art*. *International Journal of Pavement Engineering*, 2015. **16**(1): p. 39-55.
10. Tran, N.H., A. Taylor, and R. Willis, *Effect of rejuvenator on performance properties of HMA mixtures with high RAP and RAS contents*. NCAT Report, 2012: p. 12-05.
11. Roberts, F.L., et al., *Hot mix asphalt materials, mixture design and construction*. 1991.

12. Carpenter, S.H. and J.R. Wolosick, *Modifier influence in the characterization of hot-mix recycled material*. Transportation Research Record, 1980(777).
13. Mallick, R.B., et al. *Why not use rejuvenator for 100% RAP recycling?* in *Transportation research board 89th annual meeting*. 2010.
14. Shen, J., S. Amirkhanian, and B. Tang, *Effects of rejuvenator on performance-based properties of rejuvenated asphalt binder and mixtures*. Construction and Building Materials, 2007. **21**(5): p. 958-964.
15. Presti, D.L., et al., *Towards 100% recycling of reclaimed asphalt in road surface courses: binder design methodology and case studies*. Journal of cleaner production, 2016. **131**: p. 43-51.
16. Terrel, R. and J. Epps, *Using additives and modifiers in hot mix asphalt. Section A*. 1989.

CHAPTER 2 EFFECT OF TWO NOVEL BIO-BASED REJUVENATORS ON THE PERFORMANCE OF 50% RAP MIXES- A STATISTICAL STUDY ON COMPLEX MODULUS OF ASPHALT BINDERS AND ASPHALT MIXTURES

Modified from a manuscript published in Journal of Road Materials and Pavement Design

Zahra Sotoodeh-Nia^a, Nick Manke^a, R. Christopher Williams^a, Eric W. Cochran^b, Laurent Porot^c, Emmanuel Chailleux^d, Davide Lo Presti^e, Ana Jiménez del Barco Carrión^e

Abstract

An experimental study was conducted to evaluate the effectiveness of two bio-additives as rejuvenators on the properties of asphalt mixtures containing 50% RAP and their binder constituents containing 37% RAP binder. Before mixing, the rejuvenators were blended with fresh bitumen and the extracted and recovered RAP bitumen, and changes in the rheological properties of the binders were assessed using performance grading (PG) criteria. The results showed that both rejuvenators could improve the low-temperature performance of the aged RAP binder and restore its low-temperature properties. Master curves for the unaged, RTFO-aged, and PAV aged blends were constructed using both the Christensen-Anderson-Marasteanu (CAM) model and the Sigmoidal models. A comparative statistical analysis conducted on the models indicated no significant difference between the measured and predicted complex modulus values at any aging conditions. The pairwise statistical comparison between the two models showed that at unaged conditions, they can perfectly overlap as the p-values were greater than the level of significance. However, for the PAV-aged binders, this behavior appears to weaken due to the brittle behavior of the binders. Further statistical analyses revealed no significant differences between the two

^a Department of Civil, Construction, and Environmental Engineering, Iowa State University, Ames, Iowa, 50011-3232.

^b Department of Chemical and Biological Engineering, Iowa State University, Ames, Iowa, 50011-3232.

^c Kraton Chemical B.V, Almere, Netherlands.

^d LUNAM Université, IFSTTAR, Bouguenais, France.

^e Nottingham Transportation Engineering Centre, University of Nottingham, Nottingham, UK.

models at unaged conditions, however, as the binders were subjected to aging, significant differences between the two models began to appear.

Mixing was performed in two locations: lab and plant, while compaction was performed only in the lab. After mixing and compaction, mixtures were evaluated for their stiffness characteristics through dynamic modulus testing. Compared to the control mixture, rejuvenated mixtures showed lower dynamic modulus values especially at high temperatures. A statistical comparison between the lab produced, lab-compacted mixtures and plant-produced, lab compacted mixtures showed that both the rejuvenation and the location of mixing were significant factors in the stiffness measurements.

2.1 Introduction

Reclaimed asphalt pavement (RAP) has been widely used in asphalt mixtures over the past few decades. A considerable number of studies have shown that RAP can be used as a sustainable and cost-effective alternative for virgin aggregates and virgin binders in asphalt pavements (Al-Qadi, Elseifi et al. 2007, Copeland 2011). However, the greatest challenge among agencies is that high amounts of RAP could affect the long-term performance of asphalt pavements adversely, and thus not effectively reduce the costs over the pavement service life (Yu, Zaumanis et al. 2014). The concerns regarding the use of high RAP content in hot mix asphalt (HMA) primarily refer to the rheological changes that progressively occur in the RAP binder. During the pavement service life, the asphalt binder hardens through various mechanisms such as oxidation, volatilization, and separation, thus gaining more stiffness and higher viscosity (Karlsson and Isacson 2006). The durability problems related to the high stiffness and low ductility of recycled materials, coupled with concerns related to the interactions between virgin and recycled materials, make the HMA more susceptible to low-temperature and fatigue cracking (Al-Qadi, Elseifi et al. 2007).

These concerns have prompted researchers to adopt various approaches in order to effectively use high amounts of RAP in HMA without compromising the quality of the pavements. When using high amounts of RAP materials in asphalt mixtures, the mix designs often require appropriate selection of a softer virgin binder or a recycling agent (McDaniel, Soleymani et al. 2000, Tran, Taylor et al. 2012, Barco Carrión, Lo Presti et al. 2017). The effectiveness of a recycling agent can be evaluated through its ability to lower the viscosity of the recycled binder and restore its rheological properties (Kandhal and Mallick 1998). Based on this, recycling agents can be classified as softening agents which can only lower the viscosity, or rejuvenators which can also restore the rheological properties of the recycled binders (Roberts, Kandhal et al. 1991, Zaumanis and Mallick 2015). Not only does the origin of the recycling agent have a significant influence on the performance of the binders and their respective mixtures, but the dosage and the blending conditions can also affect the performance to varying extents.

This research focuses on investigating the potential of two bio-based additives as effective rejuvenators that can be used at very low dosages in high RAP mix designs. To characterize the rheological behavior of the modified binders and compare them with a control binder, the binders were tested by means of dynamic shear rheometer (DSR) and bending beam rheometer (BBR) at various temperatures and loading conditions. The critical high, intermediate, and low temperatures were determined in accordance with AASHTO T315, and the ΔT_c values were calculated from the BBR results. The results from frequency sweeps and temperature sweeps were used to construct the binder master curves at unaged, RTFO aged, and RTFO+PAV aged conditions. For this purpose, both the Sigmoidal and the Christensen-Anderson-Marasteanu (CAM) models were employed, and the differences between the two models were identified through statistical analyses using the JMP software package (Inc 1989-2019). Yusoff et al. (Yusoff, Jakarni et al. 2013) used

several mathematical models to describe the viscoelastic properties of unaged and aged bitumens and concluded that the generalized modified Sigmoidal model showed the best correlation between measured and modelled rheological properties, followed by the Sigmoidal, CAM, and Christensen and Anderson (CA) models, respectively. Asgharzadeh et al. (Asgharzadeh, Tabatabaee et al. 2015) also evaluated different models for the phase angle master curves of asphalt binders, and depending on the type of binders, whether neat or modified, proposed a practical guide for selection of the most suitable models.

The binders were then introduced to mixtures with 50% RAP content contributing 37.6% of the blended binder, and the stiffness and resistance to low-temperature cracking of the mixes were evaluated. Mixtures were produced in two locations: lab, and plant, however, all the mixing procedures were in a like manner. The dynamic modulus results from the mixes were used to construct master curves and perform a statistical analysis to investigate the effect of different temperatures as well as the locations where they were produced.

The results presented here are the preliminary findings of a research project called BioRePavation as part of the Infravation program on the use of novel bio-materials. The tasks for this proposed project are based on the investigation of the merits of application of novel bio-materials from bio-mass as potential binders and rejuvenators in the asphalt mixtures containing high amounts of RAP (Chailleux, Bessman et al. 2017). The full-scale rutting and fatigue performance of these rejuvenated mixtures have been further validated at the accelerated pavement testing facilities at IFSTTAR, and they have shown similar or better performance compared to the control mixtures (Blanc, Hornych et al. 2019).

2.2 Experimental Plan

2.2.1 Materials

A PG 64-22 virgin binder as well as the virgin aggregates and RAP materials were provided by EIFFAGE. The RAP materials were delivered in two fractions: 8/12mm and 0/8mm. To determine the binder content of the RAP, ASTM D2172 and ASTM D7906 were followed. According to these standards, each of the RAP fractions were immersed in toluene as a suitable solvent overnight. Then, the solution of RAP binder and toluene was extracted using a high-speed centrifuge. A micro-centrifugation was also performed after extraction to remove further fine particles from the solution. After extraction, the solution was drawn into a flask of a rotary evaporator to recover the asphalt binder from the solution. The distillation flask was partially immersed in an oil bath at a temperature of $140\pm 5^{\circ}\text{C}$. While rotating at 40 rpm, a vacuum of 45.3 ± 0.7 kPa was applied to the flask with a nitrogen blanket of 1000mL/min, until 200 mL of the solution was left in the flask. Then more solution was introduced to the flask and the process was continued until no more solution was left. Finally, to remove the remaining solvent from the binder, vacuum and the nitrogen flow were slowly increased to 6.7 ± 0.7 kPa and 2500mL/min, respectively. This condition was maintained for 45 minutes at a temperature of 160°C . The recovered asphalt binder was then tested by DSR and BBR instruments to determine its rheological properties. A comparison was then made between the properties of the RAP binder and all other binders studied in this paper. The binder content in the coarse and fine fractions of RAP was determined to be 2.9% and 4.4%, respectively.

The first bio-additive called BM-1 in this study, is derived from crude tall oil (CTO) as a by-product of the paper industry. It is a liquid additive that with its specific amphipathic chemical structure disperses the highly polar fractions thus limiting the agglomeration of asphaltenes (Porot

and Grady 2016). In previous studies (Turner, Taylor et al. 2015, Tran, Taylor et al. 2017) BM-1 has shown promising potential to improve the low-temperature cracking resistance and fatigue life of asphalt mixtures containing RAP. The second bio-additive called BM-2 in this study, is derived from soybean oil, epoxidized methyl soyate (EMS), which is a product of esterification and epoxidation of soybean oil.

2.2.2 Mix design

To evaluate the effectiveness of the two bio-based additives on improving the properties of asphalt mixtures with 50% RAP (34% coarse RAP and 16% fine RAP), the following three asphalt mixtures were designed and fabricated in this study:

1. A control mixture with 50% RAP and 2.8% virgin binder.
2. The BM-1 mixture with 50% RAP, 2.7% virgin binder, and 6% BM-1 by weight of RAP binder which comprises 2.3% of the total binder weight.
3. The BM-2 mixture with 50% RAP, 2.7% virgin binder, and 3% BM-2 by weight of the total binder.

For the binder evaluation, the following three binder blends were made:

1. The control blend with 62.4% virgin binder and 37.6% RAP binder.
2. The BM-1 blend with 60.1% virgin binder, 37.6% RAP binder, and 2.3% BM-1.

According to the manufacturer recommendation, BM-1 was added to the RAP binder by 6% of the weight of RAP binder. This procedure has been practiced in previous publications (Turner, Taylor et al. 2015, Tran, Taylor et al. 2017). Then the RAP binder and BM-1 blend was added to the virgin binder and manually stirred for 5 minutes.

Although no curing time was specified in the lab guidelines of BM-1, this blend was then cured in the oven for two hours at the compaction temperature to simulate the field mixing and compaction conditions.

3. The BM-2 blend with 59.4% virgin binder, 37.6% RAP binder, and 3.0% BM-2. BM-2 was first blended with the virgin binder. To ensure full blending between the virgin binder and the rejuvenator, a shear mill was used at $150^{\circ}\text{C} \pm 2^{\circ}\text{C}$ and 800 rpm for twenty minutes. This binder blend was then added to the RAP binder and stirred and cured similar to the BM-1 blend.

The asphalt mixes were produced in the lab according to Superpave and AASHTO specification methods. A summary of the mix gradation of the virgin aggregate and RAP is provided in Table 2.1. The design procedure of high RAP mixtures is similar to regular HMA mixtures, as the RAP can be treated as another stockpile for the gradation design (Al-Qadi, Elseifi et al. 2007). The mixture nominal maximum aggregate size (NMAS) was determined to be 19.0 mm.

2.2.3 Testing plan

2.2.3.1 Binder performance evaluation

Rheological measurements of asphalt binders are of paramount importance to properly characterize their behavior at various temperatures and loading conditions because asphalt binder is known as a viscoelastic material.

Table 2.1 Aggregate gradation

Sieve		Percent Passing			Requirements	
#	mm	Virgin	RAP	mix	Min	Max
1"	25	100	100	100.0	100	
3/4"	19	98.9	99.9	99.4	90	100
1/2"	12.5	66.9	92.4	80.0		90
3/8"	9.5	29.6	60.6	45.5		
#4	4.75	23.5	29.9	26.8		
#8	2.36	22.6	24.7	23.7	23	49
#16	1.18	17.1	7.6	12.2		
#30	0.60	12.9	3.6	8.1		
#50	0.30	10.0	1.3	5.5		
#100	0.15	8.1	0.4	4.1		
#200	0.075	6.6	0.1	3.2	2	8

2.2.3.2 Performance grade (PG)

To characterize the behavior of binder blend upon short-term aging and long-term aging, the three blends were subjected to testing in a rolling thin film oven (RTFO) and a pressure aging vessel (PAV) in accordance with AASHTO T240 and AASHTO R28, respectively. To determine the performance grade (PG) of the binders, they were tested by a dynamic shear rheometer (DSR) and a bending beam rheometer (BBR) instruments following AASHTO T315 and AASHTO T313, respectively. The high failure temperature of the unaged and RTFO aged binders was assessed using a 25 mm parallel plate fixture and 1mm gap in the DSR, while the intermediate failure temperature was assessed by testing the RTFO+PAV aged binder in a 8mm parallel plate fixture of the DSR with a 2mm gap. The low failure temperature was determined in accordance with AASHTO T313, by testing beams of the RTFO+PAV aged binders by means of a BBR instrument.

The performance grade for each of the blends was then determined in accordance with AASHTO M320.

2.2.3.3 Complex shear modulus (G^*)

To characterize the stiffness behavior of asphalt binders over a wide range of frequencies and temperatures, temperature-frequency sweeps were applied on the unaged binders, RTFO aged binders, and RTFO+PAV aged binders at a constant shear strain of 5%, 3%, and 0.8%, respectively. To ensure that the behavior of the binders stays within the 25-mm diameter plates and a 1-mm gap geometry were used for the unaged and RTFO aged binders, while for the RTFO+PAV aged binders the 8-mm diameter plates and a gap of 2-mm were used. The temperature-frequency sweep covered a range of temperatures from 40°C to 76°C with 6°C increments for the unaged and RTFO aged binders, and 10°C to 34°C with 6°C increments for the RTFO+PAV aged binders. The binders were tested over a frequency range of 1 to 100 rad/s. The results from temperature-frequency sweeps were then used to construct master curves of G^* at a reference temperature of 70°C for the unaged and RTFO aged binders, and 22°C for the RTFO+PAV aged binder, using both the Sigmoidal function and Christensen-Anderson-Marasteanu (CAM) model given in Equations 2.1 and 2.2, respectively (Pellinen, Witczak et al. 2004).

$$\text{Log } |G^*| = \delta + \frac{\alpha}{1 + \frac{1}{e^{\beta + \gamma \log f_R}}} \quad \text{Equation 2.1}$$

Where f_R is the reduced frequency, δ is the minimum value of $|G^*|$, $\delta + \alpha$ is the maximum value of $|G^*|$, and β, γ are fitting coefficients of the sigmoidal model.

$$|G^*| = G_g \left[1 + \left(\frac{\omega_c}{\omega} \right)^v \right]^{-\eta/v} \quad \text{Equation 2.2}$$

Where G_g is the glassy modulus, ω_c is crossover frequency, and ν and η are the CAM model parameters.

2.2.3.4 Mixture performance evaluation

To evaluate the performance of asphalt mixtures, all the specimens were mixed and compacted in the laboratory using a gyratory compactor (GC). Specimens were fabricated for dynamic modulus testing and disc-compact tension (DCT) test at the desired air void content for each test. Bulk specific gravities (G_{mb}) of the specimens were determined in accordance with AASHTO T331-13, using the CoreLok method. The maximum theoretical specific gravities (G_{mm}) of the mixtures were determined in accordance with AASHTO T 209. Table 2.2 summarizes the volumetric properties of each of the mixtures.

Table 2.2 Volumetric properties

property	Control	BM-1	BM-2	Requirements
Pb	4.5	4.5	4.5	-
Pb (virgin)	2.8	2.7	2.7	-
Pb (RAP)	1.7	1.7	1.7	-
Pa (additive)	0	0.1	0.1	-
Va	4.0	4.0	4.0	4.0
VMA	13.2	13.9	14.2	>13.0
VFA	69.5	71.0	71.8	65-78
DP	0.7	0.6	0.6	0.6-1.2
Pba	0.61	0.60	0.61	-
Pbe	3.92	3.93	3.91	-
Gmb	2.52	2.51	2.50	-
Gmm	2.63	2.61	2.60	-
% Gmm @ Nini	88.1	88.8	89.6	<90.5

2.2.3.5 Stiffness

Dynamic modulus testing was conducted in accordance with AASHTO TP79-15, using a UTM 25 machine in stress control mode to quantify the stiffness behavior of asphalt mixtures. Five replicate specimens at 7.0 ± 0.5 % air void from each group were tested at three temperatures (4, 21, and 37°C) and nine frequencies (25, 20, 10, 5, 2, 1, 0.5, 0.2, and 0.1 Hz) at each temperature. The strain level ranged between 70 and 100 micro strains for all specimens. The $|E^*|$ master curves were constructed by fitting the $|E^*|$ values at the aforementioned temperatures and frequencies to the Sigmoidal function given in Equation 2.3.

$$\text{Log } |E^*| = a + \frac{b}{1 + \frac{1}{e^{d+g \cdot \log f_R}}} \quad \text{Equation 2.3}$$

Where f_R is the reduced frequency, a is the minimum value of $|E^*|$, $a+b$ is the maximum value of $|E^*|$, and d and g are the fitting coefficients of the sigmodal model.

The shift factors were calculated using a second order polynomial function given in Equation 2.4 (Varma, Kutay et al. 2013).

$$\log(a_T(T)) = a_1 T^2 + a_2 T + a_3 \quad \text{Equation 2.4}$$

where a_1 , a_1 , and a_1 are fitting coefficients.

2.3 Results and discussions

2.3.1 Binder evaluation

Because asphalt binder is known as a viscoelastic material, rheological measurements of asphalt binders are of paramount importance to properly characterize their behavior at various temperatures and loading conditions. Rheological measurements are presented here in terms of performance grading, $|G^*|$ master curves, and black space diagrams.

2.3.1.1 Performance grading

The performance grade of the binder blends was determined in accordance with AASHTO M320. The results including the critical high, intermediate, and low failure temperatures as well as performance grades are summarized in Table 2.3. Since the RAP binder was recovered from RAP materials with a service life over 10 years, the critical high temperature was measured according to the Superpave specifications for RTFO-aged binders. Also, when tested for low failure temperatures, the RAP binder failed the BBR criteria for m-value at 0°C (0.298), and since this test procedure is recommended for testing the flexural creep of asphalt binders below ambient temperature, the test was terminated at 0°C and the low-temperature PG grade was anticipated to be -4°C. The virgin binder was blended with the RAP binder and the resulting stiffness at the high, intermediate, and low temperatures was increased due to the introduction of the higher stiffness RAP binder. Compared to the control blend, the BM-1 additive maintained the high-temperature grade at the same level, while restoring the intermediate and low temperature grades to the same degree as the virgin binder. The BM-2 additive could also restore the low-temperature grade to the same degree as that of the control binder; however, it decreased the high-temperature grade by one grade. According to Glover (Glover, Davison et al. 2005), as the binder ages, it becomes more m-controlled for the low temperature grade. Table 3 indicates that the low-temperature grading even after 1 PAV was controlled by the m-value rather than the stiffness in all cases. In addition to the grading results, a recently introduced parameter by Anderson, ΔT_c , was also determined from the BBR results, as the difference between the continuous low temperature grade for stiffness and m-value as determined for 300 MPa and 0.30, respectively. ($\Delta T_c = T_{\text{cont, S}} - T_{\text{cont, m-value}}$). The ΔT_c parameter is temperature-independent and when it exceeds -5.0°C, the drop in the ductility of the

asphalt binder results in a loss of durability and an increased susceptibility to block cracking (Anderson, King et al. 2011).

Table 2.3 Summary of performance grading

Binder	DSR failure temperature (°C)			BBR failure temperature (°C)						Cont. Grade	PG
	Original (25mm)	RTFO-aged (25mm)	RTFO+PAV aged (8mm)	RTFO+1PAV (20hrs)			RTFO+2PAV(40hrs)				
				T _{cont} (°C) m-value	T _{cont} (°C) S	ΔT _c (°C)	T _{cont} (°C) m-value	T _{cont} (°C) S	ΔT _c (°C)		
RAP	-	99.4	36.5	>0	-8.3	>-8.3	-	-	-	99.4-NA	94-4
Fresh binder	68.1	67.3	23.9	-12.6	-15.6	-3.0	-8.8	-12.9	-4.1	67.3-22.6	64-22
Control	80.6	81.9	28.7	-7.5	-11.6	-4.1	-3.2	-10.7	-7.5	80.6-17.5	76-16
BM-1	77.2	76.9	25.2	-12.1	-14.6	-2.5	-7.8	-14.5	-6.7	76.9-22.1	76-22
BM-2	71.9	73.8	24.7	-12.3	-15.1	-2.8	-11.1	-15.0	-4.9	71.9-22.3	70-22

The ΔT_c parameters for 1PAV-aged (20 hours) binders indicate that the addition of BM-1 and BM-2 has improved the ductility and relaxation properties, as compared to the control blend. To further evaluate the ΔT_c parameter, the blends were PAV-aged for 40 hours. A decrease in the ΔT_c parameter after 40 hours of long-term aging is obvious due to the significant oxidation and loss of relaxation properties. However, the BM-2 blend still showed a close ΔT_c value to -4.9 after the 40-hour aging, and therefore appears to possess a very high resistance to block cracking.

2.3.1.2 |G*| master curves

Master curves for complex shear moduli can be constructed using the time-temperature superposition principle to analyze the viscoelastic data obtained from asphalt binder specimens tested by means of the DSR instrument. The time-temperature superposition principle can relate the rheological behavior to the time of loading by shifting the data at all testing temperatures to a

reference temperature, thus obtaining a single smooth curve for $|G^*|$ with respect to temperature and applied time of loading. In this research, $|G^*|$ master curves were plotted using both the sigmoidal function and the CAM model at a reference temperature of 70°C for the unaged and RTFO-aged binders, and 22°C for the RTFO+PAV aged binders. The sigmoidal function was originally developed for fitting the dynamic modulus of asphalt mixtures (Pellinen and Witczak 2002). However, the agreement of this model with the complex shear modulus of asphalt binders has been successfully investigated by many researchers (Yusoff, Jakarni et al. 2013, Podolsky, Buss et al. 2016, Elkashef, Podolsky et al. 2017). The CAM model is considered to be used in fitting $|G^*|$ master curves to represent undamaged material responses (Marateanu and Anderson 1996).

Using both the Sigmoidal model and CAM model, the $|G^*|$ master curves of the unaged, RTFO aged, and RTFO+PAV aged binders were constructed at a reference temperature of 70 °C and are presented in Figure 2.1, Figure 2.2, and Figure 2.3. Shift factors were calculated using the Williams-Landel-Ferry (WLF) function given in Equation 2.5.

$$\log a_T = -\frac{C_1(T-T_0)}{C_2+(T-T_0)} \quad \text{Equation 2.5}$$

In order to check whether the differences between the measured and predicted complex modulus values from the two models were significant, a statistical normality test was first conducted on the measurements. The Normality of the $|G^*|$ values obtained from both methods was examined and both the measured data and predicted data were found log-normally distributed. Figure 2.4 shows an example of checking the normality assumption by constructing a normal probability plot.

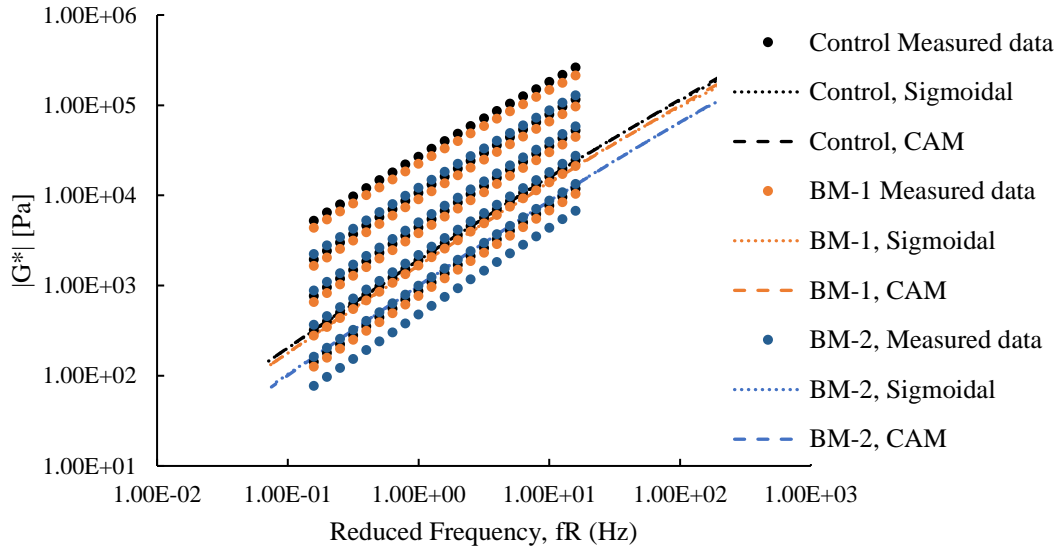


Figure 2.1 $|G^*|$ master curves for unaged binders at 70°C

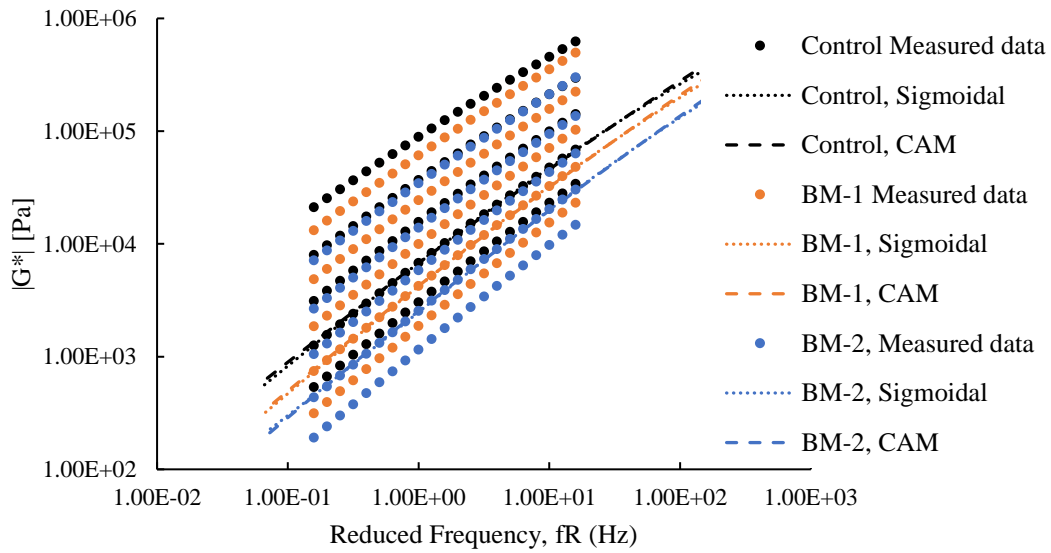


Figure 2.2 $|G^*|$ master curves for RTFO-aged binders at 70°C

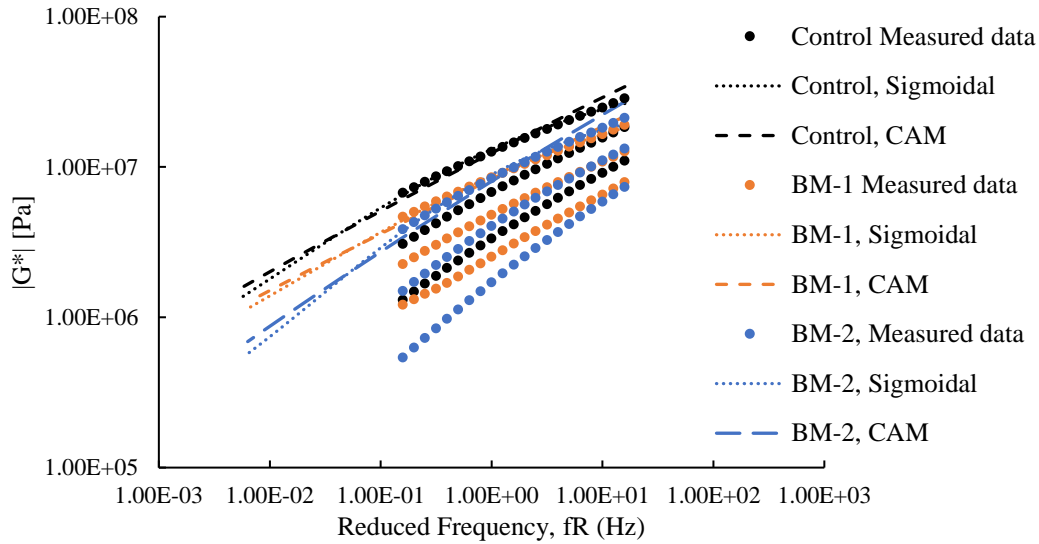


Figure 2.3 $|G^*|$ master curves for RTFO+PAV-aged binders at 22°C

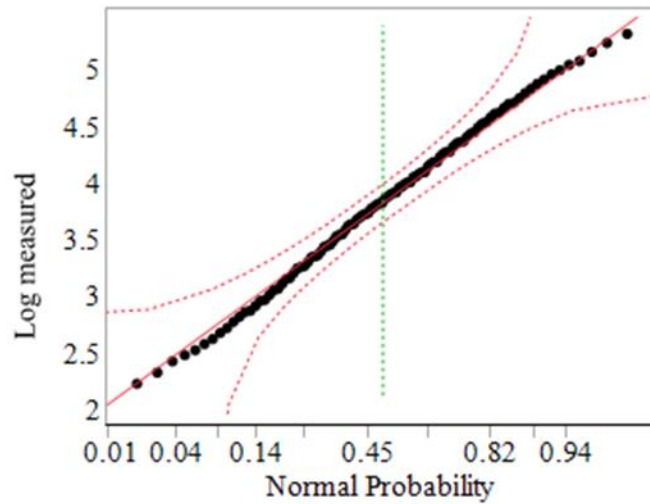


Figure 2.4 Normal quantile plot for the measured $|G^*|$

The normal probability plot allows to visually check whether the data distribution is normal. If the distribution is normal, the data points will fall along a straight line. The validity of this assumption can be furthermore evaluated by performing the Shapiro-Wilk W test on the null hypothesis where the data is from the normal distribution. P-values smaller than the level of significance (0.05) obtained from this test would reject the null hypothesis and indicate that the

data distribution is not normal at a 95% level of confidence. The p-values are presented in Table 2.4.

Table 2.4 Goodness-of-fit p-values from the normality test for measured and predicted $\log(|G^*|)$ values

	Measured			Sigmoidal model			CAM model		
	unaged	RTFO	RTFO+PAV	unaged	RTFO	RTFO+PAV	unaged	RTFO	RTFO+PAV
Control	0.612	0.500	0.230	0.582	0.452	0.130	0.679	0.656	0.784
BM-1	0.598	0.551	0.287	0.147	0.617	0.280	0.682	0.644	0.784
BM-2	0.621	0.577	0.129	0.597	0.492	0.055	0.666	0.672	0.746

To compare the predicted and measured values, the distribution of model errors defined as

$$e = \log|G^*|_{model} - \log|G^*|_{measured} \quad \text{Equation 2.6}$$

for each of the pairs should also be evaluated. Figure 2.5 shows an example of the normal probability plot for the errors, and goodness-of-fit p-values are given in Table 2.5. According to Table 2.5, the distribution of model errors was not normal in most cases and according to Figure 2.5, it appears that the tail data points contribute to this violation. Therefore, the Wilcoxon signed rank test appeared a reasonable tool for performing a pairwise comparison between the models and the measured data, as well as between the two models. The Wilcoxon signed rank test is a nonparametric matched paired test which can be used instead of the paired student t-test when the normality of the data is violated. Table 2.6 provides the p-values related to the paired comparison of measured data with each model. Since all p-values are greater than the level of significance, the null hypothesis remains true, and it can be concluded that both models could predict the $|G^*|$ values with no significant differences.

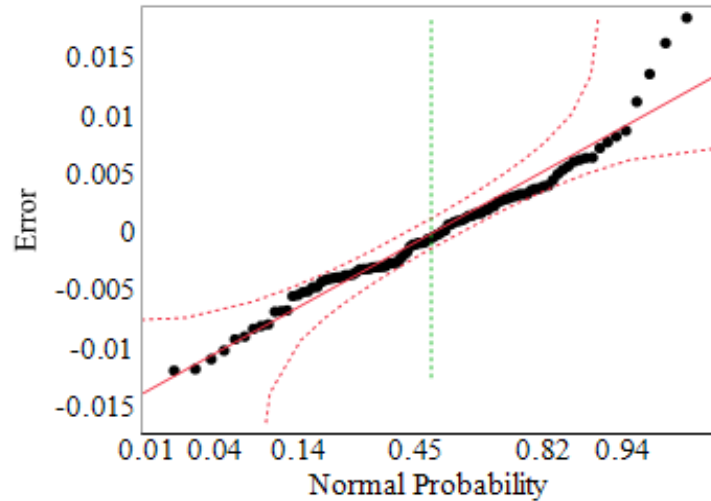


Figure 2.5 Normal quantile plot for the model error

Table 2.5 Goodness-of-fit p-values from the normality test for model errors

	Sigmoidal model error			CAM model error		
	unaged	RTFO	RTFO+PAV	unaged	RTFO	RTFO+PAV
Control	0.023	0.002	0.130	0.003	0.002	<0.0001
BM-1	<0.0001	0.001	0.006	0.002	0.137	0.063
BM-2	0.086	<0.0001	0.006	0.125	0.019	<0.0001

Table 2.6 Wilcoxon signed rank test p-values for the differences between each model and the measured values

	Sigmoidal model difference			CAM model difference		
	unaged	RTFO	RTFO+PAV	unaged	RTFO	RTFO+PAV
Control	0.853	0.492	0.930	0.644	0.406	0.210
BM-1	0.823	0.155	0.611	0.535	0.674	0.690
BM-2	0.480	0.865	0.271	0.789	0.593	0.360

At high temperatures, the results indicate that the addition of BM-1 and BM-2 have reduced the complex shear modulus of the control binder. The reduction in the dynamic modulus at high temperatures is more significant after short-term aging. The dynamic shear modulus at intermediate temperatures was also decreased due to the effect of the bio-materials. The comparison of the master curves at different aging conditions shows perfect overlap of the two models at unaged conditions, however, as the binders become more aged and stiffer, the

differences between the two models become more significant. To check whether the differences between the two models were significant, matched pairs were analyzed using the Wilcoxon signed rank test, and p-values are reported in Table 2.7. According to Table 2.7, no significant difference was observed between the two models at unaged conditions. However, after RTFO and PAV aging, significant differences were identified for the RTFO aged BM-2 binder, and for all the PAV aged binders. This trend is noticeable in Figure 2.3 where the master curves do not perfectly overlap compared to the unaged and RTFO aged conditions. This finding can be further evaluated by plotting the predicted $|G^*|$ values versus the measured values for the PAV aged binders and find the R^2 values. The higher the R^2 values, the better the correlation will be. The plots are provided in Figure 2.6 for the three binders. From Figure 2.6, it can be seen that the Sigmoidal model demonstrates better correlation with the measured data, however, according to Table 2.6 the better correlation for the Sigmoidal model does not mean that the CAM model provides predicted values that are statistically different from the measured values.

In addition to the comparison between the two rheological models, the two rejuvenated binders were also compared to the control group in terms of their complex shear modulus. Figure 2.1 shows that at high temperatures, the addition of BM-1 and BM-2 have reduced the complex shear modulus of the control binder. The reduction in the complex modulus at high temperatures is more significant after short-term aging. The dynamic shear modulus at intermediate temperatures was also decreased due to the effect of the bio-materials. Table 2.8 provides the results from conducting the Wilcoxon test on the pairs of control binder and each of the rejuvenated binders. Although the BM-1 binder has slightly lower $|G^*|$ values than the control binder at unaged conditions according to Figure 2.1, however the differences are detected significant through the statistical test results. Small p-values listed in Table 2.8 indicate that regardless of the aging

condition, the two bio-rejuvenators could significantly lower the stiffness of the control binder at high and intermediate temperatures. It should be noted that the only factor of interest in the statistical analyses was the effect of the bio-rejuvenators on lowering the stiffness of the control binder, and the effect of other variables such as curing temperature or the blending procedure was assumed negligible in this research.

Table 2.7 Wilcoxon signed rank test p-values for the differences between the two models

	unaged	RTFO	RTFO+PAV
Control	0.240	0.718	0.018
BM-1	0.150	0.163	<0.0001
BM-2	0.366	0.026	<0.0001

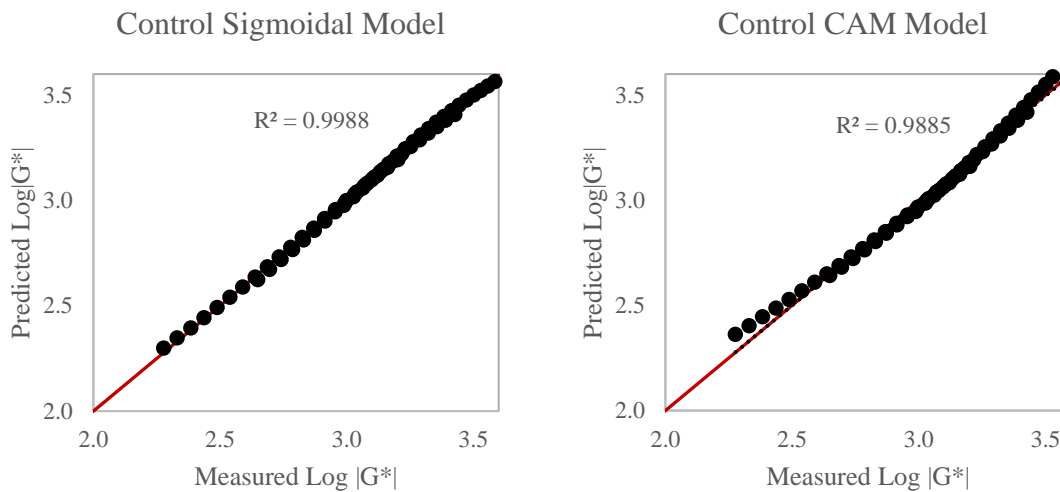


Figure 2.6 Comparison between measured and predicted $|G^*|$ for RTFO+PAV aged binders

2.3.1.3 Black space diagrams

In addition to G^* master curves, Black Space diagrams were constructed for the binders. Black Space diagrams are found to be a very useful method as they are not related to temperature and frequency, and the data needed for a master curve is directly analyzed with no mathematical shift required to account for time-temperature superposition (TTS) (King, Anderson et al. 2012). Black space diagrams are also useful tools to verify that the binders' behavior under loading is in the linear viscoelastic region (Marasteanu 2000). Figure 2.7 presents the plots of $|G^*|$ versus phase angle (δ) for the unaged, RTFO aged, and the PAV+RTFO aged. As seen earlier in Figure 2.1 and Figure 2.2, the difference in the dynamic modulus of the RTFO-aged binders was more significant than those of the unaged binders. This trend can also be seen in the Black Space diagrams. It is clear that after both short-term and long-term aging, the Black Space diagrams of the modified binders have shifted slightly to the right of the control binder, indicating greater phase angles at all stiffness levels. At the intermediate temperatures (10°C and 16°C), the long-term aged binders show discontinuities in their Black Space diagram, indicating the likelihood of thermal instability. This instability at very low strain rates after PAV aging can be attributed to the oxidation process and formation of asphaltenes which are less soluble in the matrix. Airey (Airey 2002) has also recommended that for binders having complex modulus values greater than approximately 30 MPa, other testing methods such as transient tests by a BBR should be used rather than an oscillatory test. This recommendation can be verified in Figure 2.7 where the discrepancies in the rheological data occur at complex modulus values greater than 30 MPa. Therefore, the DSR readings at the two lowest temperatures (10°C and 16°C) were discarded for construction of the master curves.

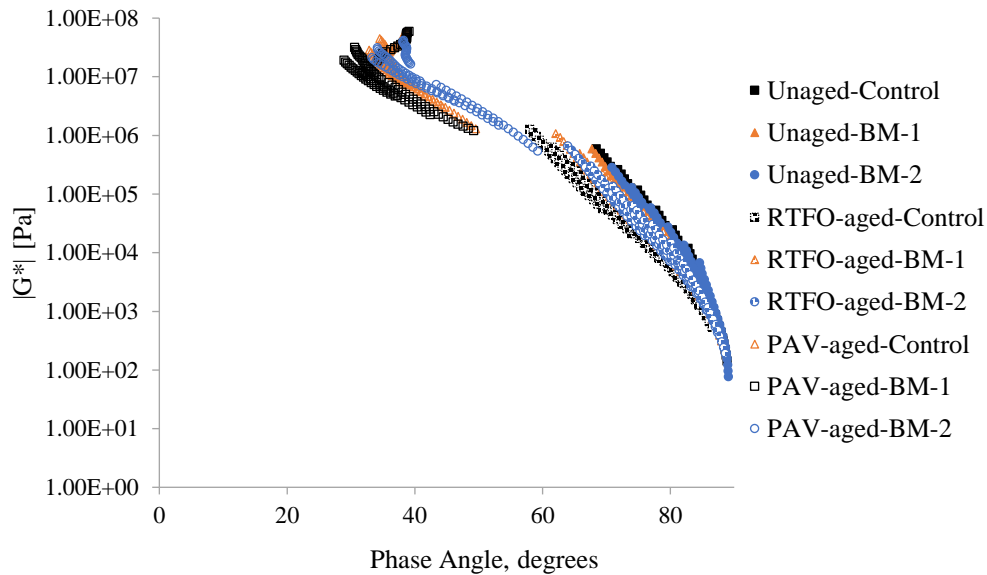


Figure 2.7 Black Space diagrams for unaged, RTFO-aged, and PAV-aged binders

2.3.2 Mixture evaluation

2.3.2.1 Dynamic modulus

Dynamic modulus testing was conducted on cylindrical specimens fabricated according to AASHTO TP79 to evaluate the stiffness of the lab-produced and plant-produced asphalt mixtures. In this test, a uniaxial sinusoidal compressive stress is applied to the test specimen, and the relationship between the maximum dynamic stress and the peak recoverable axial strain is defined as the dynamic modulus, $|E^*|$. Data were collected over a range of appropriate temperatures (4, 21, and 37°C) and frequencies (25, 20, 10, 5, 2, 1, 0.5, 0.2, and 0.1 Hz) to construct the master curves. A standard reference temperature of 21°C was then selected to shift the data at all temperatures with respect to time of loading. The dynamic modulus master curves of the mixtures after short-term aging are shown in Figure 2.8. As illustrated in Figure 2.8, the control mixture lies above the other two mixtures especially at higher temperatures and lower frequencies. At low temperatures (4°C), the differences between the $|E^*|$ values are lower than that of intermediate and high temperatures and the curves are closer to each other. To check whether these measurements are

significantly different at low, intermediate, and high temperatures, a statistical analysis similar to that conducted on the binders was performed with $\alpha=0.05$. For this purpose, the normality of the distribution of the data was first verified and all the goodness-of-fit p-values were greater than 0.05. Since the data was normally distributed, the paired student t-test was conducted, and the p-values are reported in Table 2.9 a, Table 2.9 b, and Table 2.9 c.

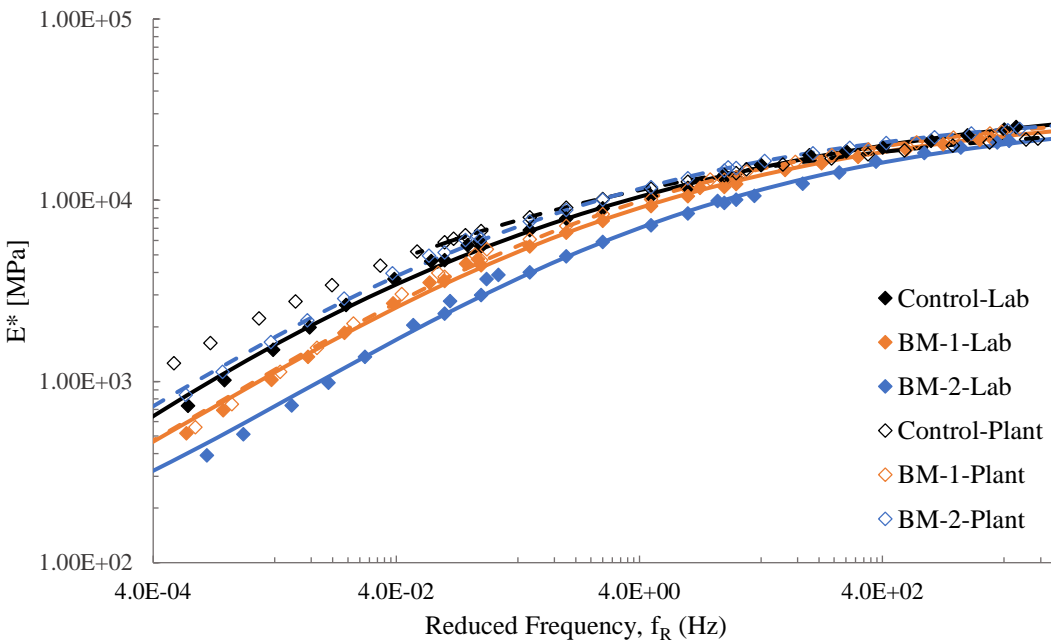


Figure 2.8 $|E^*|$ master curves for asphalt mixtures at 21°C reference temperature

At low temperatures referred to as high stiffness conditions, the BM-1 mixture performed statistically similar to the control mixture as the p-value was greater than α (0.63). However, the BM-2 mixture showed significantly higher $|E^*|$ values according to the p-value of 0.0003. At intermediate temperatures (21°C), the BM-2 mixture did not have any significant difference with the control mixture, while the BM-1 mixture exhibited lower $|E^*|$ values. At high temperatures (37°C), all pairs showed p-values smaller than α , indicating that the two bio-rejuvenators could significantly reduce the stiffness. The comparison between the lab-produced mixtures indicate that

the two rejuvenated mixtures had significantly lower $|E^*|$ values compared to the control mixture as the p-values are smaller than α . These findings demonstrate that the addition of BM-1 and BM-2 was able to lower the stiffness of the high RAP mixtures specially at high temperatures. Another conclusion from these findings is that mixtures can exhibit significantly different behaviors depending on the location where they have been produced.

Table 2.9 a P-values from statistical comparison of the dynamic modulus test results at 4°C

	Control, Plant	BM-1, Plant	BM-2, Plant	Control, Lab
Control, Lab	0.041			
BM-1, Lab		<0.0001		<0.0001
BM-2, Lab			<0.0001	<0.0001
Control, Plant		0.63	0.0003	

Table 2.9 b p-values from statistical comparison of the dynamic modulus test results at 21°C

	Control, Plant	BM-1, Plant	BM-2, Plant	Control, Lab
Control, Lab	<0.0001			
BM-1, Lab		0.0002		<0.0001
BM-2, Lab			<0.0001	<0.0001
Control, Plant		<0.0001	0.805	

Table 2.9 c p-values from statistical comparison of the dynamic modulus test results at 37°C

	Control, Plant	BM-1, Plant	BM-2, Plant	Control, Lab
Control, Lab	<0.0001			
BM-1, Lab		0.0003		<0.0001
BM-2, Lab			0.0004	<0.0001
Control, Plant		<0.0001	<0.0001	

In addition to $|E^*|$ master curves, black space diagrams were also constructed for the mixtures to evaluate the relationship between the dynamic modulus values and the phase angles regardless of their dependency on the frequency and temperature. The black space diagram also allows an estimate of the glassy modulus of the mixtures at the phase angle of 0°C. Figure 2.9 presents the Black Space diagrams of the mixtures after short-term aging. The graph shows that a

minor discontinuity appeared in the mixtures at the intermediate temperature (21°C) and a low frequency (<0.2). At high temperatures and $|E^*|$ values of approximately 1000 MPa, the mixtures show a maximum phase angle value of 32°, and then the phase angle decreases as the $|E^*|$ decreases. This behavior can be due to the strong influence of the aggregate skeleton as there are no differences in the aggregate gradation between the three mixtures.

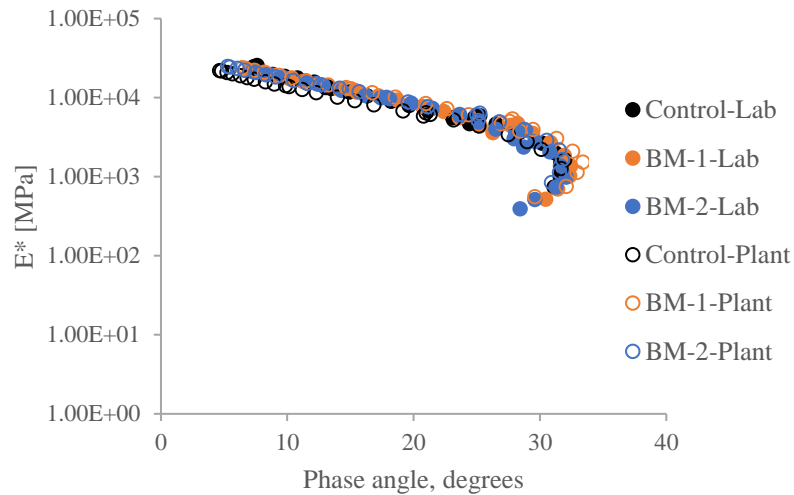


Figure 2.9 Black Space diagram for the mixtures

2.4 Conclusions

The potential utilization of a crude tall oil-derived bio-additive (BM-1) and a soybean-derived bio-material (BM-2) as rejuvenators in the production of asphalt mixtures with 50% RAP content was evaluated in this paper. BM-1 was added to the RAP by 6% of the RAP binder content, while BM-2 was added by 3% of the total binder content. The key findings of this research are summarized as follows:

- Compared to the control blend with no additive, the BM-1 additive could maintain the high-temperature grade at the same level, while restoring the low-temperature properties by one grade. The BM-2 additive also, could restore the low-temperature grade to the same

degree as that of BM-1, however, it decreased the high-temperature properties by one grade. The ΔT_c parameters for 1PAV-aged (20 hours) binders indicated that the addition of BM-1 and BM-2 can significantly improve the relaxation properties of the aged RAP binders.

- The main conclusion of this research is that high amounts of RAP could be incorporated in asphalt mixtures provided that appropriate additives are selected to rejuvenate the aged RAP binder and restore its rheological properties while providing mixtures with enhanced properties.
- The addition of small amounts of these two bio-materials to the 50% RAP mixtures resulted in lower stiffness values at intermediate and high temperatures for the unaged and aged binders.
- Both the CAM and Sigmoidal models could be successfully used to predict the $|G^*|$ values and construct the master curves of the unaged and aged binders with no significant differences detected between the measured and the predicted values.
- Statistical analysis on the dynamic modulus measurements conducted on lab-produced, lab-compacted and plant-produced, lab-compacted specimens revealed significant differences between the rejuvenated mixtures and the control mixture, leading to the conclusion that mixing and compaction of lab and plant produced mixtures can significantly influence the stiffness characteristics.

2.5 References

Airey, G. D. (2002). "Use of black diagrams to identify inconsistencies in rheological data." *Road Materials and Pavement Design* 3(4): 403-424.

Al-Qadi, I. L., et al. (2007). Reclaimed asphalt pavement—a literature review, report no. FHWA-ICT-07-001. Rantoul, IL: Illinois Center for Transportation.

Anderson, R. M., et al. (2011). "Evaluation of the relationship between asphalt binder properties and non-load related cracking." *Journal of the Association of Asphalt Paving Technologists* 80, 615-664.

Asgharzadeh, S. M., et al. (2015). "Evaluation of rheological master curve models for bituminous binders." *Materials and Structures* 48(1-2): 393-406.

Barco Carrión, A. J. d., et al. (2017). "Linear viscoelastic properties of high reclaimed asphalt content mixes with biobinders." *Road Materials and Pavement Design* 18(sup2): 241-251.

Blanc, J., et al. (2019). "Full-scale validation of bio-recycled asphalt mixtures for road pavements." *Journal of cleaner production* 227: 1068-1078.

Chailleux, E., et al. (2017). "BioRePavation: innovation in bio-recycling of old asphalt pavements: towards safe cost effective renewable pavement". *AAPA International Flexible Pavements Conference*, 17th, 2017, Melbourne, Victoria, Australia.

Copeland, A. (2011). "Reclaimed asphalt pavement in asphalt mixtures: State of the practice" (no. FHWA-HRT-11-021). Washington, DC: Federal Highway Administration. Office of Research, Development, and Technology

Elkashef, M., et al. (2017). "Preliminary examination of soybean oil derived material as a potential rejuvenator through Superpave criteria and asphalt bitumen rheology." *Construction and Building Materials* 149: 826-836.

Glover, C. J., et al. (2005). "Development of a new method for assessing asphalt binder durability with field validation." Texas Dept Transport 1872.

Inc, S. I. (1989-2019). JMP, Version Pro 13. Cary, NC, SAS Institute Inc. .

Kandhal, P. S. and R. B. Mallick (1998). Pavement recycling guidelines for state and local governments participant's reference book (no. FHWA-SA-98-042). Washington, DC: Federal Highway Administration.

Karlsson, R. and U. Isacsson (2006). "Material-related aspects of asphalt recycling—state-of-the-art." *Journal of Materials in Civil Engineering* 18(1): 81-92.

King, G., et al. (2012). "Using black space diagrams to predict age-induced cracking". *7th RILEM International Conference on Cracking in Pavements, Springer*: 453-463

Marasteanu, M. O. (2000). "Interconversions of the linear viscoelastic functions used for the rheological characterization of asphalt binders." (Thesis in Civil Engineering). Pennsylvania State University.

Marasteanu, M. and D. Anderson (1996). "Time-temperature dependency of asphalt binders--An improved model (with discussion)." *Journal of the Association of Asphalt Paving Technologists* 65.

McDaniel, R. S., et al. (2000). "Recommended use of reclaimed asphalt pavement in the Superpave mix design method." *NCHRP Web document* 30.

Pellinen, T. and M. Witczak (2002). "Stress dependent master curve construction for dynamic (complex) modulus (with discussion)." *Journal of the Association of Asphalt Paving Technologists* 71.

Pellinen, T. K., et al. (2004). "Asphalt mix master curve construction using sigmoidal fitting function with non-linear least squares optimization". *Recent advances in materials characterization and modeling of pavement systems*: 83-101.

Podolsky, J. H., et al. (2016). "Effects of aging on rejuvenated vacuum tower bottom rheology through use of black diagrams, and master curves." *Fuel* 185: 34-44.

Porot, L. and W. Grady (2016). "Effectiveness of a bio-based additive to restore properties of aged asphalt binder". *ISAP Symposium*.

Roberts, F. L., et al. (1991). "Hot mix asphalt materials, mixture design and construction." Lanham, MD: National Asphalt Pavement Association.

Tran, N., et al. (2017). "Effect of rejuvenator on performance characteristics of high RAP mixture." *Road Materials and Pavement Design* 18(sup1): 183-208.

Tran, N. H., et al. (2012). "Effect of rejuvenator on performance properties of HMA mixtures with high RAP and RAS contents." NCAT Report: 12-05.

Turner, P., et al. (2015). Laboratory evaluation of SYLVAROADTM RP 1000 rejuvenator, Draft NCAT Report, Auburn, AL.

Varma, S., et al. (2013). "Viscoelastic genetic algorithm for inverse analysis of asphalt layer properties from falling weight deflections." *Transportation Research Record: Journal of the Transportation Research Board*, 2369: 38-46.

Yu, X., et al. (2014). "Rheological, microscopic, and chemical characterization of the rejuvenating effect on asphalt binders." *Fuel*, 135: 162-171.

Yusoff, N. I. M., et al. (2013). "Modelling the rheological properties of bituminous binders using mathematical equations." *Construction and Building Materials*, 40: 174-188.

Zaumanis, M. and R. B. Mallick (2015). "Review of very high-content reclaimed asphalt use in plant-produced pavements: state of the art." *International Journal of Pavement Engineering* 16(1): 39-55.

CHAPTER 3 EFFECT OF HIGH RAP AND TWO NOVEL BIO-BASED REJUVENATORS ON THE LOW AND INTERMEDIATE TEMPERATURE PROPERTIES OF ASPHALT BINDERS AND ASPHALT MIXTURES

Modified from a manuscript under review International Journal of Fatigue

Zahra Sotoodeh-Nia^a, Nick Manke^a, R. Christopher Williams^a, Eric W. Cochran^b, Laurent Porot^c, Emmanuel Chailleux^d, Davide Lo Presti^e, Ryan Boysen^f, Jean-Pascal Planche^f

Abstract

With the purpose of improving the sustainability in the pavement industry, the use of high percentages of reclaimed asphalt pavement (RAP) coupled with softening agents and/or rejuvenators has gained a lot of attention recently. However, most of the rejuvenating agents are based on crude oil. In this study, performance characteristics of hot mix asphalt (HMA) containing 50% RAP and two novel bio-rejuvenators were evaluated. The HMA was produced in two different locations: in the laboratory and at an asphalt plant and compacted in the laboratory. The study demonstrated that compared to two control mixes and their corresponding binder blends with no rejuvenator, addition of the two bio-rejuvenators played a significant role in restoring the mechanical properties of the mixtures, and the rheological properties of the binders. The recycling agents must have compatibility with the base binder to prevent precipitation or flocculation of the binder fractions. The compatibility of the recycling agents with the binders was evaluated through differential scanning calorimetry (DSC) curves. The rejuvenators and the fresh and RAP binders were found to be compatible in the blend. Even after 40hrs of PAV aging, the rejuvenated binders still showed great resistance to block cracking as determined through the Glover-Rowe parameter.

^a Department of Civil, Construction, and Environmental Engineering, Iowa State University, Ames, Iowa, 50011-3232.

^b Department of Chemical and Biological Engineering, Iowa State University, Ames, Iowa, 50011-3232.

^c Kraton Chemical B.V, Almere, Netherlands.

^d LUNAM Université, IFSTTAR, Bouguenais, France.

^e Nottingham Transportation Engineering Centre, University of Nottingham, Nottingham, UK.

^f Western Research Institute, Laramie, Wyoming

Linear amplitude sweep (LAS) test results indicated significant improvement in fatigue life of the rejuvenated binders. A statistical comparison between the disk-shaped compact tension (DCT) results revealed that the lab-produced rejuvenated mixtures had significantly improved fracture energy compared to the lab control mixture. While the plant-produced mixtures showed greater fracture energy than the control mixture, no significant difference was found between the three groups. The fatigue properties of the mixtures were evaluated based on load cycles to failure and plateau values obtained from the ratio of dissipated energy change (RDEC) approach and it was concluded that although inclusion of rejuvenators improved the fatigue life of binders, however, the fatigue life of asphalt mixtures was not improved as much.

3.1 Introduction

The current state of the nation's infrastructure coupled with limited federal and state funding available has led the paving industry towards reducing costs by means of using recycled materials. While the concept of using recycled materials in paving is not new, the desire for an increased use of recycled materials in paving has substantially increased in recent times for two major reasons. The first reason is cost. As reported in a report by the FHWA and article by Haghshenas et al., the largest cost (upwards of 70 percent) of hot mix asphalt (HMA) paving is associated with materials (Copeland 2011, Haghshenas, Nabizadeh et al. 2016). Materials used in HMA paving include aggregates, asphalt cement binder, fillers, and modifiers where applicable. Considering that the vast majority of the nation's roadways are paved with asphalt mixtures, such material costs add up rapidly. To reduce cost, recycled materials such as RAP can be utilized to replace a portion of the required virgin (newly quarried) aggregates and asphalt binder since RAP contains both aggregates and asphalt binder.

The second reason for increasing RAP contents in paving pertains to the relatively new push for more environmentally-friendly and sustainable infrastructure. The use of RAP not only greatly reduces emissions associated with aggregate and binder production as well as material transport, but it also prevents millions of tons of HMA pavement from being used in lower value applications. While on the surface it seems prudent to use 100 percent RAP mixtures for paving nationwide, there remains many obstacles to why this is not the case currently.

RAP contains aged binder and thus, the inclusion of RAP in significant amounts can potentially adversely affect pavement performance and material characteristics. Recycled asphalt pavement materials contain nonhomogeneous characteristics in many scenarios in addition to being aged. Aged bituminous materials are oxidized and polymerized which result in a chemical alteration of molecular ratios. After extensive aging, asphalt binders contain a greater ratio of heavier, more rigid, molecular chains as compared to lighter molecules that act as lubricants within the flexible pavement system. The culmination of such effects is that the recycled material is stiffer and more brittle than their unaged elastic counterparts. A potential key to modifying RAP material and allow higher RAP contents in paving nationwide may be the use of rejuvenators. Rejuvenators are used to aid in restoring aged asphalt binders by changing chemical and physical properties of the aged binder. Essentially, rejuvenators reverse some of the aging effects on a binder if used properly. They do this by restoring the ratio of large to small molecules (asphaltenes/maltenes) which in turn lowers the aged binder viscosity and restores some elasticity (Haghshenas, Nabizadeh et al. 2016). By restoring and replacing some of the oxidized and polymerized asphalt molecules and volatilized light ends, rejuvenators not only make RAP material easier to mix and compact but also improve the cracking resistance of pavements incorporating RAP (Zaumanis, Mallick et al. 2014, Haghshenas, Nabizadeh et al. 2016).

Recently, several studies have used different rejuvenators to assess their viability of improving the rheological properties of RAP binders (Zaumanis, Mallick et al. 2014, Barco Carrión, Lo Presti et al. 2017, Borghi, Jiménez del Barco Carrión et al. 2017, Elkashef, Podolsky et al. 2017, Elkashef, Podolsky et al. 2017, Elkashef and Williams 2017, Porot, Broere et al. 2017, Tran, Taylor et al. 2017). There are many different rejuvenators available in today's market. Rejuvenators can be applied separately to the RAP or fluxed with virgin binder or other softening agents. While each rejuvenator seeks the same goals, they have a wide range of chemical properties, prescribed dosages, and origins. Some rejuvenators are derived from petroleum products while others are recycled waste products and co-products of manufacturing and food production operations. Still others are derived from bio-products for an even greater level of sustainability in paving. Many bio-agents (bio-rejuvenators) work in two stages. The first stage of the rejuvenator lowers the viscosity of the aged binder while the second stage polymerizes the binder to restore the binder stiffness after paving (Kowalski, Król et al. 2016). These multi-stage rejuvenators alter RAP physical characteristics to preferentially favor workability during mixing and construction and stiffness in situ to combat rutting after placed and compacted. Before using any rejuvenator in the production of high RAP asphalt mixtures, the compatibility of the rejuvenator with the base binder and the aged RAP binder must be verified to prevent the precipitation or flocculation of the asphaltene fractions in the binder. This can be done by using a differential scanning calorimetry (DSC) and study the thermal behavior of asphalt binders, as well as determining the glass transition temperatures, and evaluating the compatibility of the recycling agents with asphalt binders. Cucalon et al. investigated the effect of rejuvenation and aging process on recycled binder. Their research covered a range of virgin binders, as well as rejuvenated binders

and led to the conclusion that the glass transition temperature was significantly reduced when rejuvenators were introduced to the binder blends (Garcia Cucalon, King et al. 2017).

While several agencies are wary in allowing rejuvenators in flexible pavement designs incorporating high RAP contents, this paper seeks to provide evidence that the flexible pavements containing rejuvenated high RAP contents perform well in accordance with fracture resistance criteria and fatigue criteria. Such performance criteria are important in assessing a mixture's long-term stability and wear resistance against distresses such as low-temperature cracking and fatigue cracking. Since the level of improvement in the performance of the rejuvenated binders is also of great importance, assessment of their rheological properties is also provided in this paper. Therefore, the main objectives of this study can be summarized as follows.

- Incorporate pre-determined dosages of two bio-based rejuvenators in a blend of fresh binder and RAP binder as well as two control mixtures.
- Investigate the compatibility of the rejuvenators with the base binder and RAP binder.
- Evaluate the ductility of the rejuvenated binders and their resistance to fatigue cracking.
- Obtain lab-produced and plant-produced mixtures and compact them using a gyratory compactor in the lab.
- Measure the DCT fracture energy and fatigue cracking resistance in accordance with AASHTO/ASTM standards.

3.2 Experimental Plan

3.3.1 Materials

The EIFFAGE Company provided the virgin binder as well as the virgin aggregates and the RAP materials. The virgin binder was a 50/70 penetration grade binder which later in the study

was graded as a PG 64-22 binder according to Superpave specifications. The virgin aggregates were delivered in three different sizes: coarse aggregate (10/14 mm), fine aggregate (0/2 mm), and filler. RAP was fractionated into two sizes: coarse RAP (8/12mm) and fine RAP (0/8mm).

The first bio-based rejuvenator was provided by the Kraton Company and is called SYLVAROAD™ RP1000. It is a pine chemical derived from crude tall oil, which is a co-product of the paper industry. This product has been found as a promising rejuvenator in past studies (Turner, Taylor et al. 2015, Chailleux, Bessman et al. 2017, Porot, Broere et al. 2017, Tran, Taylor et al. 2017), and is coded as BM-1 in this study.

The second bio-based rejuvenator used in this study was provided by ADM Company and is called epoxidized methyl soyate (EMS). EMS is a product of esterification and epoxidation of soybean oil and is highly competitive in cost relative to petroleum-based additives. This rejuvenator is coded as BM-2 in this study.

These two bio-rejuvenators not only differ by their molecular structure, but also by their working mechanism and interactions with asphalt binder; therefore, they are not considered as direct competitors in this study and are only compared with the control group composed of no rejuvenators. Also, it should be noted that these products are made from non-food source oil and are co-products thus, do not compete with the food chain.

3.3.2 Extraction and recovery

ASTM D2172 and ASTM D7906 were followed to extract the RAP binder from the two RAP fractions and recover the binder from solution by means of a rotary evaporator. The rheological properties of the recovered RAP binder were then evaluated using DSR and BBR instruments. After recovering the binder, RAP binder content was determined as shown in Table 3.1.

Table 3.1 Binder contents of the fractionated RAP

Fraction	Coarse RAP	Fine RAP
Binder content (%)	2.9	4.4

3.3.3 Mix design

One group of asphalt mixtures were mixed and compacted in the lab, while the other group were mixed at the plant and compacted in the lab. The control group of lab-produced mixtures had the same gradation and mix design as the rejuvenated groups (GB5), while the control group of the plant-produced mixtures had a different gradation and mix design (EME2). The GB5 mix design proportion and the two different gradations are shown in Table 3.2 and Figure 3.1, respectively. The GB5 mix design was proposed based on an optimization process in which the goal was to achieve void contents in the range of 3.0-4.5% with 100 number of gyrations (Olard and Pouget 2015, Pouget, Olard et al. 2016). The EME2 mix design was developed in France and has been used for over 30 years ago and is worldwide known as a high modulus mix design. The 20% RAP content chosen proposed for this control group is the typical percentage of RAP practically used in France. The nominal maximum aggregate size (NMAS) for all lab-produced mixtures and plant-produced mixtures except the control plant-produced mixture which was a 19.0 mm dense-graded mixture. The NMAS for plant control mixture was determined to be 12.5 mm. Note that according to the mix design in Table 3.2 and the RAP binder contents determined in Table 3.1, 50% RAP materials in the asphalt mixture introduces 37.6% RAP binder to the total binder content. Therefore, to evaluate the binders, the following proportions listed in Table 3.3 were used and blended.

Table 3.2 Mix design proportions

Fraction	Virgin Aggregate			RAP		Virgin binder + rejuvenator
	10/14 mm	0/2 mm	Filler	RAP 8/12mm	RAP 0/8mm	
% in mix	37.2	7.7	2.3	34.0	16.0	2.8

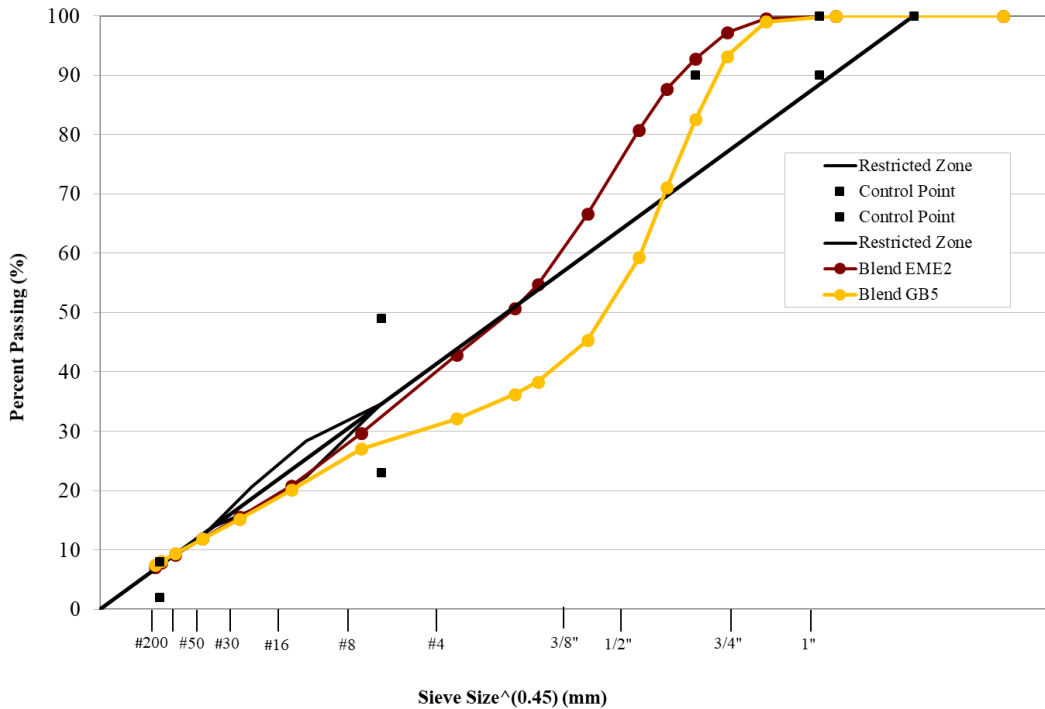


Figure 3.1 Mix design gradations

Table 3.3 Proportions of fresh binder, RAP binder, and the rejuvenators

Groups	% in total binder		
	RAP binder	Virgin binder	Rejuvenator
Control	37.6	62.4	None
BM-1	37.6	60.1	2.3
BM-2	37.6	59.4	3.0

3.3.4 Testing plan

The testing plan of this study is shown in Figure 3.2. First, the compatibility of the rejuvenators with the RAP binder and the virgin binder was evaluated through DSC measurements. The ductility and resistance to block cracking of the binders was assessed through the Glover-Rowe

parameter. Also, the fatigue cracking resistance of the binders was evaluated by conducting the linear amplitude sweep (LAS) test on the aged binders. Next, the performance of the corresponding mixtures was evaluated with disc-compact tension (DCT) and flexural beam fatigue testing. All specimens were fabricated at the desired dimensions and air void content for each test. Prior to testing, bulk specific gravities (G_{mb}) of each of the specimens and maximum theoretical specific gravities (G_{mm}) were determined in accordance with AASHTO T331-13 and AASHTO T 209, respectively.

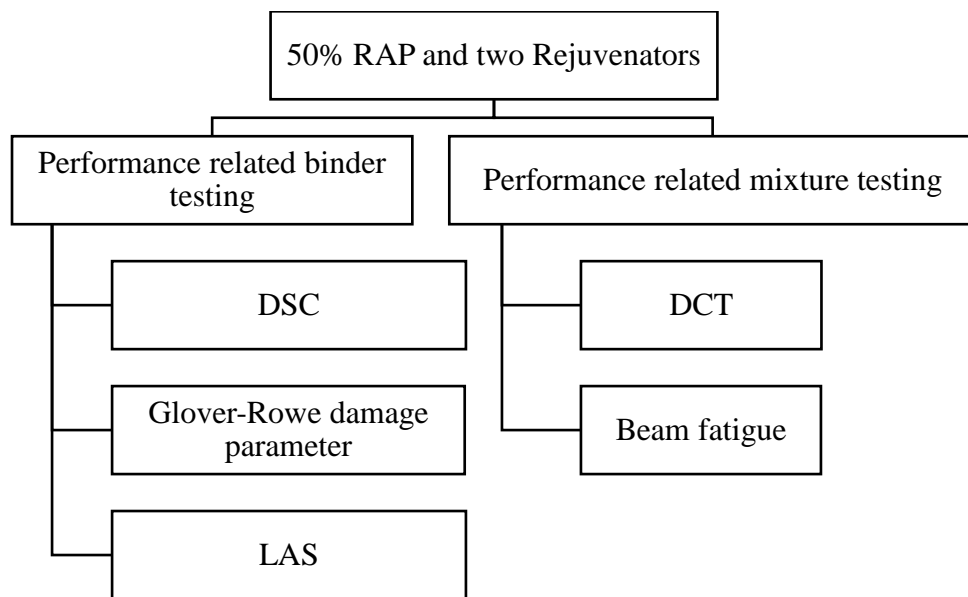


Figure 3.2 Testing plan

3.3.4.1 Rejuvenator compatibility

A TA Instruments Q2000 differential scanning calorimeter (DSC), equipped with a liquid nitrogen cooling system was used in this research. 7-10 mg of each binder as well as the rejuvenators were placed in standard hermetic aluminum pans. The samples were heated up to 100°C and underwent isotherm for 2 minutes. The samples were then quenched to -90°C at a rate of 3°C/minute. Data analysis was conducted using TA universal analysis software.

3.3.4.2 Glover-Rowe damage parameter

In order to investigate the effect of aging on the ductility of the binders, the Glover-Rowe (G-R) damage parameter tests were conducted. For this purpose, RTFO-aged binders were first subjected to 0, 20, 40, and 80 hours of PAV aging. Then, they were tested using the 8mm parallel plate geometry of a DSR, and their complex modulus and phase angles were measured. The G-R parameter is expressed in terms of G^* and δ , using Equation 3.1:

$$G - R = \frac{G^*(\cos \delta)^2}{\sin \delta} \quad \text{Equation 3.1}$$

Two critical values of this parameter, 180 kPa and 450 kPa, define two stages of damage as the onset of damage and significant cracking, respectively.

3.3.4.3 Binder fatigue properties

In addition to performance grading and stiffness evaluation, a DSR was used to conduct the linear amplitude sweep (LAS) test on the RTFO+PAV aged binders. Following AASHTO TP101, all binders were tested at the intermediate performance grade of the control blend for subsequent comparison. The LAS test is based on the definition of fatigue damage and consists of a series of cyclic loads at linearly increasing strain amplitudes from 0.1% to 30% at a constant frequency of 10 Hz. Prior to the LAS test, a frequency sweep test was also performed to obtain undamaged material properties, using a very low strain amplitude of 0.1%.

3.3.4.4 Mixture low-temperature cracking

The disc-shaped compact tension (DCT) test was conducted on the mixtures in accordance with ASTM D7313 to obtain fracture properties of the mixtures at low temperatures. Five replicates of each group were tested at -12°C which is 10°C higher than the low-temperature performance grade of the rejuvenated mixtures. The main results of interest from DCT test are the

fracture energy (G_f), the peak load, and crack mouth opening displacement (CMOD) of the specimens. Fracture energy can be computed by integrating the area under the curve obtained from plotting the applied load versus CMOD, normalized by the dimensions of the specimens. The fracture energy was then computed using Equation 3.2.

$$G_f = \frac{AREA}{B.(W-a)} \quad \text{Equation 3.2}$$

where:

G_f = fracture energy (J/m^2);

AREA= area under load-CMOD curve;

B= specimen thickness (m); and

W-a= initial ligament length (m).

3.3.4.5 Mixture Fatigue cracking

Several test methods can be utilized to characterize the fatigue behavior of asphalt mixtures. In this research, asphalt mixture beam specimens were subjected to repeated flexural bending load in accordance with AASHTO T321. Testing was conducted at controlled-strain mode and three different levels of stain (300, 600, and 1000 μs). The flexural stiffness and number of load cycles were recorded. The test was terminated when the flexural stiffness reduced from the initial value, as measured at the 50th load cycle, by 50 percent.

3.3 Results and discussion

3.4.1 Rejuvenator compatibility

The compatibility of the rejuvenators with the base binder can be evaluated through plots of heat capacity versus temperature when they are tested in a DSC instrument. From DSC test results, the glass transition temperature of the binders can also be determined. The glass transition temperature is related to the asphalt binder performance at low temperatures. Below the glass

transition temperature, the brittleness of the binder is extensively increased and the potential for stress relaxation is reduced (Velasquez, Tabatabaee et al. 2011). Figure 3.3 presents changes in the the heat flow curves of the binders caused by addition of the bio-rejuvenators.

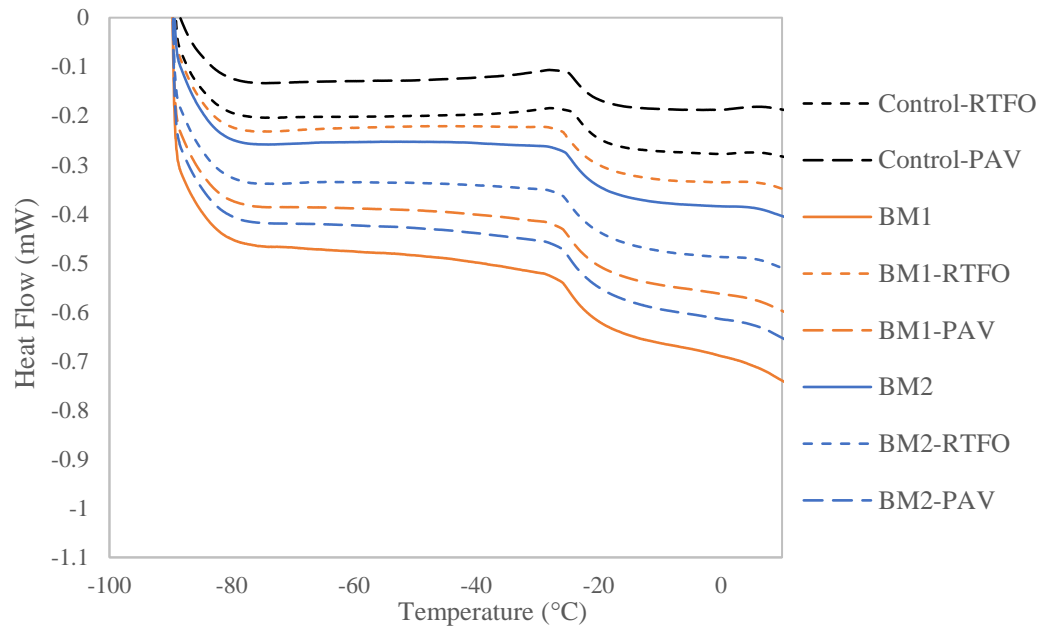


Figure 3.3 Heating curves obtained from DSC testing

The glass transition temperature of the binders was determined by calculating the inflection point on the curves, using TA Instruments' software. The T_g values of the rejuvenated binders were determined slightly lower than the T_g values of the control binder. A possible reason for this observation that the reductions were not significant could be that the glass transition behavior highly depends on the heating/cooling rates as well as the thermal program (modulated/standard) selected to study the heat flow (Kriz, Stastna et al. 2008). Compared to the rejuvenated blends, the control binder shows an exothermic flow before the glass transition region. This decrease in the heat flow could be due to crystallization of asphaltenes which have been polymerized during the pavement service life, and cause less interaction between the recycled binder and the fresh binder.

Therefore, it can be concluded that the inclusion of the these bio-based rejuvenators can possibly disaggregate the asphaltenes in the recycled binder and restore the balance between the maltene and asphaltene phases to some extent. The compatibility of the recycling agents with the base binders is usually determined by the number of distinct glass transition temperatures that a blend exhibits. If multiple inflection points are detected, it is an indication that two or more separate amorphous phases exist in the blend (Song, Hourston et al. 1998, Huang, Qin et al. 2014). As illustrated in Figure 3.3, the presence of only one inflection point below 0°C verifies the compatibility of the rejuvenators with the binder.

3.4.2 Glover-Rowe damage parameter

The Glover-Rowe parameter was first introduced by Glover et al. to relate the ductility and age-related cracking of asphalt binders to their DSR measurements and track the pavement aging (Glover, Davison et al. 2005). To evaluate the ductility of the binders at different stages of aging, they were subjected to 0, 20, and 40 hours of PAV aging and their G^* and phase angle values were plotted in Black Space diagram Figure 3.4. Two failure curves corresponding to 5 cm ductility and 3 cm ductility are also shown in Figure 3.4. These two curves are plotted based on the equations related to damage onset and significant cracking, respectively:

$$|G^*|((\cos \delta)^2 / \sin \delta) = 180 \text{ kPa} \quad \text{Equation 3.3}$$

$$|G^*|((\cos \delta)^2 / \sin \delta) = 450 \text{ kPa} \quad \text{Equation 3.4}$$

The G^* and phase angle values are recommended to obtain at 15°C and loading rate of 0.005 rad/s, however, because testing at such a low rate of loading is time-consuming, testing was conducted at temperature ranges between 10°C and 34°C, and the results were fitted to a master curve at a reference temperature of 15°C using the Christensen-Anderson-Marasteanu (CAM) model. The $|G^*|$ and phase angle values corresponding to 0.005 rad/s were then obtained from

these master curves and plotted. As shown in Figure 3.4, the two rejuvenated binders presented lower G^* values and higher phase angles at the three aging conditions compared to the control binder. After 40 hours of PAV aging the control binder was close to obtaining the damage onset curve, while the other two binders showed excellent resistance to fatigue and block cracking even after 40 hours of PAV aging.

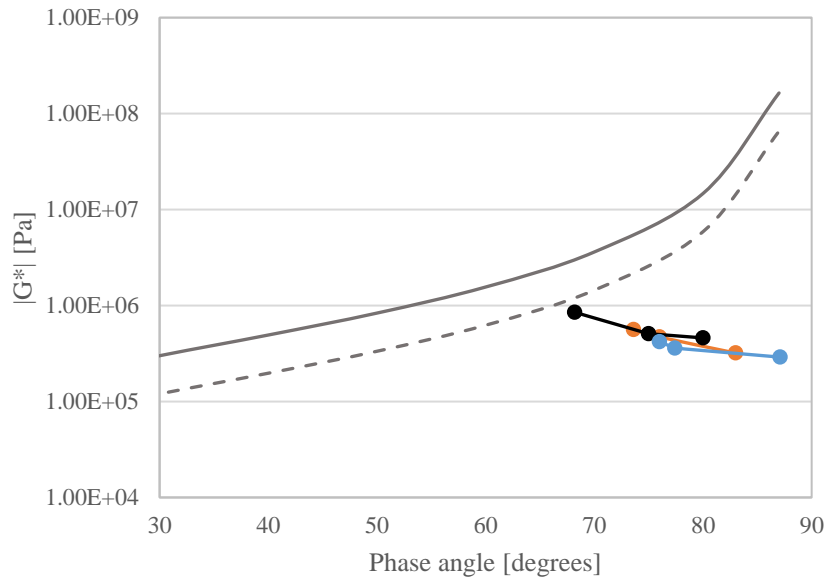


Figure 3.4 Glover-Rowe diagram

3.4.3 Binder fatigue properties

Linear amplitude sweep test results can be analyzed based on the principle of viscoelastic continuum damage (VECD). VECD has been used in several studies to model the complex fatigue behavior of asphalt binders and mixtures (Park, Kim et al. 1996, Christensen Jr and Bonaquist 2005, Hintz, Velasquez et al. 2011). By utilizing VECD, the damage growth in asphalt binder can be modeled following Schapery's work potential theory. According to Schapery's theory, work is related to damage by Equation 3.5.

$$\frac{dD}{dt} = \left(\frac{\partial W}{\partial D} \right)^\alpha \quad \text{Equation 3.5}$$

Where D is the damage intensity, t is time, W is the work performed, and α is a material constant related to the rate of damage progress, which is computed using Equation 3.6.

$$\alpha = 1 + \frac{1}{m} \quad \text{Equation 3.6}$$

Where m is the slope of a log-log plot of relaxation modulus versus time (Hintz, Velasquez et al. 2011). To quantify work in terms of damage intensity, two equations are used: Equation 3.7 quantifies work performed using dissipated energy under strain controlled loading (Kim, Lee et al. 2006), and Equation 3.8 relates $|G^*| \sin \delta$ to the damage intensity by fitting a power law (Johnson and Bahia 2010).

$$W = \pi \cdot \gamma_0^2 \cdot |G^*| \sin \delta \quad \text{Equation 3.7}$$

$$|G^*| \sin \delta = C_0 - C_1(D)^{C_2} \quad \text{Equation 3.8}$$

Where γ_0 is shear strain, and C_0 , C_1 , and C_2 are model coefficients. C_0 is taken as the average value of $|G^*| \sin \delta$ during the 0.1% strain amplitude load step, and C_1 , and C_2 were derived by using the simplified linearization procedure which can be used in place of the optimization method (Hintz, Velasquez et al. 2011).

The derivative of Equation 3.8 with respect to D was substituted into Equation 3.5, and after integration and simplification, the following Equation 3.9 can be achieved which defines the relationship between the number of cycles to failure and strain amplitude for a defined failure criterion.

$$N_f = A(\gamma_{max})^B \quad \text{Equation 3.9}$$

where,

$$A = \frac{f(D_f)^k}{k(\pi I_D C_1 C_2)^\alpha} \quad \text{Equation 3.10}$$

and,

$$B = 2\alpha \quad \text{Equation 3.11}$$

Where D_f is the damage accumulation at failure, I_D is the initial un-damaged value of $|G^*|$, f is the loading frequency, and $k = 1 + (1 - C_2)\alpha$. As recommended by Johnson and Bahia (Johnson and Bahia 2010), A was computed using the damage intensity corresponding to 35% decrease from the initial $|G^*| \sin \delta$ value.

A log-log plot of the number of cycles to failure versus strain rate based on Equation 3.9 is shown in Figure 3.5 Cycles to failure at 28°C. All the binders were tested at 28°C. The results indicate that the addition of BM-1 and BM-2 has considerably improved the fatigue life of the control binder. Borghi et al. have also observed improvement in fatigue resistance when BM-1 was used (Borghi, Jiménez del Barco Carrión et al. 2017). At low strains (2.5%), the level of improvement in the number of cycles to failure was not significantly different for the two bio-additives but is more than 5 times better than the control. At higher strains (5% and 10%), the improvement by the recycling agents was more than 10 and 26 times better than the control, respectively.

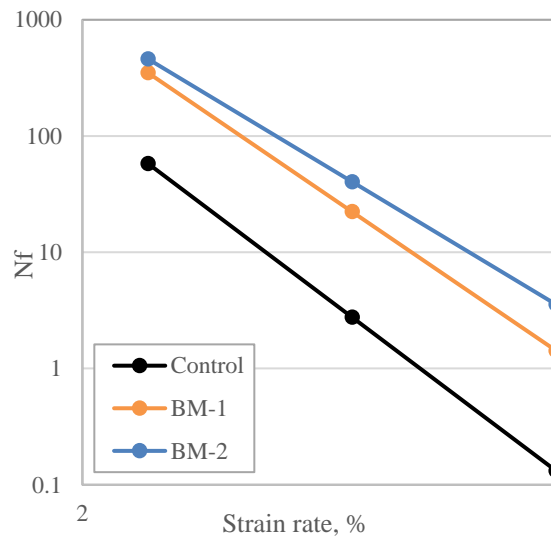


Figure 3.5 Cycles to failure at 28°C

3.4.4 Low temperature mixture fracture resistance

To determine the fracture properties of the mixtures at low temperatures, they were tested using the disk-shaped compact tension (DCT) geometry in accordance with ASTM D7313-13. The fracture energy parameter (G_f) obtained from this test is useful in differentiating the mixtures whose service life is dominated by cracking at low temperatures. For each of the groups studied in this research, 5 specimens were mixed and compacted to 150 mm diameter and 50 mm height specimens at 7% air voids. As mentioned earlier, the specimens were produced both in the lab and at a plant but compacted in the lab. A 1.5 mm notch was fabricated along the diameter of each of the specimens. As recommended by ASTM D7173, a test temperature of 10°C greater than the low temperature grade of the asphalt binder was selected. The low temperature grade of the control blend (-16°C) was one grade greater than those of the bio-modified blends (-22°C). However, for the ease of comparison, the control mixtures were tested at -12°C instead of -6°C. The DCT test was performed with a constant crack mouth opening displacement rate of 0.017 mm/s until the post-peak load level had been reduced to 0.1 kN. The fracture energy of the specimens was then computed using the area under the load-displacement curve, normalized by the thickness and the initial ligament length of the specimens. Figure 3.6 and Figure 3.7 present the comparison between the peak load and the fracture energy of the mixtures, respectively. It can be concluded from both figures that the addition of bio-materials has improved the fracture behavior of the asphalt mixtures at low temperatures. Research by Elkashef et al. (Elkashef and Williams 2017) has also shown that the addition of soybean-derived rejuvenators has improved the low-temperature cracking resistance of asphalt mixtures by approximately 13%. Porot et al. (Porot, Broere et al. 2017) have also shown that the addition of a crude tall oil (CTO)-derived rejuvenator has positively affected the performance of asphalt mixtures through restoring their flexibility. The significant decrease in

the low-temperature fracture resistance of mixtures containing 40% RAP with no rejuvenating agent was also observed in a study by Li et al. (Li, Marasteanu et al. 2008).

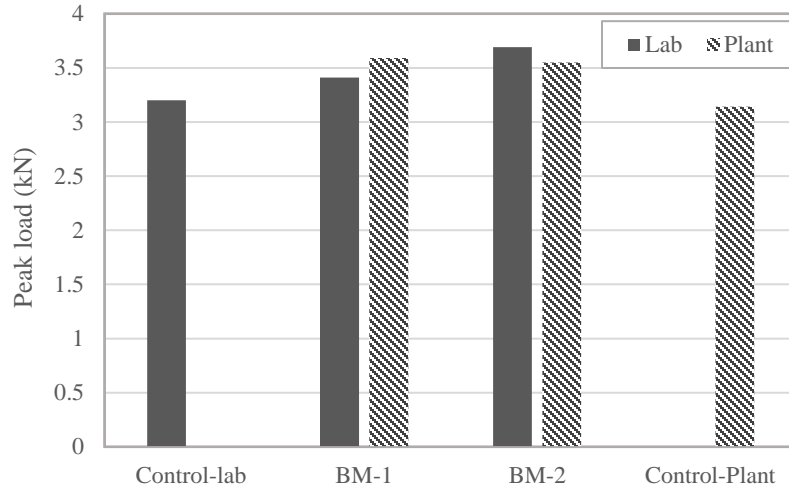


Figure 3.6 Mean peak load results obtained from DCT testing

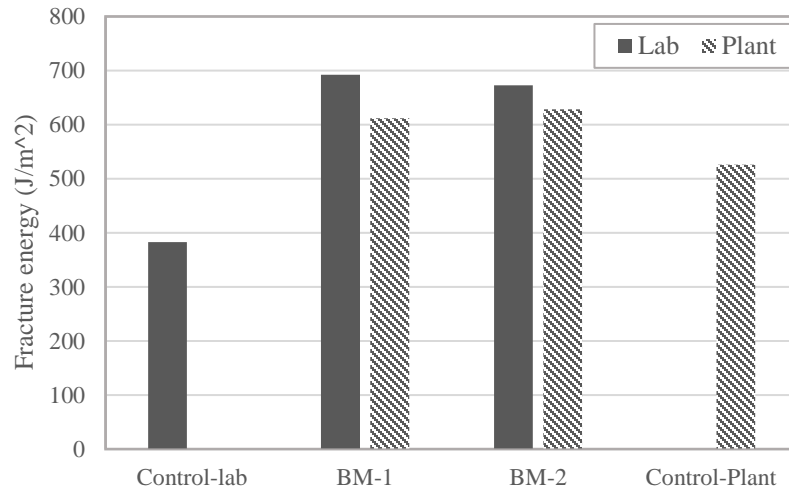


Figure 3.7 Mean peak load results obtained from DCT testing

However, it is important to statistically analyze the data to verify that the bio-materials have significantly improved the performance. For this purpose, a one-way ANOVA analysis was performed on the fracture energy values and peak load values of the lab-produced mixtures and the two rejuvenated mixtures were compared to the control mixtures using the Dunnett test method which provides individual comparison of the control group with any other group. Because the

control plant-produced mixtures only contained 20% RAP, and the difference in the RAP content is assumed to have a significant effect on the results, the statistical comparison was not performed between the control plant-produced mixtures and the rejuvenated plant-produced mixtures. However, the effect of lab and plant production could be assessed by performing a two-sample t-test on the fracture energy and peak load values of the two rejuvenated mixtures.

Before conducting the comparisons, the normality of the distribution of all data was examined through the Shapiro-Wilk W test on the null hypothesis where the distribution is normal if the p-values are larger than the level of significance (0.05). The equal variances test was also conducted on each of the comparisons and variances were found to be equal. The results of statistical analysis on the peak load and fracture energy of lab-produced mixtures are provided in Table 3.4 and

Table 3.5, respectively. A p-value greater than 0.05 for the peak load of BM-1 indicates no significant difference with the control mixture. However, p-values smaller than the level of significance for the fracture energy results indicate that the two rejuvenators have significantly improved the fracture energy of the control mixture. Therefore, it is always essential to compare asphalt mixtures based on their fracture energy as well as the peak loads to obtain more realistic conclusions.

Table 3.4 Statistical comparison between the control and the rejuvenated mixtures-peak load

Level	Level	Difference in peak load	Lower CL	Upper CL	p-value
BM-1-lab	Control-lab	0.21	-0.0197	0.613	0.362
BM-2-lab	Control-lab	0.48	0.077	0.887	0.021

Table 3.5 Statistical comparison between the control and the rejuvenated mixtures-fracture energy

Level	Level	Difference in fracture energy	Lower CL	Upper CL	p-value
BM-1-lab	Control-lab	244.6	112.7	376.5	0.0011
BM-2-lab	Control-lab	221.6	89.7	353.5	0.0023

Prior to perform a comparison between the lab-produced and plant-produced rejuvenated mixtures, the outlier data were discarded (one fracture energy and one peak load from the BM-2 plant-produced mixtures). A two-sample t-test was then conducted between fracture energy values and peak load values, and the results are summarized in Table 3.6 and Table 3.7.

Table 3.6 Statistical comparison between the lab and plant-produced rejuvenated mixtures-peak load

Level	Level	Difference in peak load	Lower CL	Upper CL	p-value
BM-1-lab	BM-1-plant	0.173	-0.301	0.647	0.788
BM-2-lab	BM-2-plant	0.316	-0.671	0.038	0.037

Table 3.7 Statistical comparison between the lab and plant-produced rejuvenated mixtures-fracture energy

Level	Level	Difference in fracture energy	Lower CL	Upper CL	p-value
BM-1-lab	BM-1-plant	35.80	-149.6	78.0	0.245
BM-2-lab	BM-2-plant	86.4	-183.0	10.2	0.036

The box and whisker plots are also provided in Figure 3.8 and Figure 3.9. From these results, it can be inferred that the mix scale, whether small (in the lab) or large (at the plant), does not have significant effect on the properties of the BM-1 mixtures as indicated by p-values greater

than 0.05 for both the peak load and the fracture energy. However, small p-values for the BM-2 mixture is an indication of significant difference in the low-temperature properties of lab-produced mixtures and plant-produced mixtures. This could be due to the process control variations in large-scale production or the relevantly high coefficients of variation (COV) among DCT test results and the hidden effects of other influencing factors such as variations in the void content as well as the mixing and compaction temperatures.

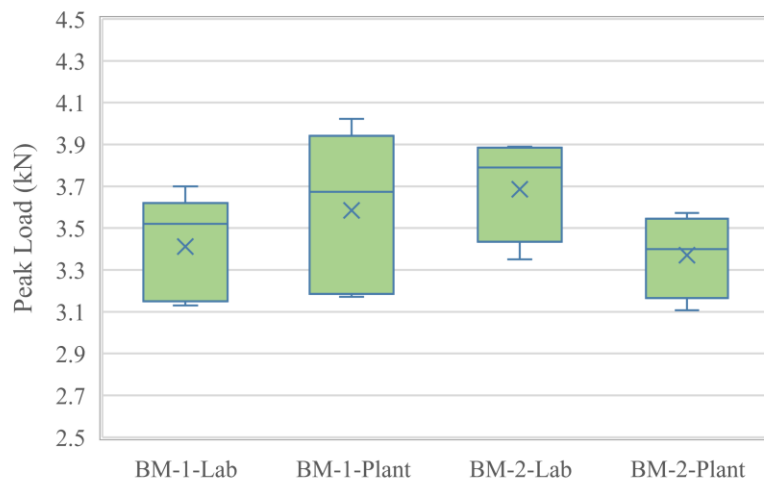


Figure 3.8 Variation of peak load in the rejuvenated mixtures

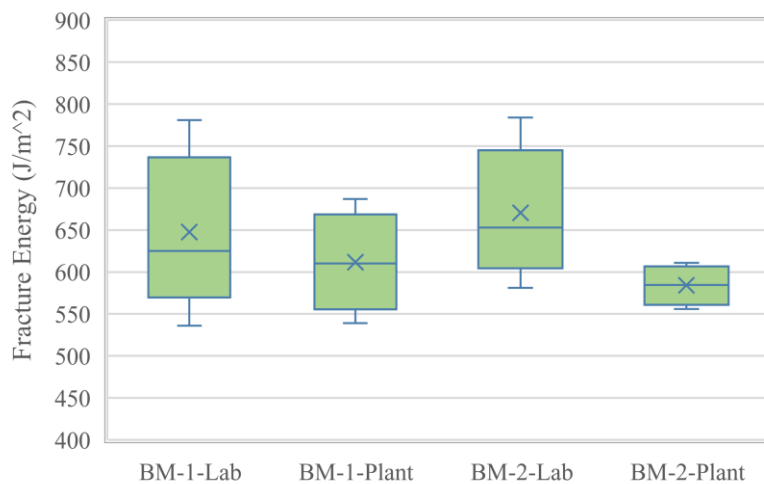


Figure 3.9 Variation of fracture energy in the rejuvenated mixtures

The correlation between mixture fracture properties obtained from DCT testing and binder low-temperature properties obtained from BBR testing was also investigated in this research. For this purpose, the DCT test was conducted on mixtures at three different temperatures: -6°C , -12°C , and -18°C . The BBR test was also conducted on binders at the same temperatures. To determine the correlations, comparisons were made once between the fracture energy results and binder stiffness results, and once between the fracture energy results and m-value results. Figure 3.10 and Figure 3.11 show the relatively linear relationship between these parameters. The relatively high correlation coefficient of 0.99 for fracture energy and m-values indicate a strong correlation between these two parameters. A lower correlation coefficient of 0.89 for the fracture energy and stiffness values also indicates a relatively strong correlation between the two parameters, however, it appears that as the temperature increases, the stiffness values become more scattered from the trendline.

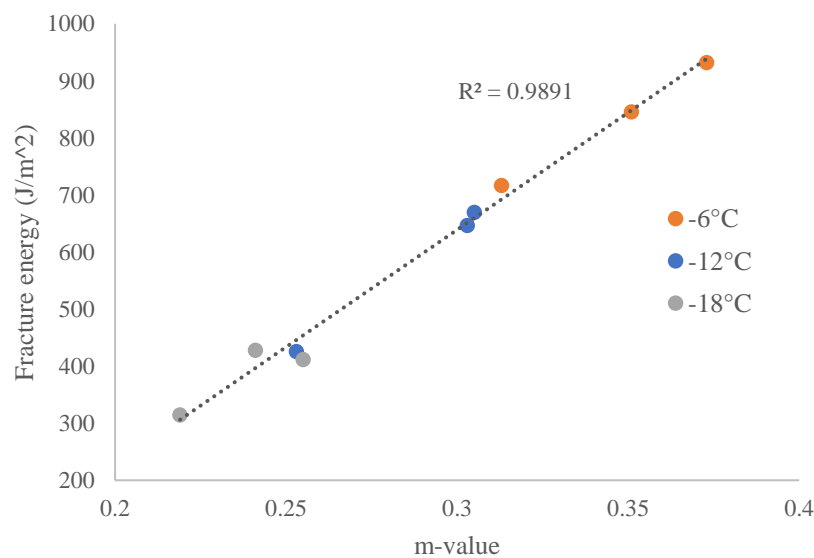


Figure 3.10 Correlation between mix fracture energy and binder m-value

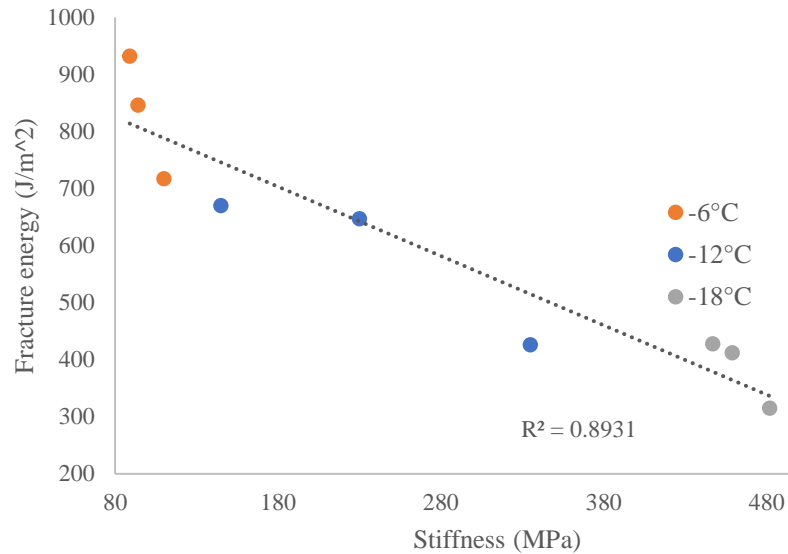


Figure 3.11 Correlation between mix fracture energy and binder stiffness

3.4.5 Mixture fatigue resistance

Fatigue cracking resistance of asphalt mixture has been extensively studied by many researchers. Traditionally, the fatigue life of asphalt mixtures could be determined by using the following equation which relates the number of load repetitions to the flexural tensile strain at the bottom of the asphalt layer mixtures: (Monismith, Epps et al. 1970, Tayebali, Deacon et al. 1993)

$$N_f = K_1(1/\varepsilon)^{K_2} \quad \text{Equation 3.12}$$

where N_f is the fatigue life or the number of load repetitions, ε is the flexural tensile strain, and K_1 and K_2 are the experimentally determined coefficients. Recently, researchers have shown that this relationship between the fatigue life and the tensile strain cannot be obtained at low strain levels where the asphalt mixtures reach a fatigue endurance limit below which they exhibit almost no fatigue damage (Carpenter, Ghuzlan et al. 2003). Through further investigation, researchers employed the dissipated energy concept which can represent a measure of damage due to the incremental dissipated energy between the consecutive cycles, and introduced the ratio of

dissipated energy change (RDEC) as a true indication of fatigue damage, regardless of testing conditions: (Ghuzlan and Carpenter 2000)

$$RDEC = \frac{(DE_{n+1} - DE_n)}{DE_n} \quad \text{Equation 3.13}$$

where DE_{n+1} and DE_n are dissipated energy at load cycles $n+1$ and n , and RDEC is the ratio of dissipated energy change. The damage curve obtained from plotting RDEC values versus loading cycles consists of three distinct stages from which the second one is of special interest when characterizing the fatigue behavior of the beams. A schematic of the damage curve is shown in Figure 3.12 (Ghuzlan 2001). In the second stage, known as the plateau stage, a nearly constant value of RDEC represents a constant rate of damage accumulation before failure. The value of RDEC at this stage is shown to have a strong correlation with the number of cycles to failure, thus being a reliable measure of damage accumulated in the beams (Ghuzlan and Carpenter 2000, Shen and Carpenter 2005).

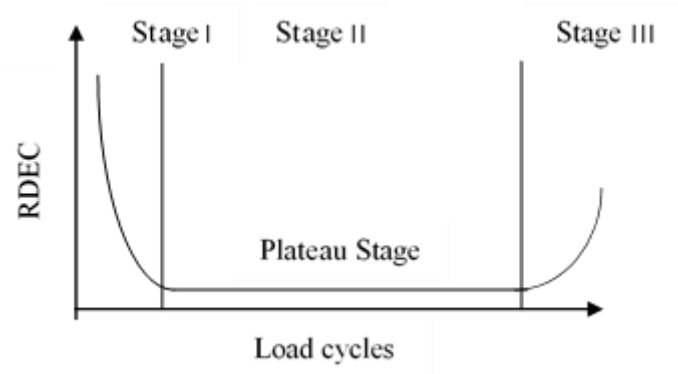


Figure 3.12 Schematic of RDEC curve(Ghuzlan 2001)

The beam fatigue testing was performed on a total of six specimens from each group: three specimens at 600 microstrain and three specimens at 1000 microstrain. All specimens were pre-conditioned in the chamber for 2 hours to obtain the testing temperature of 20°C. The test was terminated when the initial flexural stiffness of the beams was reduced by 50% and the dissipated

energy values were directly obtained from the testing program. The plateau values (PV) of the different beams were calculated by using Equation 3.13 and the average values were selected for comparing the different groups. Figure 3.13 shows the comparison between the control mixture and the two rejuvenated mixtures. Since the effectiveness of this approach in comparison to the traditional approach was also of interest in this research, the number of load cycles to failure for the different groups were averaged and summarized in Figure 3.14.

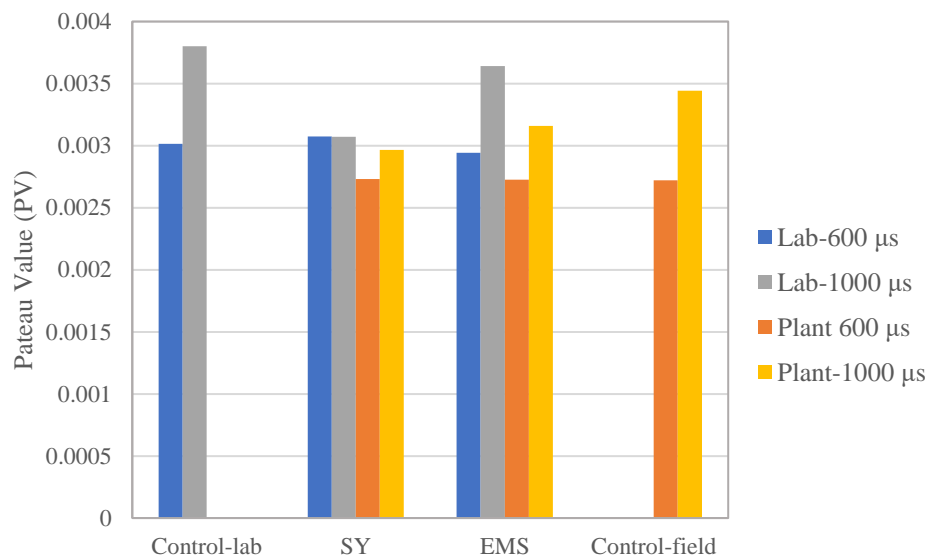


Figure 3.13 Comparison of PVs obtained from flexural beam fatigue testing

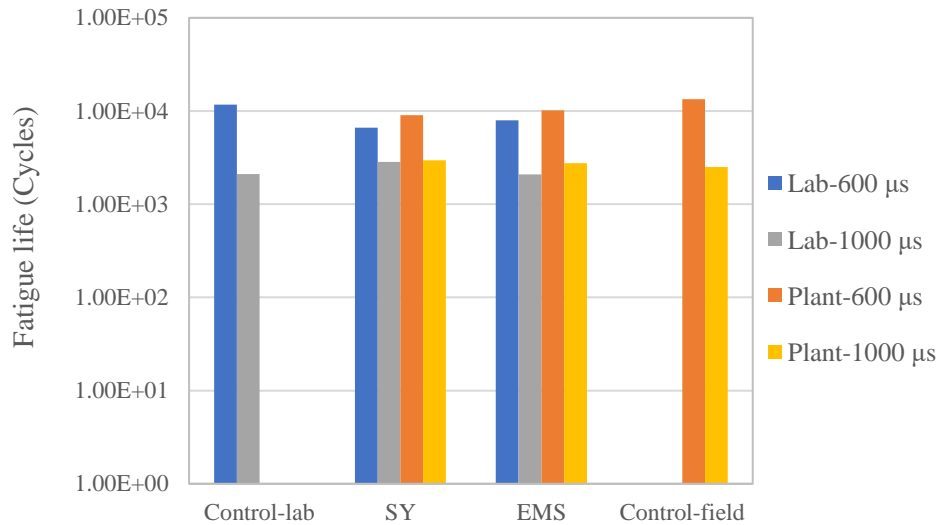


Figure 3.14 Comparison of Fatigue life obtained from flexural beam fatigue testing

In Figure 3.13, the PV of the lab-produced mixtures and plant-produced mixtures tested at 600μs are slightly different from the control group, while at 1000μs greater differences are observed. Since the PV is an indication of the accumulated damage, greater values indicate more damage accumulated in the beams at a certain strain level before reaching 50% of the initial flexural stiffness which is measured at the 50th load cycle. At 600μs and small-scale production, the control mixtures failed at greater number of load cycles, hence anticipated to have higher plateau values than the rejuvenated mixtures. However, the lab-produced BM-1 mixtures showed higher plateau values than the control mixtures indicating more damage accumulated in the beams. Similarly, at 600μs and large-scale production, while the control mixtures failed later than the two rejuvenated mixtures, identical plateau values for all the three groups indicates more damage accumulated in the rejuvenated mixtures. At 1000μs and small-scale production, the BM-1 mixture failed slightly later than the other two mixtures, however, less damage was accumulated in the BM-1 beams. At 1000μs and large-scale production, while the three groups performed similarly in terms of fatigue load cycles, more damage was accumulated in the control mixtures compared

to the two rejuvenated mixtures. Another observation from Figure 3.13 is that compared to the lab-produced mixtures, the PV obtained for the plant-produced mixtures were smaller, indicating less damage accumulated in the beams when produced and mixed in larger quantities. Furthermore, these findings can be compared with the LAS test results which were obtained and discussed in section 3.4.3 to study the fatigue behavior of the binders. According to Figure 3.5, the rejuvenated binder blends tested at 28°C showed better fatigue performance in comparison to the control blend specially at higher strain levels. The opposite of this behavior was observed when mixtures were subjected to low strain levels while at high strain levels mixtures performed similarly. Since these results are not consistent with the LAS test results, previous research can be verified that the number of load cycles to failure at a certain strain level cannot exclusively be a representative of the fatigue behavior of asphalt mixtures, while the plateau value criterion appears more reasonable and more consistent with the binder fatigue behavior (Ghuzlan and Carpenter 2000, Shen and Carpenter 2005, Shu, Huang et al. 2008). Also, it should be noted that according to previous studies (Mannan, Islam et al. 2015, Kim, Mohammad et al. 2018), at low RAP contents (<25%), inclusion of rejuvenators can reduce the stiffness, thus improving the fatigue life. However, as the RAP content increases, as a result of partial blending between the RAP binder and the fresh binder, the excessive amount of stiffness cannot be diminished by the softening effect of the rejuvenators, thus reducing the fatigue life of the mixtures.

3.5 Conclusions and Recommendations

The effectiveness of two bio-based rejuvenators in the production of asphalt mixtures containing 50% RAP materials and their respective asphalt binders was investigated in this study. Mixtures were produced in two locations: lab and plant and were compacted in the standard specimen size for DCT and flexural beam fatigue testing. The experimental plan included

investigation of the compatibility of the bio-rejuvenators with the base binder and the RAP binder, evaluation of the brittleness of the control binder and the rejuvenated binders through Glover-Rowe parameter, and evaluation of the fatigue performance of the control and rejuvenated binders under cyclic loading. Mixtures were evaluated through DCT and beam fatigue testing. The DCT results were furthermore used to perform a statistical analysis and identify the significant differences between the rejuvenated mixtures and the control mixtures as well as between the locations where they were produced. The key findings from this research are reported as follows:

- The compatibility of the two bio-based rejuvenators with the asphalt mixtures was evaluated and the blends were found to be compatible. The addition of bio-rejuvenators possibly resulted in disaggregation of some of the asphaltene particles as no heat flow associated with crystallization was observed in their DSC curves, as opposed to the control binder.
- The Glover-Rowe parameter for the binders at different aging conditions was obtained and it was found that compared to the control binder, the rejuvenated binders showed improved ductility and improved resistance to block cracking even after 40 hours of PAV aging.
- At intermediate temperatures, the LAS test results on the binders revealed that the fatigue cracking resistance of the rejuvenated binders was significantly improved compared to the control binder.
- From DCT testing, it was found that the fracture resistance of the asphalt mixtures was improved by incorporating the rejuvenators in their formulation. The statistical analysis on the peak load and fracture energy results showed significant differences between the fracture energy values of the control group and those of the rejuvenated group. No significant difference in the peak loads of the control and the BM-1 mixture indicated that

the peak load values are not solely enough in the evaluation of the performance of the mixtures. Statistical analysis on the small (lab) and large-scale (plant) production of the two rejuvenated mixtures showed significant differences for the BM-2 mix, while no significant difference was observed for the BM-1 mixtures. Since the variations in the fracture energy values are usually high when conducting DCT tests, it is recommended to conduct this test on a larger number of specimens in order to identify the differences more realistically.

- From the LAS test on binders it was anticipated that the rejuvenated mixtures would exhibit longer fatigue life compared to the control mixture. However, from the flexural beam fatigue results, it appears that fatigue life of mixtures is adversely influenced by the effect of high RAP content and the rejuvenators cannot completely restore the stiffness of the control mixtures. Moreover, the fatigue behavior of asphalt mixtures depends on several factors other than the rheological properties of binders, such as layer thickness and variations in the air voids. It is therefore recommended to take all the important factors into account when comparing different mixtures for their fatigue cracking resistance.

3.6 References

Barco Carrión, A. J. d., et al. (2017). "Linear viscoelastic properties of high reclaimed asphalt content mixes with biobinders." *Road Materials and Pavement Design* 18(sup2): 241-251.

Borghi, A., et al. (2017). "Effects of laboratory aging on properties of biorejuvenated asphalt binders." *Journal of Materials in Civil Engineering* 29(10): 04017149.

Carpenter, S. H., et al. (2003). "Fatigue endurance limit for highway and airport pavements." *Transportation Research Record* 1832(1): 131-138.

Chailleux, E., et al. (2017). "BioRePavation: innovation in bio-recycling of old asphalt pavements: towards safe cost effective renewable pavement". *AAPA International Flexible Pavements Conference*, 17th, 2017, Melbourne, Victoria, Australia.

Christensen Jr, D. W. and R. Bonaquist (2005). "Practical application of continuum damage theory to fatigue phenomena in asphalt concrete mixtures (with discussion and closure)." *Journal of the Association of Asphalt Paving Technologists* 74.

Copeland, A. (2011). "Reclaimed asphalt pavement in asphalt mixtures: State of the practice". (no. FHWA-HRT-11-021). Washington, DC: Federal Highway Administration. Office of Research, Development, and Technology

Elkashef, M., et al. (2017). "Preliminary examination of soybean oil derived material as a potential rejuvenator through Superpave criteria and asphalt bitumen rheology." *Construction and Building Materials* 149: 826-836.

Elkashef, M., et al. (2017). "Introducing a soybean oil-derived material as a potential rejuvenator of asphalt through rheology, mix characterisation and Fourier Transform Infrared analysis." *Road Materials and Pavement Design*: 1-21.

Elkashef, M. and R. C. Williams (2017). "Improving fatigue and low temperature performance of 100% RAP mixtures using a soybean-derived rejuvenator." *Construction and Building Materials* 151: 345-352.

Garcia Cucalon, L., et al. (2017). "Compatibility of recycled binder blends with recycling agents: Rheological and physicochemical evaluation of rejuvenation and aging processes." *Industrial & Engineering Chemistry Research* 56(29): 8375-8384.

Ghuzlan, K. and S. Carpenter (2000). "Energy-derived, damage-based failure criterion for fatigue testing." *Transportation Research Record: Journal of the Transportation Research Board*(1723): 141-149.

Ghuzlan, K. A. (2001). "Fatigue damage analysis in asphalt concrete mixtures based upon dissipated energy concepts", University of Illinois at Urbana-Champaign.

Glover, C. J., et al. (2005). "Development of a new method for assessing asphalt binder durability with field validation." *Texas Dept Transport* 1872.

Haghshenas, H., et al. (2016). "Research on High-RAP Asphalt Mixtures with Rejuvenators and WMA Additives." Report SPR-P1(15) M016, *Nebraska Transportation Center*.

Hintz, C., et al. (2011). "Modification and validation of linear amplitude sweep test for binder fatigue specification." *Transportation Research Record: Journal of the Transportation Research Board*(2207): 99-106.

Huang, S.-C., et al. (2014). "Influence of rejuvenators on the physical properties of RAP binders." *Journal of Testing and Evaluation* 43(3): 594-603.

Johnson, C. and H. U. Bahia (2010). "Evaluation of an accelerated procedure for fatigue characterization of asphalt binders." *Submitted for publication in Road Materials and Pavement Design*.

Kim, M., et al. (2018). "Fatigue performance of asphalt mixture containing recycled materials and warm-mix technologies under accelerated loading and four point bending beam test." *Journal of cleaner production* 192: 656-664.

Kim, Y., et al. (2006). "A Simple Testing Method to Evaluate Fatigue Fracture and Damage Performance of Asphalt Mixtures (With Discussion)." *Journal of the Association of Asphalt Paving Technologists* 75.

Kowalski, K. J., et al. (2016). "Eco-friendly materials for a new concept of asphalt pavement." *Transportation Research Procedia* 14: 3582-3591.

Kriz, P., et al. (2008). "Glass transition and phase stability in asphalt binders." *Road Materials and Pavement Design* 9(sup1): 37-65.

Li, X., et al. (2008). "Effect of reclaimed asphalt pavement (proportion and type) and binder grade on asphalt mixtures." *Transportation Research Record: Journal of the Transportation Research Board*(2051): 90-97.

Mannan, U. A., et al. (2015). "Effects of recycled asphalt pavements on the fatigue life of asphalt under different strain levels and loading frequencies." *International Journal of Fatigue* 78: 72-80.

Monismith, C. L., et al. (1970). Asphalt mixture behavior in repeated flexure.

Olard, F. and S. Pouget (2015). "A new approach for aggregate grading optimization for mixtures", *Advances in Asphalt Materials*, Elsevier: 427-457.

Park, S. W., et al. (1996). "A viscoelastic continuum damage model and its application to uniaxial behavior of asphalt concrete." *Mechanics of Materials* 24(4): 241-255.

Porot, L., et al. (2017). "Asphalt and binder evaluation of asphalt mix with 70% reclaimed asphalt." *Road Materials and Pavement Design* 18(sup2): 66-75.

Porot, L., et al. (2017). "Asphalt and binder evaluation of asphalt mix with 70% reclaimed asphalt." *Road Materials and Pavement Design*: 1-10.

Pouget, S., et al. (2016). "GB5® Mix Design: A New Approach for Aggregate Grading Optimization for Heavy Duty Flexible Pavements". *8th RILEM International Conference on Mechanisms of Cracking and Debonding in Pavements*, Springer.

Shen, S. and S. Carpenter (2005). "Application of the dissipated energy concept in fatigue endurance limit testing." *Transportation Research Record: Journal of the Transportation Research Board*(1929): 165-173.

Shu, X., et al. (2008). "Laboratory evaluation of fatigue characteristics of recycled asphalt mixture." *Construction and Building Materials* 22(7): 1323-1330.

Song, M., et al. (1998). "Modulated differential scanning calorimetry: XVI. Degree of mixing in interpenetrating polymer networks1." *Thermochimica acta* 315(1): 25-32.

Tayebali, A. A., et al. (1993). "Modeling fatigue response of asphalt-aggregate mixtures." *Asphalt Paving Technology* 62: 385-385.

Tran, N., et al. (2017). "Effect of rejuvenator on performance characteristics of high RAP mixture." *Road Materials and Pavement Design* 18(sup1): 183-208.

Turner, P., et al. (2015). "Laboratory evaluation of SYLVAROADTM RP 1000 rejuvenator", Draft NCAT Report, Auburn, AL.

Velasquez, R., et al. (2011). "Low temperature cracking characterization of asphalt binders by means of the single-edge notch bending (SENB) test." *Asphalt Paving Technology-Proceedings Association of Asphalt Technologists* 80: 583.

Zaumanis, M., et al. (2014). "Influence of six rejuvenators on the performance properties of Reclaimed Asphalt Pavement (RAP) binder and 100% recycled asphalt mixtures." *Construction and Building Materials* 71: 538-550.

CHAPTER 4 HIGH TEMPERATURE PERFORMANCE OF ASPHALT MIXTURES AND ASPHALT BINDERS CONTAINING HIGH AMOUNTS OF RAP AND TWO NOVEL BIO-BASED REJUVENATORS

Modified from a manuscript under review Journal of Cleaner Production

Zahra Sotoodeh-Nia^a, Nick Manke^a, R. Christopher Williams^a, Eric W. Cochran^b, Luarent Porot^c, Emmanuel Chailleux^d, Juliette Blanc^d

Abstract

Over the past decades, reclaimed asphalt pavement (RAP) materials have been increasingly used in asphalt pavements due to their significant contribution in reducing asphalt production costs and energy consumption. However, using high amounts of RAP in the asphalt mixtures can cause early pavement failures and result in higher maintenance costs; therefore, certain actions need to be taken to improve their performance. The most common practice to offset the adverse effects of RAP is to use recycling agents known as rejuvenators in the asphalt mix design. In this paper, two novel bio-additives with rejuvenating properties were used in the production of asphalt mixtures containing 50% RAP materials. At high temperatures, where rutting is the major distress that the asphalt pavement experiences, the behavior of a mixture is substantially affected by the rheological properties of the asphalt binder. Therefore, accurate investigation of the rheological properties of the binders including viscosity and dynamic modulus is important. Using a dynamic shear rheometer (DSR), the rheological properties of binders at various temperatures and loading conditions was determined. In addition to the binder rheological properties, characterizing the

^a Department of Civil, Construction, and Environmental Engineering, Iowa State University, Ames, Iowa, 50011-3232.

^b Department of Chemical and Biological Engineering, Iowa State University, Ames, Iowa, 50011-3232.

^c Kraton Chemical B.V, Almere, Netherlands.

^d LUNAM Université, IFSTTAR, Bouguenais, France.

rutting and stripping resistance of the asphalt mixtures is also an integral part of performance evaluation at high temperatures. In this paper, asphalt mixtures were produced in two locations: in the lab, and at the plant. The specimens were then compacted in the lab, and the flow number test and the Hamburg wheel tracking test were conducted on the specimens to characterize their rutting and stripping resistance. Finally, asphalt binder was recovered from the tested specimens, and the differences between the performance grade of the original and RTFO aged blended binders and that of the recovered binders were identified.

4.1 Introduction

Reclaimed asphalt pavement (RAP) has been widely used in asphalt mixtures over the past decades. A considerable number of studies have shown that RAP can be used as a sustainable and cost-effective alternative for virgin aggregates and virgin binders in asphalt pavements (Al-Qadi, Elseifi, & Carpenter, 2007; Copeland, 2011). However, the most common issue of debate amongst agencies is that high amounts of RAP could affect the long-term performance of asphalt pavements adversely, and not effectively reduce the costs over the pavement service life (Yu, Zaumanis, Dos Santos, & Poulidakos, 2014). The concerns regarding the use of high RAP content in hot mix asphalt (HMA) refers to the chemical, physical, and rheological changes that occur in the RAP binder during the pavement service life. Oxidation and exposure to severe climatic conditions occurring in the RAP binder leads to a phenomenon known as aging. During the aging process, asphalt binder loses some of its volatile components and reacts with oxygen; therefore, it becomes significantly stiffer than the virgin binder. Due to the stiffening effect of aged RAP binder, when RAP materials are introduced into asphalt mixtures, there is a need to restore the chemical and rheological properties of the aged binder. One approach to reduce the stiffness of the RAP binder is to use rejuvenators or recycling agents in the mix design. Currently, many researchers have been

assessing rejuvenators that can help improve the mechanical performance of asphalt mixtures as well as providing cost savings and addressing environmental concerns (Cavalli, Zaumanis, Mazza, Partl, & Poulidakos, 2018; Zaumanis, Mallick, Poulidakos, & Frank, 2014). A successful rejuvenator is one that can be applied to the mix design in low dosages while restoring the chemical and rheological properties of the aged RAP binder as well as improving the performance of mixtures to adequate levels. Overall, the mix design also needs to be economical. Table 4.1 below summarizes some of the rejuvenators available along with rejuvenator origins and descriptions (Ali and Mohammadafzali, 2015; Haghshenas, Nabizadeh, Kim, & Santosh, 2016; Zaumanis, et al., 2014).

Table 4.1 Common Types of Rejuvenators

Rejuvenator Category	Examples	Description
Paraffinic Oils	Waste Engine Oil (WEO) Storbit®	Refined from waste lubricating oils (petroleum-derived)
Aromatic Extracts	Hydrolene® Reclamite® ValAro 130A®	Refined from crude oil with polar aromatic additives (potentially carcinogenic)
Naphthenic Oils	Ergon HyPrene® Naphthenic Base Oils	Engineered hydrocarbons (maltenes, saturates, and acidifins from crude oil source)
Triglycerides and Fatty Acids	Waste Vegetable Oil Waste Vegetable Grease Brown Grease	Refined vegetable oils (many derived from waste oils and grease from food industry)
Tall Oils	Sylvaroad™ RP1000 Hydrogreen® Hydrogreen S™	Coproducts of the paper mill industry (can be used in crude form or refined)
Bio-Rejuvenators	Rapeseed Oils Linseed Oils Pine Oils	Rejuvenators refined (often using rapid pyrolysis) from sustainable organic materials

As seen in Table 4.1, there are many variations in available rejuvenator origin materials and derivations. While each rejuvenator accomplishes relatively the same goal in pavements containing RAP, the varying physical and chemical properties of each must be considered.

Manufacturer or supplier guidance should always be consulted when choosing a specific rejuvenator to use and selecting an appropriate dosage to be used.

The influence of rejuvenators or recycling agents on the properties of RAP-containing binders can be determined through evaluation of rheological, chemical, and physical characteristics of the rejuvenated binders at different temperatures. At high temperatures, when the asphalt pavement experiences repeated heavy loads, rutting or permanent deformation becomes the major distress in the asphalt structure. Several methods have been practiced by researchers to evaluate the rutting resistance of asphalt binders and asphalt mixtures. At high temperatures, the behavior of asphalt pavement is primarily influenced by the rheological properties of asphalt binder. Therefore, it is essential to properly characterize the behavior of rejuvenated binders when employing the recycling agents in their mix design. The rheological properties of asphalt binder at high temperatures are usually determined in terms of dynamic modulus and viscosity. Dynamic modulus properties can be obtained by testing the asphalt binders using a dynamic shear rheometer (DSR) at the desired testing conditions. Viscosity properties in a steady state are usually measured by a viscometer or a DSR, while in dynamic state the measurements are mostly done by means of a DSR. The contribution of asphalt binder to the rutting resistance of asphalt pavement has been studied by researchers through different specification parameters from which the $G^*/\sin \delta$ and the zero shear viscosity (ZSV) are the most commonly used. Although the $G^*/\sin \delta$ has shown promising results in characterizing and rating the asphalt binders based on their rutting resistance (D. A. Anderson et al., 1994), however, some researchers have suggested that in the case of polymer-modified binders the contribution of this parameter with the rutting resistance cannot be fully captured (D. Anderson, Le Hir, Planche, Martin, & Shenoy, 2002). On the other hand, ZSV, which is defined as the viscosity at very low

shear rates, has been found to have a good correlation with the rutting performance in asphalt mixtures (Phillips and Robertus, 1996; Rowe, D'Angelo, & Sharrock, 2002; Saboo, Singh, Kumar, & Vikram, 2018).

Several studies have investigated the effect of RAP and rejuvenators on the rutting and stripping resistance of asphalt mixtures and have concluded that the inclusion of RAP may improve the rutting resistance (Shu, Huang, Shrum, & Jia, 2012; Zhao, Huang, Shu, Jia, & Woods, 2012), while the use of rejuvenators along with RAP may reduce it (Mogawer, Austerman, Kluttz, & Puchalski, 2016). Other studies on the stripping and moisture susceptibility of the rejuvenated mixtures have shown an improvement in these properties by using recycling agents (Hajj, Souliman, Alavi, & Salazar, 2013; Im and Zhou, 2014). A study conducted by Podolsky et al. suggested that the use of rejuvenators may sometimes improve the rutting and stripping of the control mixtures due to the better adhesion that the rejuvenator may provide for the mixture (Podolsky, Sotoodeh-Nia, Huisman, Williams, & Cochran, 2019).

The objective of this research was to incorporate two novel bio-based additives with rejuvenating effects in an asphalt mix design containing 50% RAP materials and evaluate the effectiveness of them to restore the rheological properties of the binder and improve the mixture performance in terms of resistance to rutting and stripping. To this end, binders and the rejuvenators were first blended in pre-determined dosages. The blends were then tested by means of a rotational viscometer and a DSR instrument for their rheological properties. The experimental study on asphalt mixtures was focused on flow number and Hamburg wheel tracking device (HWTD) tests. Finally, the binders were recovered from the lab- and plant-produced mixtures, and their performance grades were compared.

4.2 Experimental Materials and Mix Designs

4.2.1 Materials

For binder evaluation prior to mixing and compaction, RAP binder was recovered from two sources of RAP materials: coarse RAP (8/12mm), and fine RAP(0/8mm). The coarse RAP fractions contributing to 34% of the mix design, contained 2.9% RAP binder, and the fine RAP fractions contributing to 16% of the mix design contained 4.4% RAP binder. These results were validated between the three institutions collaborating in this research. For the purpose of this study, the total binder content was set to 4.5%. 50% RAP materials in the mixture contributed to 1.7% of RAP binder in the mixture, and 37.4% of RAP binder in the total binder. To reach 4.5% binder content in the mixture, 2.8% of fresh binder including the rejuvenators was added to the mixture.

The first rejuvenator, SYLVAROAD™ RP1000, was provided by the Kraton Company and is derived from crude tall oil. The second rejuvenator, EMS (epoxidized methyl soyate), was provided by the ADM Company and is derived from soybean oil. In this study, these two rejuvenators are coded as BM-1 and BM-2, respectively. BM-1 has been suggested by its providing company to be used in the total mixture by 6% of the weight of the RAP binder. In order to determine the appropriate dosage of BM-2, it was blended with the RAP and the fresh binder in different dosages from 3 to 6% of the weight of the total binder. Considering both low- and high-temperature rheological properties of the rejuvenated blends, and based on performance grading test results, the 3% dosage performed better than the higher dosages. Therefore, to stay within the scope of this study, 3% was selected as the optimum dosage of BM-2 to incorporate in the mix design.

4.2.2 Mix design

Table 4.2 shows the proportions of the different binders that were blended and tested for their rheological properties.

Table 4.2 Binder mix design

Groups	% in total binder		
	RAP binder	Virgin binder	Rejuvenator
Control	37.6	62.4	None
BM-1	37.6	60.1	2.3
BM-2	37.6	59.4	3.0

For mixture evaluation, two groups of asphalt mixtures were fabricated: 1. lab-produced, lab compacted mixtures, and 2. plant-produced, lab compacted mixtures. The asphalt specimens were compacted using a gyratory shear compactor (GSC) and the compaction was terminated when the target air void was achieved based on the volumetric calculations. For the lab-produced mixtures, the control group and the rejuvenated groups (BM-1 and BM-2) were mixed following the same mix design containing 50% RAP materials. This mix design, known as GB5 in previous publications (Olard and Pouget, 2015; Pouget, Olard, & Hammoum, 2016), has been developed to produce asphalt mixtures with 3.0 to 4.5% air void content, compacted with 100 number of gyrations.

For the plant-produced mixtures, the control group was mixed based on a mix design containing 20% RAP, known as EME2, which was developed in France as a high modulus mix design and has been used worldwide for over 30 years. The two rejuvenated plant-produced mixtures followed the GB5 mix design for the subsequent comparisons between the lab- and plant produced rejuvenated mixtures. The differences in the gradations of GB5 and EME2 are presented in Figure 3.1. The nominal maximum aggregate size (NMAS) for GB5 and EME2 mix designs was determined to be 19.0 and 12.5 mm, respectively. As shown in Figure 3.1, the EME2 mix

design contains more fine aggregates than the GB5 mix design and by the shape of its curve, this mix design can be classified as a dense-graded mix.

BM-1 has been designed as a pre-treatment of RAP materials and therefore it was added to the RAP prior to mixing with the virgin materials. However, BM-2 was first blended with the virgin binder, and then added to the mixture at the same time with RAP and virgin aggregates.

After all asphalt mixture specimens were fabricated and tested according to the experimental plan, the specimens were crushed and prepared for binder extraction and recovery. The recovered binders from lab-produced and plant-produced binders were then evaluated for their rheological properties and performance grading.

4.2.3 Laboratory testing

4.2.3.1 Binder temperature dependency

The temperature dependency of the binders was evaluated through viscosity testing. The viscosity was measured using a rotational viscometer as well as a DSR instrument. Using the DSR at the strain-controlled mode, the values of complex viscosity (η^*) were obtained at frequency sweeps ranging from 0.1 to 100 rad/s and a temperature range from 40°C to 70°C, increasing by 10°C increments.

4.2.3.2 Mixture rutting

The flow number test was performed on four of the dynamic modulus specimens at a temperature of 54°C, in accordance with AASHTO TP79-15 to evaluate the rutting resistance of the asphalt mixtures. The flow number test applies a haversine axial compressive load pulse of 0.1 s every 1.0 s. The test was conducted until the completion of 5% permanent strain or 10,000 cycles, whichever occurred first. The flow number is defined as the number of cycles at which the asphalt

specimen begins shear deformation or tertiary flow. The flow number is commonly obtained by using the Francken model given in Equation 4.1, which is recommended in AASHTO TP79-15.

$$\varepsilon_p = AN^B + C(e^{DN} - 1) \quad \text{Equation 4.1}$$

Where:

ε_p = permanent axial strain;

N = number of cycles; and

A , B , C and D = fitting coefficients.

4.2.3.3 Stripping and moisture Susceptibility of the mixtures

The Hamburg wheel-tracking test is currently the most common performance test to evaluate the rutting and stripping potential of asphalt mixtures at the same time. In this test, a cylindrical asphalt specimen is submerged in a water bath which can maintain the desired testing temperature, and a steel wheel is passed over the surface of the specimen backward and forward until a certain number of load cycles is reached. After the test, the rut depth data are plotted versus the number of load passes, and from the resulting curve the creep slope, stripping slope, and the stripping inflection point (SIP), where the two slopes intersect, are determined.

In this research, the specimens were fabricated in standard size and tested in three pairs, in accordance with AASHTO T 324. For the ease of comparison, a testing temperature of 50°C was selected for all pairs of specimens. The test was terminated when 10,000 load cycles (20,000 passes) or a rut depth of 20 mm was reached, whichever occurred first.

4.3 Results and Discussion

4.3.1 Rotational Viscosity

The rotational viscosity testing was conducted on the binders using a Brookfield viscometer in accordance with AASHTO T316. The variation in viscosity versus temperature is presented in Figure 4.1. Each binder blend was tested at 120, 135, 165, and 180°C at 20 rpm. The

allowable viscosity ranges for mixing and compaction of asphalt mixtures based on the Superpave specification are also marked in Figure 4.1 by green and red dashed lines, respectively. From Figure 4.1 it is evident that the two bio-rejuvenators have significantly reduced the mixing and compaction temperatures of the control binder. It can also be seen that as the temperature increases, the two rejuvenated binders tend to perform similarly as the virgin binder.

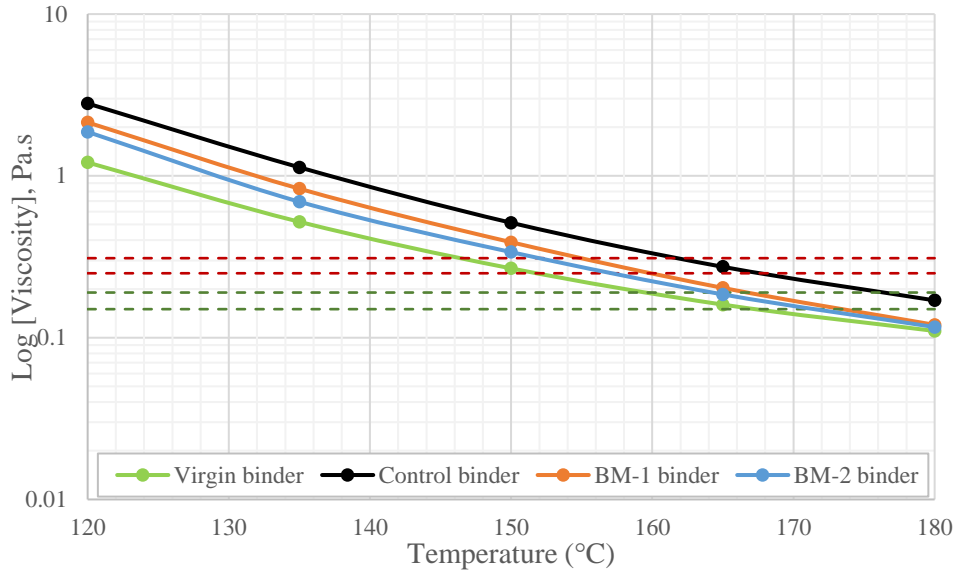


Figure 4.1 Conventional viscosity measurements

From the results of the rotational viscosity test, the temperature susceptibility of the asphalt binders can also be assessed. To this aim, the ASTM viscosity-temperature susceptibility (VTS) parameter was calculated for the binders according to the following equation:

$$\log \log \eta = A + VTS \log T_R \quad \text{Equation 4.2}$$

where η is the viscosity in cP, T_R is the temperature in Rankine, A is the regression intercept, and VTS is the regression slope. The calculated VTS values are given in Table 4.3 and the results indicate that the two rejuvenated binders have slightly higher temperature

susceptibility than the virgin binder, however, they have slightly improved the temperature susceptibility of the control binder.

Table 4.3 VTS values

Binder	Virgin	Control	BM-1	BM-2
VTS	-2.979	-3.248	-3.228	-3.229

4.3.2 Superpave specification parameter, $G^*/\sin(\delta)$

Superpave specification suggests that the $G^*/\sin(\delta)$ parameter at 10 rad/s gives a reasonable estimation of the rutting behavior of asphalt binders. The calculated $G^*/\sin(\delta)$ values at 10 rad/s for the control binder and the rejuvenated binders versus temperature are plotted in Figure 4.2. In this figure, the control binder shows higher $G^*/\sin(\delta)$ values compared to the two rejuvenated binders. This indicates that the addition of bio-rejuvenators will increase the rutting susceptibility to some extent. Although researchers have found that for modified binders this parameter underestimates the binder rutting performance (Bahia et al., 2001), however it still seems to provide a correct ranking between the binders in terms of rutting resistance (Elkashef, Podolsky, Williams, & Cochran, 2017; Hajikarimi, Rahi, & Moghadas Nejad, 2015).

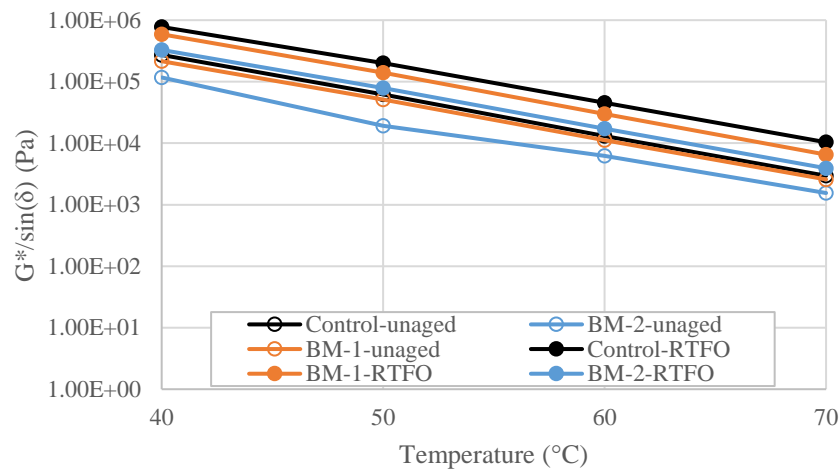


Figure 4.2 Variation of rutting parameter $G^*/\sin(\delta)$ with temperature

4.3.3 Complex Viscosity and shear rate influence

The complex viscosity of the binders was measured by a DSR instrument at different temperatures and frequencies. Figure 4.3 shows the variation of complex viscosity with shear rate and temperature. At 40°C, the binders have the highest complex viscosity and by increasing the shear rate the viscosity decreases at a higher rate compared to higher temperatures. As the temperature increases, the plateau region in the viscosity curves expands over a wider range of shear rates, indicating a wider area where the viscosity is independent of shear rate, and exhibits behavior closer to Newtonian fluids. This behavior was also seen when the two bio-rejuvenators were added to the control binder, and extended the plateau region at low shear rates, known as the zero shear viscosity region.

In order to assess the significant differences between the control binder and the rejuvenated binders in terms of complex viscosity, a paired t-test was conducted on the viscosity measurements, using the JMP statistical software. The independent variable was the shear rate which was equal for each pair. Prior to the test, a normality test was conducted on the measurements to ensure the differences between pairs are approximately normally distributed. To this aim, the Shapiro-Wilk W test with a significance level of 0.05 was used and all p-values were greater than 0.05, validating normal distribution of the differences between pairs. An example of the normal quantile plot is shown in Figure 4.4. The paired t-test was then conducted on the pairs of control binder and each rejuvenated binder at different temperatures and aging conditions, and in all cases very small p-values (<0.0001) revealed significant differences between the pairs of viscosity measurements for the control binder and each of the rejuvenated binders.

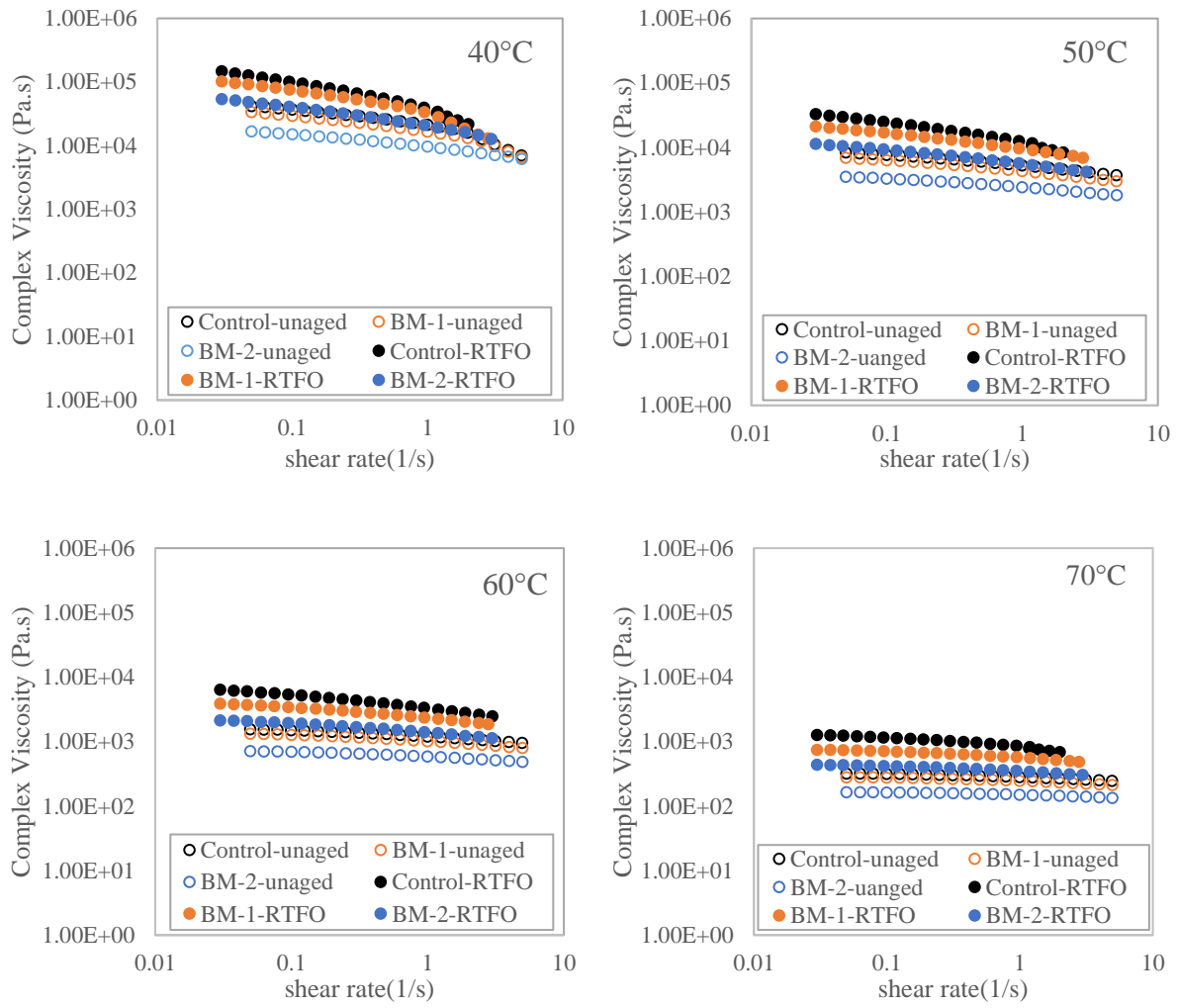


Figure 4.3 Variation of complex viscosity with shear rate and temperature for the control and the rejuvenated binders

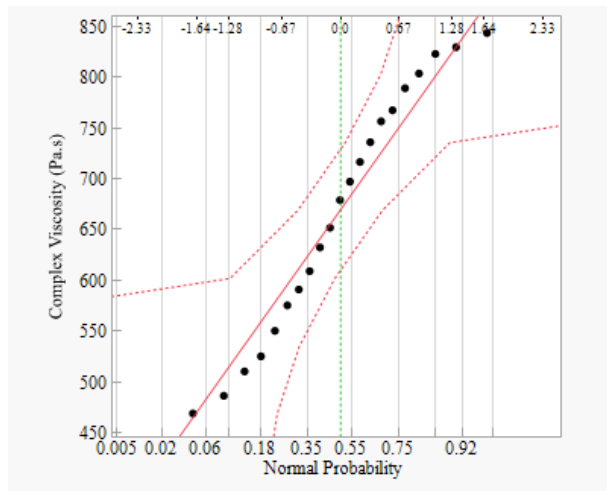


Figure 4.4 Normal quantile plot for the differences between pairs

4.3.4 Zero Shear Viscosity and Cross model

The viscosity of the asphalt binder at zero shear rate is as an intrinsic property of asphalt binders. This concept known as zero shear viscosity (ZSV), can be measured under particular conditions when a shear stress is acting on the material at a shear rate approaching to zero. It has been shown that especially in the case of modified asphalt binders, this parameter can better capture the stiffness of the binder and its resistance to rutting than the current Superpave specification, $G^*/\sin(\delta)$, which depends on the frequency testing (Bahia, et al., 2001; Binard, Anderson, Lapalu, & Planche, 2004; De Visscher, Soenen, Vanelstraete, & Redelius, 2004; Rowe, et al., 2002). The complex viscosity values of the unaged and RTFO-aged binders were employed to obtain the ZSV values of the binders by using the simplified Cross model presented in Equation 4.3 (Cross, 1965).

$$\eta = \eta_{\infty} + \frac{\eta_0 - \eta_{\infty}}{1 + (k \cdot f)^m} \quad \text{Equation 4.3}$$

where η is the measured viscosity data in Pa.s, η_{∞} is the infinite viscosity in Pa.s, η_0 is the zero shear viscosity in Pa.s, f is the frequency in Hz, k is the time constant, and m is the dimensionless rate constant. The inverse of the time constant, $1/k$, is known as the critical shear rate, or the shear rate at which the onset of shear thinning behavior occurs. The measured viscosity data at frequencies ranging from 0.1 to 100 Hz and temperatures ranging from 40°C to 70°C were fitted to the cross model and the ZSV and regression coefficients were obtained using the Solver tool in Excel. Figure 4.5 and Figure 4.6 present a comparison between the mean ZSV and the mean critical shear rate parameters obtained from six replicates of the unaged and RTFO-aged binders. As illustrated in Figure 4.5, the ZSV decreases with increase in temperature, and increases by aging. The ZSV value for the bio-rejuvenated binders is lower than the control binder. Figure 4.6 shows that by increasing the

temperature from 40°C to 50°C, the critical shear rate slightly increases, and at higher temperatures this increase becomes more significant. It can be seen that by incorporating the bio-rejuvenators in the control binder, the critical shear rate increases, indicating that the onset of shear-thinning behavior occurs at higher shear rates and they exhibit a more Newtonian-like behavior at low shear rates. This may be an indication of the rejuvenators' significant potential for restoring the balance between asphaltene and maltene fractions and lower the excess asphaltene portion which was present in the highly aged RAP binder.

Figure 4.6 also provides evidence that the critical shear rate decreases after RTFO-aging. This may be attributed to the higher asphaltene fractions in the aged binder which cause a non-linear behavior in the binder matrix. In order to investigate the significant differences between the ZSV values at different temperatures, a statistical analysis using one-way ANOVA with a significance level of 0.05 was conducted on the ZSV values. Prior to the test, an equal variances test was conducted on the groups that were analyzed together in the same ANOVA test, and p-values greater than 0.05 revealed no significant differences between the variances. Therefore, the ANOVA test could be used assuming that each ZSV value was taken from a normally distributed population. Because the purpose of this study was to compare each of the rejuvenated binders with the control binder, the Dunnett test was used to determine the significant differences between the groups. Therefore, the ANOVA test could be used assuming that each ZSV value was taken from a normally distributed population. Because the purpose of this study was to compare each of the rejuvenated binders with the control binder, the Dunnett test was used to determine the significant differences between the groups.

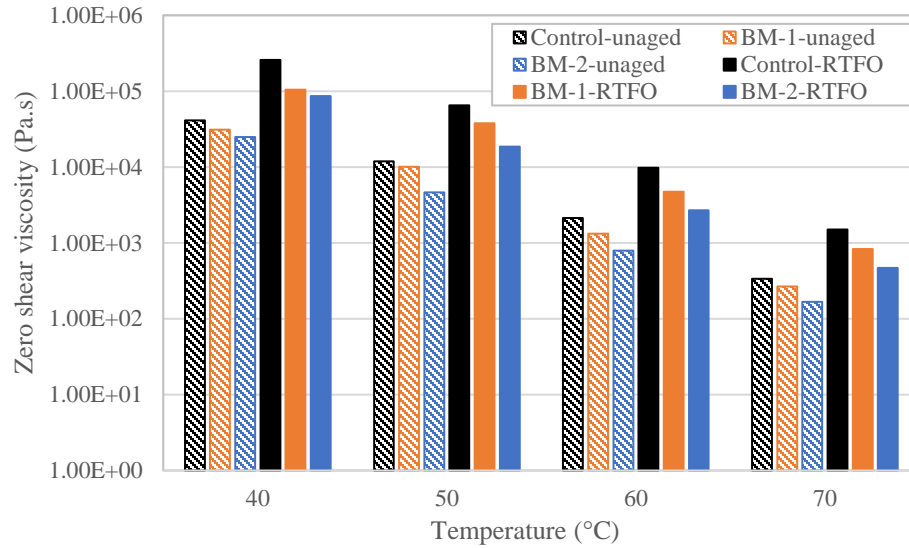


Figure 4.5 Variation of ZSV with temperature and aging conditions for the binders

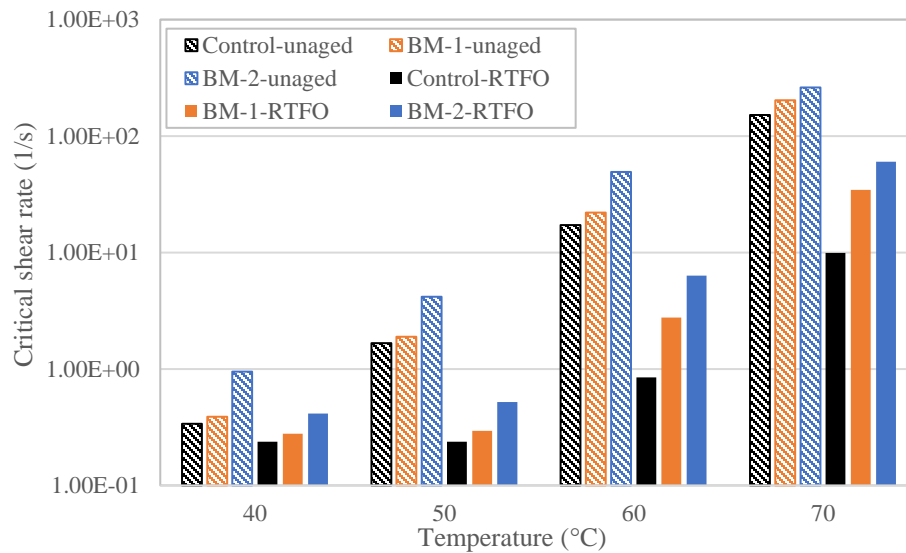


Figure 4.6 Variation of critical shear rate with the temperature and aging conditions for the binder

The results of the ANOVA test using Dunnett method at the four different testing temperatures revealed significant differences between the ZSV values of the rejuvenated binders and the control binder as the p-values obtained from Dunnett test were smaller than the significance level. Table 4.4 provides a comparison between the mean ZSV values and the decision limits for the control binder. An example of the Dunnett test output is also shown

in Figure 4.7 for the test temperature of 70°C and unaged conditions. Because the ZSV values of BM-1 and BM-2 binders are outside the decision limit (LDL-UDL) of the control least square mean, they are considered to be significantly lower than the ZSV of the control binder.

Table 4.4 ANOVA test results for the ZSV measurements

	Temperature (°C)							
	40		50		60		70	
	Unaged	RTFO	Unaged	RTFO	Unaged	RTFO	Unaged	RTFO
Control Mean	41199.2	258076	11928.5	65273.1	2194.1	9745.4	336.7	1505.1
RA1 Mean	31104.3	104596	10092.5	37775.5	1272.0	5245.4	266.8	832.5
RA2 Mean	24853.2	86485	4646.8	18601.2	788.6	2678.0	168.0	469.2
Control Decision Limits	32660.0- 49738.4	225647.8- 290504.0	10519.6- 13337.4	58171.3- 72374.9	1992.5- 2395.6	8273.7- 11217.1	282.5- 390.9	1377.5- 1632.75

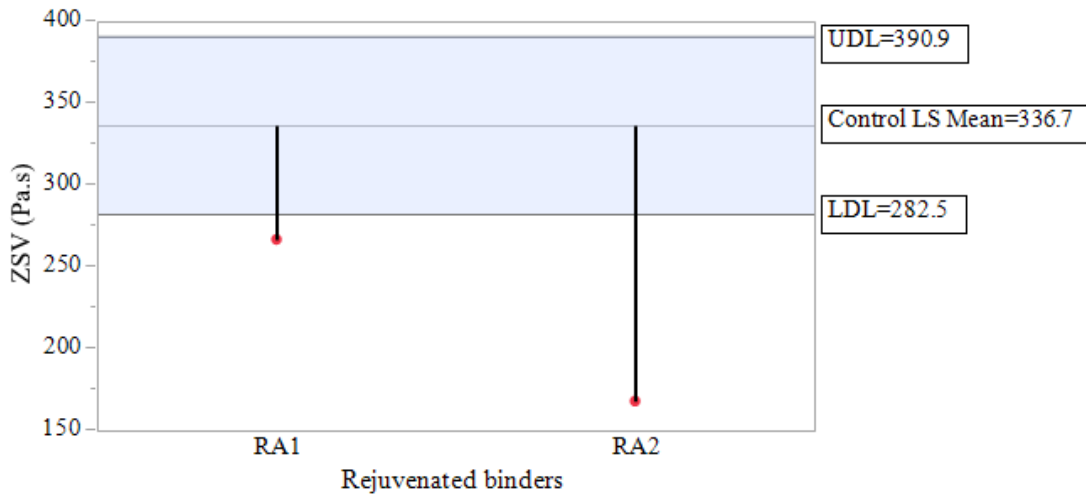


Figure 4.7 Example of Dunnnett test output showing significant differences between the ZSV values of the control binder and the rejuvenated binders

The variation of ZSV with temperature for the different binders at the two aging condition was also assessed, and an exponential relationship with R^2 values greater than 0.98 was found in all cases. This relationship was earlier found by Saboo et al. (Saboo, et al., 2018) and is confirmed here. This relationship can be used for constructing the master curves of the viscosity of the binders.

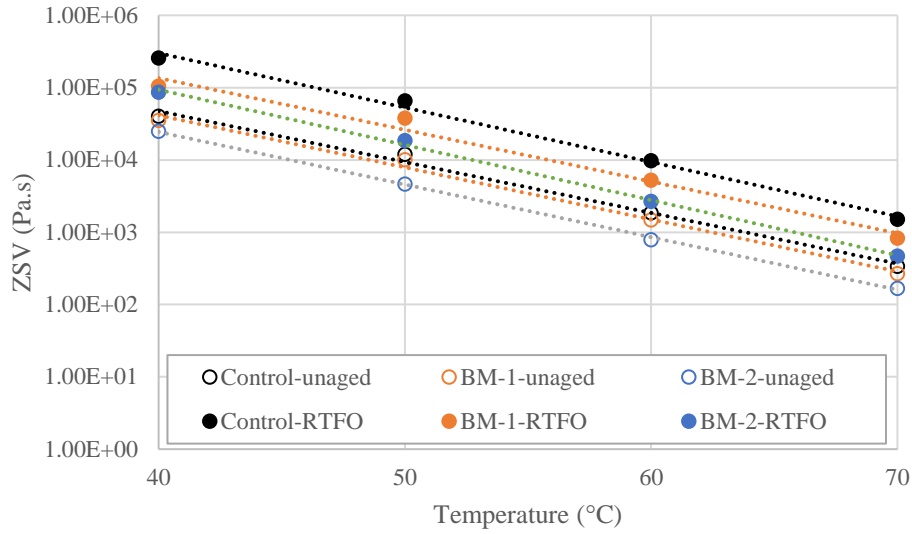


Figure 4.8 Variation of ZSV with temperature

4.3.5 Flow number

The rutting resistance of the asphalt mixtures was evaluated by the flow number test in accordance with AASHTO TP79-15. The test was performed on four dynamic modulus specimens that were tested for their stiffness characteristics in previous publications. The specimens were tested at a temperature of 54°C. Under repeated loading, asphalt mixtures undergo three main stages of deformation: primary, secondary, and tertiary. The flow number, which is the number of cycles at which the asphalt specimen begins tertiary flow, was obtained by using the Francken model. The Francken model is a composite mathematical model of a power law equation and an exponential equation. This model has been recommended over several other models because it captures all three stages of permanent deformation. Figure 4.9 displays an example of a flow number test result, as well as the flow number determined with a MATLAB program.

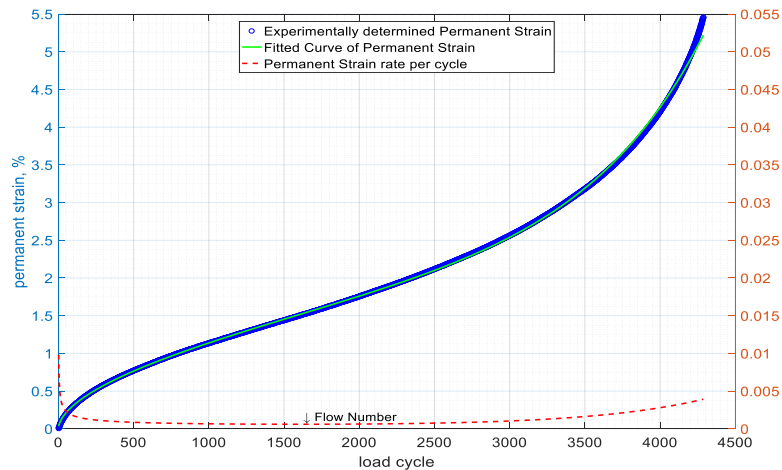


Figure 4.9 Example of MATLAB output for determining the flow number

Figure 4.10 presents the flow number of the mixtures at 54°C. It is clear that the control mix having higher stiffness/modulus shows greater resistance to rutting than the mixes modified with the bio-rejuvenators. In fact, after the aggregate interlocking terminates at some point under repeated loading, the behavior of the mixtures will be primarily influenced by the rheological properties of the binder, and binders with lower stiffness will fail earlier due to permanent deformation. At small scale production, the two modified mixtures met the minimum average flow number requirement of 190 for medium traffic (10 to ≤ 30 million ESALs), but not 740 for heavy traffic, as listed in the AASHTO TP79-15 standard. At large-scale production, however, both rejuvenated mixtures passed the criteria for heavy and medium traffic. Research by Tran et al. (Tran, Taylor, & Willis, 2012) has also shown that the addition of 6.8% of the BM-1 rejuvenator by weight of the RAP binder did not contribute towards improving the rutting performance of a 50% laboratory produced RAP mixture, however the medium traffic level requirement was still met and no further damage was observed compared to the standard mix.

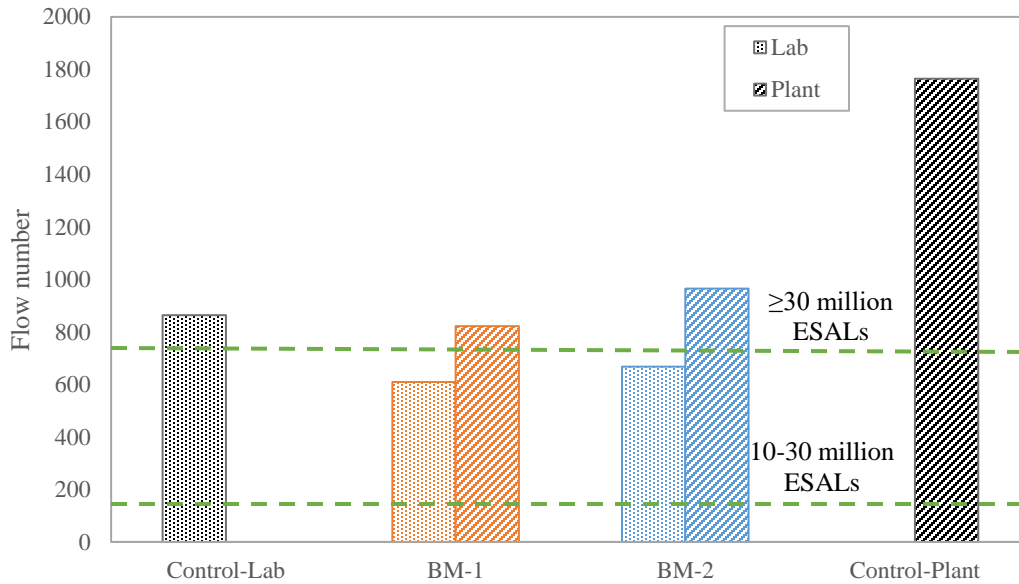


Figure 4.10 Comparison of rutting resistance

4.3.6 Stripping and moisture Susceptibility

The Hamburg wheel-tracking test was performed on three replicates per group at 50°C and in all cases the test was terminated after reaching 20,000 passes. This indicates the good resistance of the rejuvenated mixtures to early rutting and premature failure. Figure 4.11 shows an example of the rutting and stripping curve for the BM-1 mixtures where no SIP was identified before 20,000 wheel passes. In previous studies the same behavior was observed that mixtures containing some rejuvenators such as distilled tall oils, organic oils, and aromatic extracts did not reach stripping inflection points before 20,000 wheel passes (Zaumanis, et al., 2014). The average rut depth values for the lab-produced and plant-produced mixtures are shown in Figure 4.12. According to Figure 4.12, among the lab-produced mixtures, the two rejuvenated mixtures showed greater rut depth compared to the control mixture. However, at the large-scale production, because the control mixtures only contained 20% RAP in their mix design, their rut depth was greater than the BM-2 mixtures, but not than the BM-1 mixtures.

Studies on the influence of high RAP contents on moisture susceptibility are divided. The high variability potential of RAP material is likely a key factor to such discrepancies in results. Haghshenas et al. point out that the pre-coated aggregates in RAP likely inherently increase the moisture resistance of mixtures containing high RAP contents (Haghshenas, et al., 2016). This leads one to conclude that under optimal conditions and material quality, asphalt pavements containing high RAP contents should have similar or greater moisture resistance as their virgin material counterparts. However, non-homogeneity within the pavement system such as “black rock” resulting from insufficient material mixing can prove detrimental to such assumptions about material performance produced at the plant. Extensive laboratory testing and quality control can help in alleviating some of the uncertainty surrounding the effect of not only RAP, but rejuvenated RAP on a mixture’s moisture susceptibility.

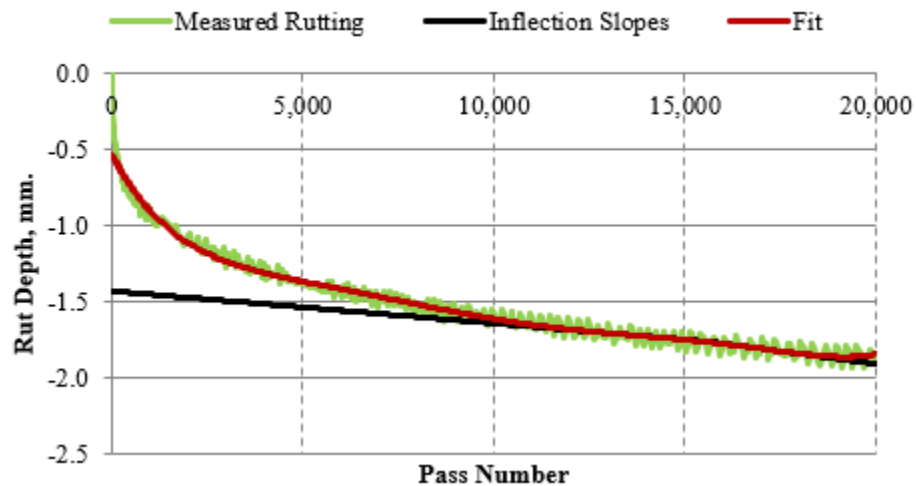


Figure 4.11 Example of HWTD output

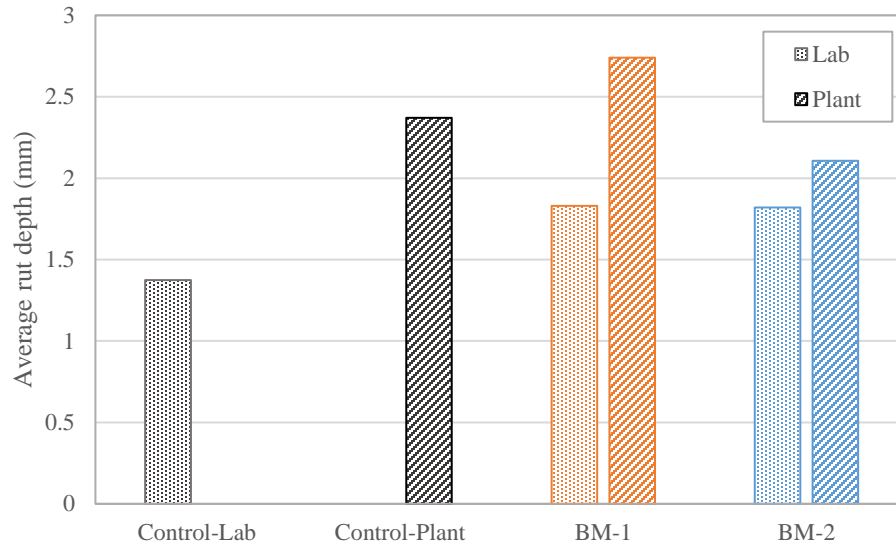


Figure 4.12 average rut depth for lab-produced and plant-produced groups

4.3.7 Study on the recovered binders

After testing for dynamic modulus and flow number, the lab-produced and plant-produced specimens were separately heated in sealed trays at 80°C for 2 hours and then crushed and immersed in toluene for the extraction and recovery processes. According to ASTM D2172 and ASTM D7906, the binders were extracted and recovered using two extraction units and a rotary evaporator. The binders were then tested using a DSR instrument for their original and RTFO high-temperature performance grade, and a comparison was made between the binders recovered from lab-produced mixtures and those of plant-produced mixtures. Because the recovered binders had been exposed to aging during production of asphalt specimens, the RTFO grading was performed on the non-RTFO aged recovered binders as well as the RTFO aged recovered binders. This procedure was employed to assess the differences in the high-temperature grades with/without further aging of the binders. In addition, a comparison was conducted between the blended binders in the lab and the recovered binders in order to determine the effect of RTFO aging and plant aging on the performance grade of the binders. All these comparisons were conducted using the ANOVA analysis and the normality of the

data and equal variances assumptions were checked and verified. Performance grading was conducted on six replicates from each group in order to perform a more precise evaluation based on the statistical results. Because the recovered binder from the plant-produced mixtures had a different RAP binder dosage, this binder was not included in the ANOVA analysis and the control lab-recovered binder was compared with the control lab-blended binder and the two rejuvenated lab-recovered binders. The significant differences between the groups are reported in the form of Tukey HSD connecting letters with those not connected by the same letters indicating significant differences. Because the comparison between the control lab-blended and the control lab-recovered binders only contained two groups, the connecting letters were assigned based on the resulting p-value. The blended binders which were obtained by blending the different constituents (RAP binder and fresh binder with/without rejuvenators) in the lab using a high speed shear mill and were labeled with the letter B. Binders recovered from lab-produced specimens were labeled as LR, and binders recovered from plant-produced specimens were labeled as PR. Table 4.5,

Table 4.6, and Table 4.7 present the ANOVA analysis results for the control, BM-1, and BM-2 binders, respectively. From the results it can be concluded that during the mixing and compaction of asphalt mixtures and through the recovery of asphalt binders, the binders are to some extent aged and their PG is significantly increased by one or two grades. The results also indicate that the recovered binders from the plant-produced mixtures exhibit higher failure temperatures than those of lab-produced mixtures, leading to the conclusion that they might have been exposed to more oxidation and aging conditions. The comparison between the RTFO on original results of the recovered binders with the RTFO on RTFO results of the blended binders show that during the production, the binders have not been aged to the same

level as the RTFO procedure does ages them in the lab. An exception from this observation is the BM-2 binder which the recovered binder from plant-produced mixtures has a higher PG than the RTFO-aged blended binder when both being tested under RTFO mode of the DSR program. This may be attributed to the mixing and compaction procedures at the plant where a high mixing temperature may have been exposed to the mixture and result in volatilizing the rejuvenator and diminish its rejuvenating effect on the mix. By looking at the flow number and Hamburg results, this hypothesis would not be validated and may lead to the conclusion that during the recovery of the binder from the BM-2 specimens, BM-2 may have been volatilized.

Table 4.5 ANOVA results for PG of the control binder

	Original			RTFO on Original			RTFO on RTFO		
	Mean Failure temperature (°C)	High temperature PG	t test Grouping	Mean Failure temperature (°C)	High temperature PG	t test Grouping	Mean Failure temperature (°C)	High temperature PG	t test Grouping
Control-B	80.6	76	B				81.9	76	A
Control-LR	85.6	82	A	78.1	76		84.1	82	B

Table 4.6 ANOVA results for PG of the BM-1 binder

	Original			RTFO on Original			RTFO on RTFO		
	Mean Failure temperature (°C)	High temperature PG	Tukey HSD Grouping	Mean Failure temperature (°C)	High temperature PG	Tukey HSD Grouping	Mean Failure temperature (°C)	High temperature PG	Tukey HSD Grouping
BM-1-B	77.2	76	B	-	-	-	76.9	76	B
BM-1-LR	83.4	82	A	74.3	70	A	78.2	76	B
BM-1-PR	83.1	82	A	75.9	70	A	83.2	82	A

Table 4.7 ANOVA results for PG of the BM-2 binder

	Original			RTFO on Original			RTFO on RTFO		
	Mean Failure temperature (°C)	High temperature PG	Tukey HSD Grouping	Mean Failure temperature (°C)	High temperature PG	Tukey HSD Grouping	Mean Failure temperature (°C)	High temperature PG	Tukey HSD Grouping
BM-2-B	71.9	70	B	-	-	-	73.8	70	C
BM-2-LR	81.7	76	A	73.2	70	A	81.0	76	B
BM-2-PR	82.1	82	A	75.0	70	A	83.2	82	A

4.4 Conclusions

- The two bio-rejuvenators were able to slightly improve the temperature-susceptibility of the control binder. When tested by the rotational viscometer, it was found that as the temperature increases, the two rejuvenated binders would likely behave in a similar way to the virgin binder used in their formulation.
- The conventional $G^*/\sin(\delta)$ parameter appears to provide a correct rating of the rutting behavior of the different binders, however, this parameter depends on the frequency of testing. To overcome the dependency on frequency, zero shear viscosity (ZSV) of the binders can be determined. The two rejuvenators caused a decrease in the ZSV of the control binder, and an increase in its critical shear rate, indicating a more Newtonian-like behavior at lower shear rates. Small P-values (<0.001) obtained from the Dunnett statistical test on the ZSV values revealed significant differences between the control binder and its rejuvenated counterparts. ZSV values were computed from the measured complex viscosity values using a DSR instrument. The statistical analysis on the complex viscosities also revealed significantly lower viscosity measurements for the two rejuvenated binders.
- The rutting resistance of the mixtures decreased by adding the bio-rejuvenators yet meeting the AASHTO standard requirements for a medium traffic level. The main output of the Hamburg test is the stripping inflection point (SIP), where the two steady-state portions in the plot of rut depth vs. number of load cycles cross each other. In this study, all the alternatives as well as their control groups exhibited superior performance against stripping since all of them passed 20,000 load cycles without any SIP.
- Compared to the binders blended in the lab according to the proportions in the mix design, the recovered binders from the lab-produced and plant-produced mixtures exhibited higher

performance grades, indicating the aging mechanisms they have been exposed to during the mixing and compaction efforts. After being recovered, the binders exhibited lower performance grades compared to their RTFO aged counterparts which were sampled from the blended binders. This may lead to the conclusion that the RTFO aging in the lab imposes more extreme aging on the binders compared to reality. It is also important to account for the effect of the extraction and recovery processes on the aging of the recovered binders. Generally, the rejuvenators contain some extent of light components with boiling points lower or close to the temperature where the recovery of the binder occurs; therefore, it is likely that these components volatilize and inhibit correct measurements of the rheological properties of the recovered binders. Therefore, further evaluation of the rejuvenated binders through some analytical techniques such as mass spectrometry is needed to attain a better understanding of the binder's components after recovery.

4.5 References

- Al-Qadi, I. L., Elseifi, M., & Carpenter, S. H. (2007). *Reclaimed asphalt pavement—a literature review* 0197-9191).
- Ali, H., & Mohammadafzali, M. (2015). *Long-term aging of recycled binders*.
- Anderson, D., Le Hir, Y., Planche, J.-P., Martin, D., & Shenoy, A. (2002). Zero shear viscosity of asphalt binders. *Transportation Research Record: Journal of the Transportation Research Board*(1810), pp. 54-62.
- Anderson, D. A., Christensen, D. W., Bahia, H. U., Dongre, R., Sharma, M., Antle, C. E., & Button, J. (1994). Binder characterization and evaluation, volume 3: Physical characterization. *Strategic Highway Research Program, National Research Council, Report No. SHRP-A-369*
- Bahia, H. U., Hanson, D., Zeng, M., Zhai, H., Khatri, M., & Anderson, R. (2001). *Characterization of modified asphalt binders in superpave mix design*. (No. Project 9-10 FY'96)

- Binard, C., Anderson, D., Lapalu, L., & Planche, J. (2004). *Zero shear viscosity of modified and unmodified binders. Proceedings of the 3rd euraspalt and eurobitume congress held vienna*, May 2004.
- Cavalli, M. C., Zaumanis, M., Mazza, E., Partl, M. N., & Poulikakos, L. D. (2018). Effect of ageing on the mechanical and chemical properties of binder from RAP treated with bio-based rejuvenators. *Composites Part B: Engineering*, 141, pp. 174-181.
- Copeland, A. (2011). *Reclaimed asphalt pavement in asphalt mixtures: State of the practice*.
- Cross, M. M. (1965). Rheology of non-Newtonian fluids: a new flow equation for pseudoplastic systems. *Journal of colloid science*, 20(5), pp. 417-437.
- De Visscher, J., Soenen, H., Vanelstraete, A., & Redelius, P. (2004). *A comparison of the zero shear viscosity from oscillation tests and the repeated creep test*. Proceedings of 3rd Euraspalt & Eurobitume Congress, Vienna.
- Elkashef, M., Podolsky, J., Williams, R. C., & Cochran, E. W. (2017). Introducing a soybean oil-derived material as a potential rejuvenator of asphalt through rheology, mix characterisation and Fourier Transform Infrared analysis. *Road Materials and Pavement Design*, pp. 1-21.
- Haghshenas, H., Nabizadeh, H., Kim, Y.-R., & Santosh, K. (2016). Research on High-RAP Asphalt Mixtures with Rejuvenators and WMA Additives, Report SPR-P1(15) M016, *Nebraska Transportation Center*.
- Hajikarimi, P., Rahi, M., & Moghadas Nejad, F. (2015). Comparing different rutting specification parameters using high temperature characteristics of rubber-modified asphalt binders. *Road Materials and Pavement Design*, 16(4), pp. 751-766.
- Hajj, E. Y., Souliman, M. I., Alavi, M. Z., & Salazar, L. G. L. (2013). Influence of hydrogreen bioasphalt on viscoelastic properties of reclaimed asphalt mixtures. *Transportation Research Record*, 2371(1), pp. 13-22.
- Im, S., & Zhou, F. (2014). Field performance of RAS test sections and laboratory investigation of impact of rejuvenators on engineering properties of RAP/RAS mixes. (No. FHWA/TX-14/0-6614-3). *Texas. Dept. of Transportation. Research and Technology Implementation Office*.
- Mogawer, W. S., Austerman, A. J., Kluttz, R., & Puchalski, S. (2016). Using polymer modification and rejuvenators to improve the performance of high reclaimed asphalt pavement mixtures. *Transportation Research Record*, 2575(1), pp. 10-18.
- Olard, F., & Pouget, S. (2015). A new approach for aggregate grading optimization for mixtures *Advances in Asphalt Materials* (pp. 427-457): Elsevier.

- Phillips, M., & Robertus, C. (1996). Binder rheology and asphaltic pavement permanent deformation; the zero-shear-viscosity. *Eurasphalt & eurobitume congress*, strasbourg, 7-10 may 1996. Volume 3. Paper e&e. 5.134.
- Podolsky, J. H., Sotoodeh-Nia, Z., Huisman, T., Williams, R. C., & Cochran, E. W. (2019). Practical Approach to Mix Design with High Binder and Aggregate Replacement in Iowa using Fractionation. *Transportation Research Record*, p 0361198119834303.
- Pouget, S., Olard, F., & Hammoum, F. (2016). *GB5® Mix Design: A New Approach for Aggregate Grading Optimization for Heavy Duty Flexible Pavements*. 8th RILEM International Conference on Mechanisms of Cracking and Debonding in Pavements.
- Rowe, G. M., D'Angelo, J. A., & Sharrock, M. J. (2002). *Use of the zero shear viscosity as a parameter for the high temperature binder specification parameter*. 2nd International Symposium on Binder Rheology and Pavement Performance.
- Saboo, N., Singh, B., Kumar, P., & Vikram, D. (2018). Study on viscosity of conventional and polymer modified asphalt binders in steady and dynamic shear domain. *Mechanics of Time-Dependent Materials*, 22(1), pp. 67-78.
- Shu, X., Huang, B., Shrum, E. D., & Jia, X. (2012). Laboratory evaluation of moisture susceptibility of foamed warm mix asphalt containing high percentages of RAP. *Construction and Building Materials*, 35, pp. 125-130.
- Tran, N. H., Taylor, A., & Willis, R. (2012). Effect of rejuvenator on performance properties of HMA mixtures with high RAP and RAS contents. *NCAT Report*, pp. 12-05.
- Yu, X., Zaumanis, M., Dos Santos, S., & Poulikakos, L. D. (2014). Rheological, microscopic, and chemical characterization of the rejuvenating effect on asphalt binders. *Fuel*, 135, pp. 162-171.
- Zaumanis, M., Mallick, R. B., Poulikakos, L., & Frank, R. (2014). Influence of six rejuvenators on the performance properties of Reclaimed Asphalt Pavement (RAP) binder and 100% recycled asphalt mixtures. *Construction and Building Materials*, 71, pp. 538-550.
- Zhao, S., Huang, B., Shu, X., Jia, X., & Woods, M. (2012). Laboratory performance evaluation of warm-mix asphalt containing high percentages of reclaimed asphalt pavement. *Transportation Research Record*, 2294(1), pp. 98-105.

CHAPTER 5 CONCLUSIONS AND RECOMMENDATIONS

This research is focused on investigating the feasibility of using two bio-based rejuvenators in asphalt pavements containing 50% RAP materials. To this end, the BioRePavation project was proposed by IFSTTAR institute in France, and four other institutes collaborated to meet the goals. The tasks assigned to the research group at ISU involved a thorough evaluation of the mixtures as well as their respective binders. Further research was conducted alongside the objectives of this project to address some of the current challenges in the field.

5.1 Effect of bio-rejuvenators and mix scale on the complex modulus of binders and mixtures

In the early stage of this research, in order to assess the effect of the two bio-rejuvenators on the overall performance of the mixtures, pre-determined proportions from the RAP binder, the fresh binder, and the rejuvenators were blended, and the respective binders were prepared in the lab. The full investigation of the binders' performance in terms of rheological and physical properties proved their ability to enhance the low and intermediate-temperature properties and to reduce the critical high-temperature performance grade.

Research on two of the most common models for predicting the binder complex modulus values- the Sigmoidal model and the CAM model- suggested that the two models could perfectly predict the complex modulus values at unaged and RTFO-aged conditions as shown by P-values greater than the level of significance when comparing the measured and the predicted values, however, as the binder is more aged, the deviation of the predicted data vs. measured data from the line of equity becomes more noticeable. This deviation makes the two models to present significantly different complex modulus values for the PAV-aged binders, with better prediction by the Sigmoidal model. The CAM model, however, still shows a very high R^2 value between the

predicted and the measured data and the deviation from the equality line is for the tail data points. Therefore, for the construction of binder master curves at intermediate temperatures ($<25^{\circ}\text{C}$) the Sigmoidal model is recommended over the CAM model.

The Black diagrams of the binders also indicate that testing at temperatures below 16°C cannot provide accurate measurements for the complex viscosities and very low constant shear strain ($<0.8\%$) is needed to obtain the correct measurements at low temperatures.

The mixture stiffness evaluation at two different mixing locations suggests that the dynamic modulus measurements for identical mixtures can be significantly different depending on where they have been produced (lab/plant). Therefore, it is recommended to take more control of the mixing process especially at the plant due to the high variability in the operations.

5.2 Effect of bio-rejuvenators and mix scale on the low and intermediate temperature properties of asphalt binders and asphalt mixtures

In the second part of this research, binders were tested for their heat flow properties using a DSC. It was found that the rejuvenators were fully miscible in the binders, and they could disaggregate some of the asphaltene particles in the control binder. The rejuvenators were also able to greatly improve the ductility of the control binder as seen from the Glover-Rowe diagrams.

From the LAS test results, significant improvement was seen in the fatigue life of the control binder after rejuvenation, but not in the mixtures. Even the results from the dissipated energy approach could not provide a correct evaluation of the fatigue life after rejuvenation, and this could be an indication of the incapability of the beam fatigue testing in capturing a realistic fatigue behavior of asphalt mixtures with high RAP contents.

From the low-temperature performance grades in the previous chapter, it was anticipated that the rejuvenated mixtures would outperform the control mixture in the DCT test. The DCT test results verified this observation, and a very high correlation was found between the m-values obtained from BBR test on the binders and the fracture energy values obtained from DCT test on the mixtures. This correlation appears to fade out as the test temperature approaches zero. The effect of mix scale on the DCT measurements was evaluated through statistical analysis of both the peak load values and the fracture energy values, and significant differences were identified indicating that the different batching and mixing operations in the lab may not always provide a correct estimation of the performance of the mixtures prepared at the asphalt plant. Higher variation observed in the fracture energy of the lab-produced mixtures also suggests that separate batching and mixing of the specimens in the lab could largely contribute to this variation.

5.3 Effect of bio-rejuvenators and mix scale on the high temperature properties of asphalt binders and asphalt mixtures

Research on the viscosity of the binders was conducted in this part of the study. Although the results from the conventional method using a viscometer showed significant decrease in the mixing and compaction temperature, however, the mixing temperature ranges were slightly high (~165°C -170°C) and the rejuvenators would possibly lose some of their volatilizing components at these temperatures. The temperature susceptibility of the binders was also assessed by the conventional viscosity measurements and the rejuvenated binders showed slight improvement compared to the control binder.

The Superpave rutting specification for the asphalt binders indicated greater rutting susceptibility for the rejuvenated binders, as it was anticipated from their lower critical high-temperature performance grade. However, the rating between the binders was not in the same order

as that of the mixtures. Less rutting susceptible BM-1 binder compared to the BM-2 binder led to an earlier failure of the BM-1 mixture, although the mix proportions and the aggregate gradations were identical. This leads to the conclusion that the method of incorporating rejuvenators in the mix (directly to the RAP aggregates, BM-1, or blended with the virgin binder, BM-2) could be an influencing factor in the final rutting performance.

The flow number test results also provide this comparison between the lab-produced (50% RAP) and plant-produced (20% RAP) control mixtures that although excessive amount of RAP can introduce greater stiffness to the mix, however, the rutting resistance can be adversely influenced. This observation was further evaluated by the Hamburg test results and an opposite behavior for the control mixtures was seen. In the Hamburg test results analysis, a higher rut depth for the plant-produced control mix in comparison to all other mixtures better described what would occur in practice when using lower RAP contents. Therefore, it is recommended to perform the Hamburg test other than the flow number test when evaluating high RAP mixtures for their rutting resistance.

The zero shear viscosity values and critical shear rates calculated by using the Cross model were also compared and the rejuvenated binders exhibited a more Newtonian-like behavior at lower shear rates indicating their effectiveness in restoring the balance between the asphaltene and maltene fractions.

5.4 Recovered binders after short-term aging

At the final stage of this research, binders were extracted and recovered from the lab-produced and plant-produced mixtures and a statistical analysis was conducted on their high-temperature performance grades to identify the effect of aging during their production. It was

found that during the mixing and compaction of asphalt mixtures the performance grade of the binders was increased by one or two grades. The heating process during the recovery of asphalt binder could also contribute to this increase.

5.5 Future research

In future work, investigating the blending level between the fresh binder and the RAP binder through analytical, chemical, and microscopic characterization such as mass spectrometry, SARA fractionation, and scanning electron microscopy might prove important.

A comprehensive statistical design of experiments involving the effect of several influencing factors such as the RAP dosage, the rejuvenator dosage, the blending temperature, and the blending time on several responses such as the performance grade, the glass transition temperature, and the SARA analysis is needed to find out the optimum alternative rejuvenated binder with the most contribution to improved performance and sustainability of road pavements.

Future research on the fatigue characterization of high RAP asphalt mixtures is needed to address the current limitations in analyzing the beam fatigue data and propose other techniques to consider the viscoelastic properties of the mixtures in the analysis.

Due to the potential for some of the volatile compounds of the rejuvenators to adversely impact the long-term performance of the asphalt pavement, further studies should investigate the effect of long-term aging on the performance of asphalt mixtures containing high RAP contents and rejuvenators.